Experimental Investigation and Thermodynamic Analysis of a Cross-Flow Humidifier

BY

Ibrahim Saad Al-Shalawi

A Thesis Presented to the
DEANSHIP OF GRADUATE STUDIES

KING FAHD UNIVERSITY OF PETROLEUM & MINERALS

DHAHRAN, SAUDI ARABIA

In Partial Fulfillment of the
Requirements for the Degree of

MASTER OF SCIENCE

In

MECHANICAL ENGINEERING

May, 2014

KING FAHD UNIVERSITY OF PETROLEUM AND MINERALS

DHAHRAN- 31261, SAUDI ARABIA

DEANSHIP OF GRADUATE STUDIES

This thesis, written by IBRAHIM SAAD ALSHALAWI under the direction his thesis advisor and approved by his thesis committee, has been presented and accepted by the Dean of Graduate Studies, in partial fulfillment of the requirements for the degree of MASTER OF SCIENCE in MECHANICAL ENGINEERING.

Thesis Committee

Dr. Mohamed A. Antar (Advisor)

Dr. Syed M. Zubair (Member)

Dr. Mostafa H. Elsharqawy (Member)

Dr. Zuhair M. Gasem
Department Chairman

Dr. Salam A. Zummo
Dean of Graduate Studies

15/11/15

Date

بِسْمِ اللهِ الرَّحمَنِ الرَّحِيمْ

In the name of Allah, the most Gracious, and the most Merciful

Dedicated

To

My beloved parents, my brothers and sisters, my Wife, my daughter Miriam and my son Yaser

ACKNOWLEDGMENTS

All praise be to Allah, the Lord of all creation, the most gracious, the most merciful for his beneficence that he granted me the strength, health and knowledge to complete this Thesis. And all prayers and blessings of Allah be upon our master, the most noble Prophet Muhammad (P.B.U.H.).

Thereafter, I am so thankful to the authority King Fahd University of Petroleum and Minerals for giving me the opportunity to pursue my Master degree in Mechanical Engineering.

I acknowledge the directions, advices, encouragements, supports and valuable time given to me by my thesis advisor, Dr. Mohammed A. Antar. Also, I am grateful to my thesis committee members, Dr. Syed M. Zubair and Dr. Mostafa H. Elsharqawy for their guidance and valuable comments, during the whole period of my research activities.

Moreover, my warm thanks are due to my parents, brothers and sisters for their prayers and support during my master program.

I also would like to appreciate and thank my colleagues at the university for their help and collaboration in my study.

May Allah bless everyone with happiness.

TABLE OF CONTENTS

LIST OF TABLES

LIST OF FIGURES

THESIS ABSTRACT (ENGLISH)

Name : **IBRAHIM SAAD ALSHALAWI**

Thesis Title : **EXPERIMENTAL INVESTIGATION AND THYRMODYNAMIC ANALYSIS OF A CROSS-FLOW HUMIDIFIER**

Major Field : **MECHANICAL ENGINEERING**

Date of Degree : **RAJAB 1435 (H) (MAY 2014 G)**

Humidification constitutes one of the main processes of humidification-dehumidification desalination systems (HDH) in which evaporation of some amount of water vapor into the air is a necessary stage to extract desalinated water from the humidified air by condensation in the dehumidifier. In the current study the performance of a cross-flow humidifier is intended to be evaluated and experimentally investigated based on the analysis of first and second law of thermodynamics. The experimental work includes variation of three input parameters: the mass flow rate ratio, the packed bed length and the water inlet temperature. The performance of the system is examined by air and water effectiveness, Merkel number, entropy generation, and second law efficiency as a function of the three beforehand mentioned variables. The results showed that the best operating conditions of the cross-flow humidifier happen when the heat capacity rates of air and water streams are equal to each others.

MASTER OF SCIENCE DEGREE

KING FAHD UNIVERSITY OF PETROLEUM AND MINERALS

DHAHRAN, SAUDI ARABIA

ملخص رسالة (باللغة العربية)

الاسم : **إبراهيم سعد الشلوي**

عنوان الرسالة : **الاختبار التجريبي و التحليل الديناميكي الحراري للمرطب الذي يعمل بالجريان التقاطعي**

مجال التخصص : **الهندسة الميكانيكية**

تاريخ الدرجة : **رجب ١٤٣٥ هـ ، الموافق مايو ٢٠١٤ م**

يشكل الترطيب واحدة من العمليات الرئيسية في أنظمة تحلية المياه بالترطيب والتجفيف (اتش دي اتش) ، والتي يكون من أحد مراحلها الأساسية تبخير كمية من بعض بخار الماء في الهواء ، لاستخراج المياه المحلاة من الهواء المرطب بواسطة التكثيف في مزيل الرطوبة (معادل الرطوبة) . وفي الدراسة الحالية ، نهدف إلى تقييم أداء المرطب الذي يعمل بالجريان التقاطعي ودراسته واختباره من الناحية التجريبية ، استنادا الى القانون الأول والثاني للديناميكا الحرارية . ويشمل العمل التجريبي على إدخال ثلاثة عوامل متغيرة وهي : نسبة معدل تدفق الكتلة ، طول العمود المعبأ ، و درجة حرارة دخول المياه . ويتم فحص واختبار أداء النظام عن طريق فعالية الهواء والمياه ، رقم ميركل ، التوليد الانتروبي ، وكفاءة وفعالية القانون الثاني كدالة على المتغيرات الثلاثة المذكورة سلفا .وأظهرت النتائج أن أفضل الظروف التشغيلية للمرطب الذي يعمل بالجريان التقاطعي تحدث عندما تكون معدلات السعة الحرارية لتيارات الهواء والماء مساوية لبعضها البعض .

درجة الماجستير في العلوم

جامعة الملك فهد للبترول والمعادن

الظهران، المملكة العربية السعودية

CHAPTER 1

INTRODUCTION

1.1 THE WATER CRISIS IN THE WORLD

The easily reached drinking water in the world is decreasing everyday and at the same time the demand for clean water by human beings is increasing very fast. On the other hand, polluted water resources are the main cause of many diseases that many people nowadays are suffering from. Even today, due to the industrial pollutions and some other activities, many countries face water scarcity. In the near future, it is expected that the lack in drinkable water will be the biggest problems worldwide, and this is due to the fact that the current consumptions rates are high as well as the world population is increasing continuously. Meanwhile, the wastes from industries are contributing in increasing the impurity of clean water resources. [1]

Almost 40% of people on earth are affected by water scarcity. And by 2025, it is expected that 1.8 billion people will be living in countries with high water scarcity. Moreover, the highest population growth will occur in countries that are already facing water stress and such level of population growth may lead to more difficult situations. Concerned researchers in water resources provided figures on the

amount of water on earth as a step to facilitate recommendations and solutions for future water crisis. So, it has been estimated that the total volume of water on the earth is nearly 1.4 billion cubic kilometers; almost 97.5% of it is salt water and the rest 2.5% is fresh water. Most of the fresh water is in the form of ice and snow over the mountains, also almost 30% of the fresh water is ground water resources and the remaining 0.3% is in the rivers and lakes which is the amount available for human beings. [2].

Therefore, in order to beat the challenge associated with future water scarcity, development of new resources of clean water is badly needed. Hence, desalination of sea water is a good alternative because the only available and largest source of water is the ocean.

In addition to the problem of water shortage, the needed energy for sea water desalination processes forms another problem because it requires huge amount of energy input. It is estimated that to produce one million cubic meter of water per day requires ten million tons of oil per year [3, 4].

1.2 DESALINATION PROCESSES

1.2.1 Overview

Producing fresh water from ocean needs appropriate separation process which can be achieved in different methods. As shown in figure 1.1, when sea or brackish water is fed into any type of separation units two streams will be produced, one is the fresh water and the other is the rejected brine which will be with high salt

concentration and in order to achieve such process of separation an energy must be added to the desalination unit and this energy might be in the form of mechanical, electrical or thermal energies [5, 6].

Historically, the first desalination units used for producing fresh water were based on the evaporation of water though adding heat from the sun. In recent years, many desalination technologies are used and the two main types of evaporative units used these days are Multiple Effect Distillation (MED) and Multi Stage Flash (MSF) desalination. And the other famous used type of processes is the membrane desalination technology or specifically the reverse osmosis units (RO). Figure 1.2 shows the classifications and different types of some desalination processes.

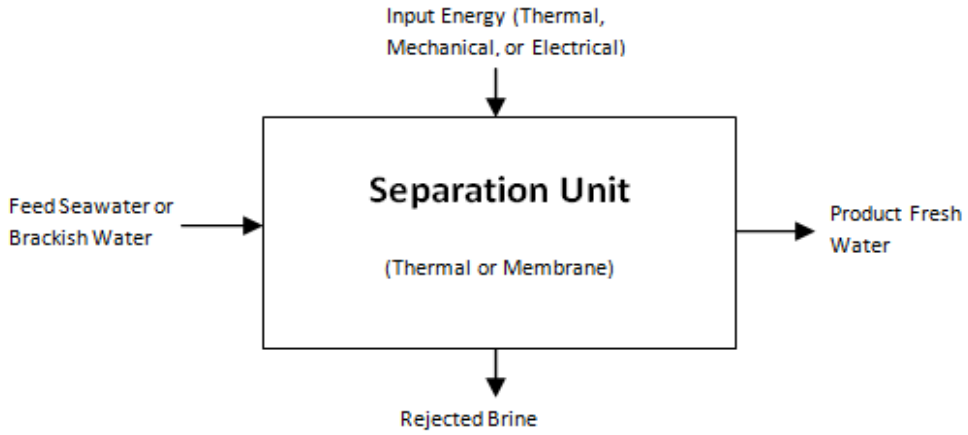

Figure 1.1 Separation process in desalination systems [6]

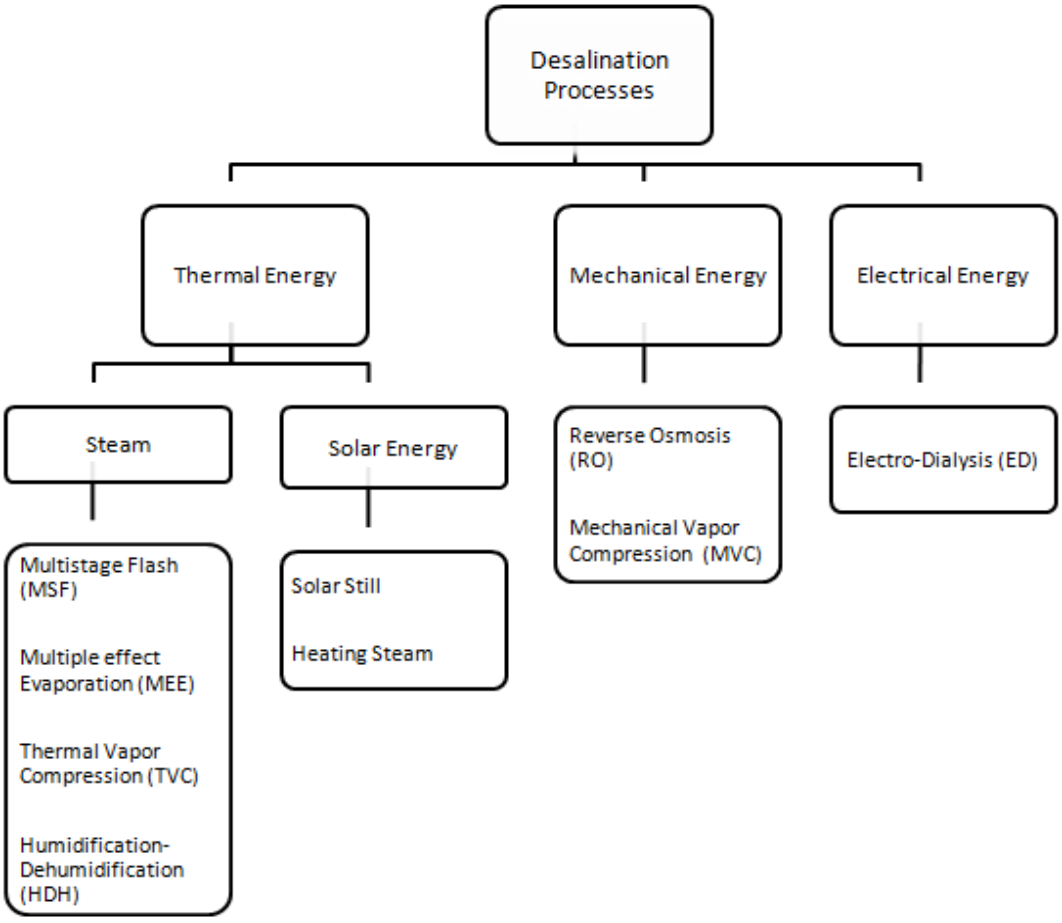

Figure 1.2 Classification of sea water desalination technology [6]

From the classifications of processes shown in figure 1.2, the thermal energy processes are categorized into two groups, one is adding energy to the process such as MSF, MED, and humidification-dehumidification and the other type is removing energy from the system such as freezing. In the processes of adding energy, the heating steam is these units can be obtained from power generation plant, or from solar energy [6]. The separation process in these systems is achieved by utilizing the high energy associated with hot steam to evaporate the saline solution and obtain vapor which is then condensed to produce pure water.

In light of the above overviews about global water crisis and existing desalination processes, it is very important to put more efforts for providing desalination units with better performances at all basis. From economical point of view, for remote areas, such better performances can be approached through three main criterions:

1. The capital cost must be low and/or effective.
2. The system is reliable and requires simple maintenance.
3. It is suitable for small scale application.

Solar stills which are one of the oldest desalination units require large areas to produce pure water even though their maintenance is simple, therefore, they are not economically feasible up to date. Moreover, Reverse osmosis systems which are the most used ones in the world nowadays do not fall under the last two criterions [7].

The desalination process that meets all mentioned criterion is the humidification-dehumidification desalination (HDH) systems.

1.2.2 Humidification-Dehumidification Desalination System (HDH)

HDH system imitates the natural water cycle very closely and this happens when the water is heated in solar panel or electric water heater then sprayed over a dry air stream in the humidifier section of HDH unit as shown in figure 1.3.

As the air and water flows over the surfaces of packing material and mixes with each other, there is a driving potential for heat transfer due to temperature difference between both streams and another driving potential for mass transfer due to difference in water-vapor concentration, therefore, some water evaporates from water stream and absorbed into the air. The moisture content of air increases during this process and its temperature increases.

The hot and humid air leaving the humidifier section is then enters the dehumidification section where the water vapor contained in the air is condensed over the coils of the incoming cold water, and such stream of cold water is preheated as it flows out of the dehumidifier to the sprayers in the humidifier. This particular cycle is called closed air-open water cycle (CAOW). There are different and many cycles of HDH systems which are described in details in [8].

There is a separate component for each process in the humidification-dehumidification desalination unit which allows flexibility of thermodynamic designing for evaporation in the humidifier, condensation in the dehumidifier and heating of water in the solar collector or other source of heating. The advantage of HDH systems over solar stills is that they have higher GOR (the ratio of the latent heat of evaporation of the water produced to the net energy input to the cycle). And

the advantages HDH has over other desalination systems include its low initial cost, simple design, less maintenance and also its ability to handle wide range of raw water qualities while the main disadvantage of it is that it requires high energy input compared to the other available systems[9, 10, 11].

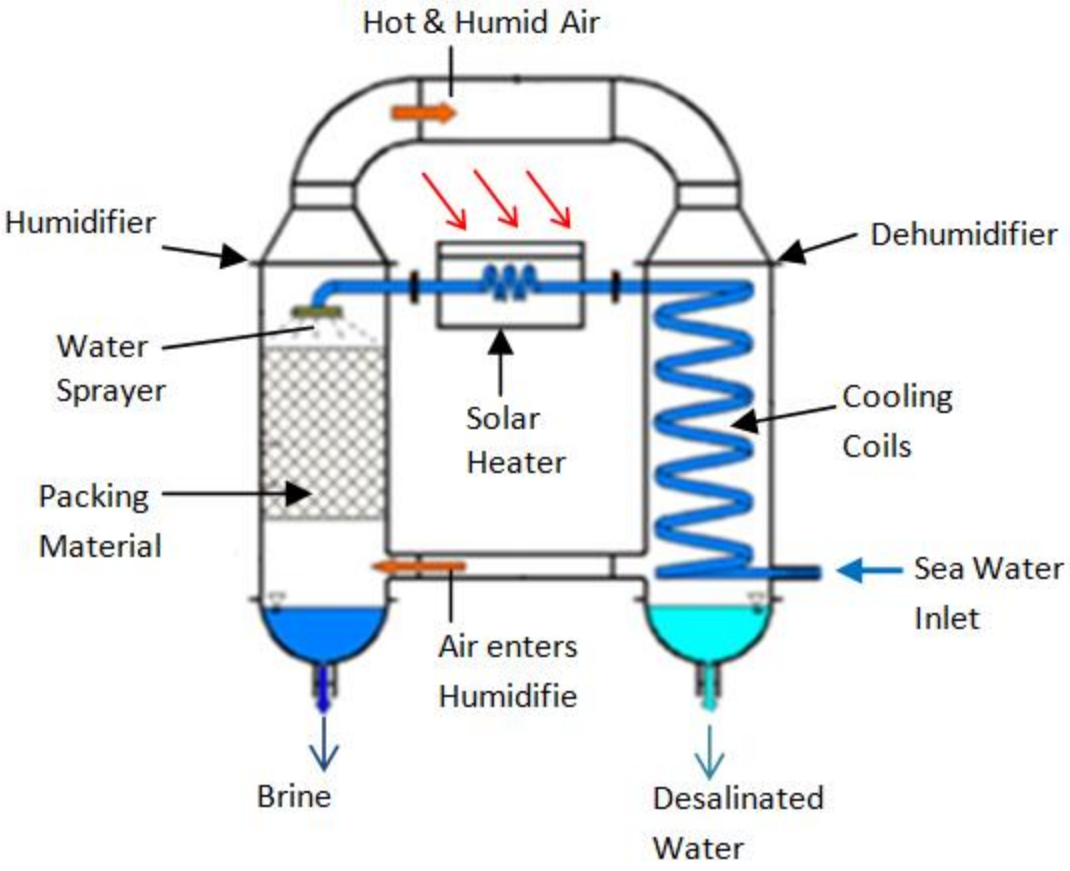

Figure 1.3 Humidification-dehumidification desalination unit [4]

1.3 HUMIDIFIERS

1.3.1 What is a Humidifier

A humidifier is a device that transfers mass and heat between water and air, and this process takes place when the hot water is sprayed over a cold air stream as can be seen in figure 1.4. When the two streams get in contact with each other, some fractions of water evaporate from water liquid stream and absorbed into the unsaturated air stream due to the potential difference in temperature and water concentration between water and air.

In such humidification process, part of the latent heat of vaporization that comes from the water is absorbed by air and as a result increases the temperature of air and consequently cools the water.

The water vapor content in the air can be quantified in different ways. One of these ways is to relate the mass of water vapor in a unit mass of dry air and this is called the humidity ratio and it is denoted by symbol ω:

$$\omega = \frac{m_v}{m_a} \tag{1.1}$$

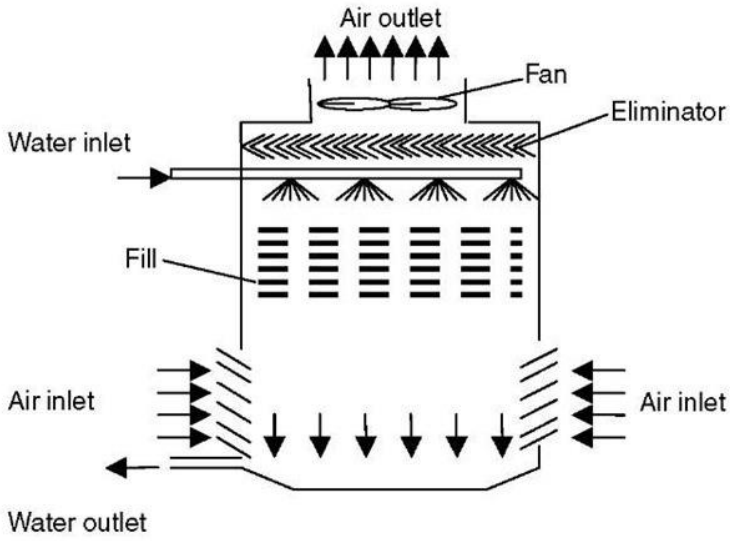

Figure 1.4: Counter-flow humidifier [12]

Water vapor in air can be treated as an ideal gas below the saturation pressure at 50^{o}C (i.e. below 12.3 KPa) and such approximation does not affect the accuracy of the result very much but with negligible error of less than 0.2%. Therefore, water vapor in air obeys the ideal gas relation *Pv=RT* and as a result the atmospheric air which is a mixture of dry air and water vapor can be treated as ideal gas too and the total pressure of it is the sum of the partial pressure of dry air P_a and that of water vapor P_v[13]:

$$P = P_a + P_v \tag{1.2}$$

Humidity ratio can also be expressed in terms of total pressure and partial pressure of water vapor as follows:

$$\omega = \frac{0.622\ P_v}{P - P_v} \tag{1.3}$$

The other way of defining the water vapor content in the air is the relative humidity, which relates the amount of water vapor the air holds (m_v) and the maximum amount of water vapor the air can hold at the same temperature (m_g):

$$\emptyset = \frac{m_v}{m_g} \tag{1.4}$$

This relation can also be expressed in other form as follows:

$$\omega = \frac{0.622\ \emptyset P_g}{P - \emptyset P_g} \tag{1.5}$$

It is obvious from the previous relations that the relative humidity of air changes with temperature even if the humidity ratio remains constant. And because the

water vapor in air changes as the temperature changes and the dry air remains constant, the total enthalpy of air mixture is expressed per unit mass of dry air and can be evaluated as sum of the enthalpies of dry air and water vapor:

$$H = H_a + H_v = m_a h_a + m_v h_v \quad (1.6)$$

Divide by m_a gives:

$$h = h_a + \omega h_v \quad (1.7)$$

Or,

$$h = h_a + \omega h_g \quad (1.8)$$

Without going into the details of various forms of heating and humidification of air, the process shown in figure 1.5 is one of heating and humidification processes applied to air.

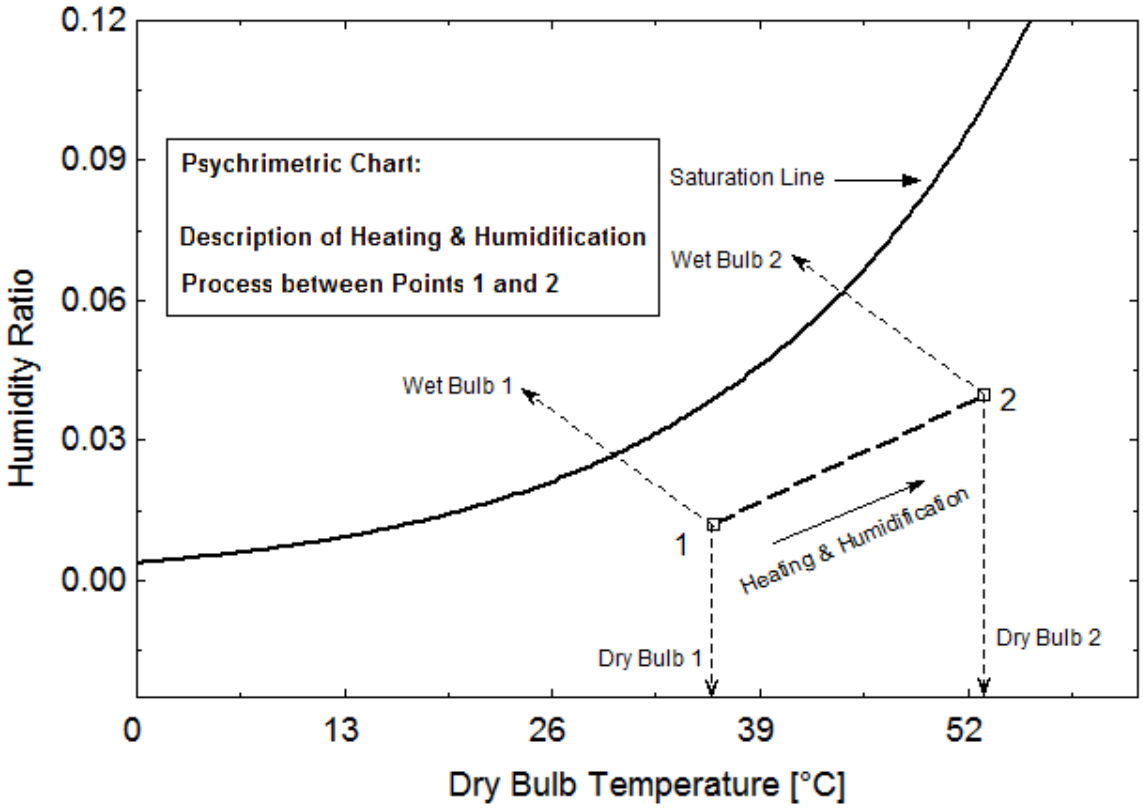

Figure 1.5 Representation of heating and humidification process in the Psychrometric chart

The air in such process is heated while it is humidified and this happens when the sprayed water is hot and it would be the case for all work presented in current study. The humidifier works in almost the same way as the cooling tower but the goal for humidifier is to humidify and cool or heat the air while the cooling tower objective is to cool the process water; therefore, the analysis of both systems is nearly alike.

1.3.2 Types of humidifiers

There are different types of humidifiers and they are categorized according to the method used to move the air stream though the system, that is, mechanical or natural draft, and based on the configuration of the air and water flows through the packing material inside the humidifier, that is, cross and counter flow. The mechanical draft systems can either be forced or induced draft. The forced draft type is shown in figure 1.6; the fan in such type is located at the inlet of the humidifier where the air stream enters the system and hence forcing it through column of the humidifier. The induced type as already shown in figure 1.4, has its fan located at the exit of the humidifier [14].

In the natural draft type, as shown in figure 1.7, the air is not forced by a fan or blower to flow inside the humidifier, instead, the difference in density between the heated humid air inside the humidifier and the cold denser ambient air outside the humidifier is what makes the air flows from the bottom of the humidifier and exit at the top of it.

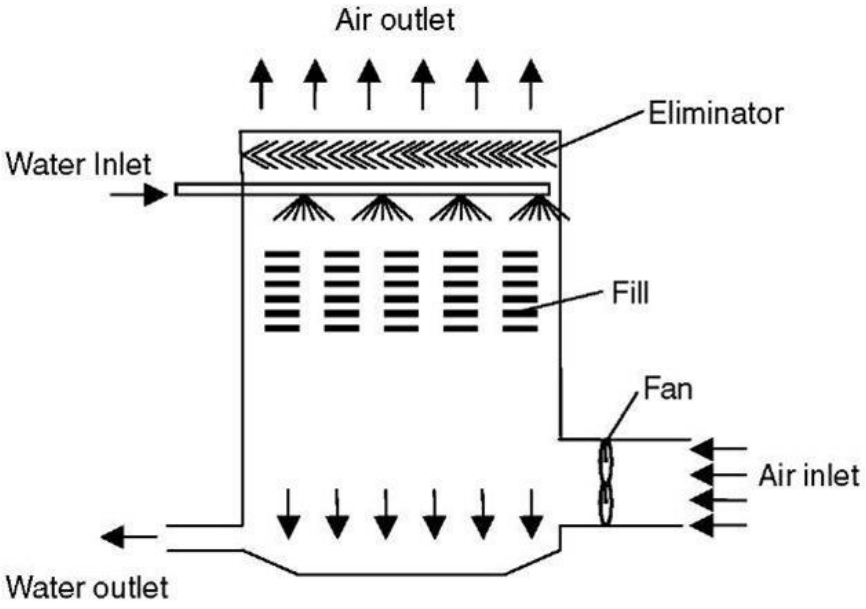

Figure 1.6 Forced draft counter-flow humidifier [12]

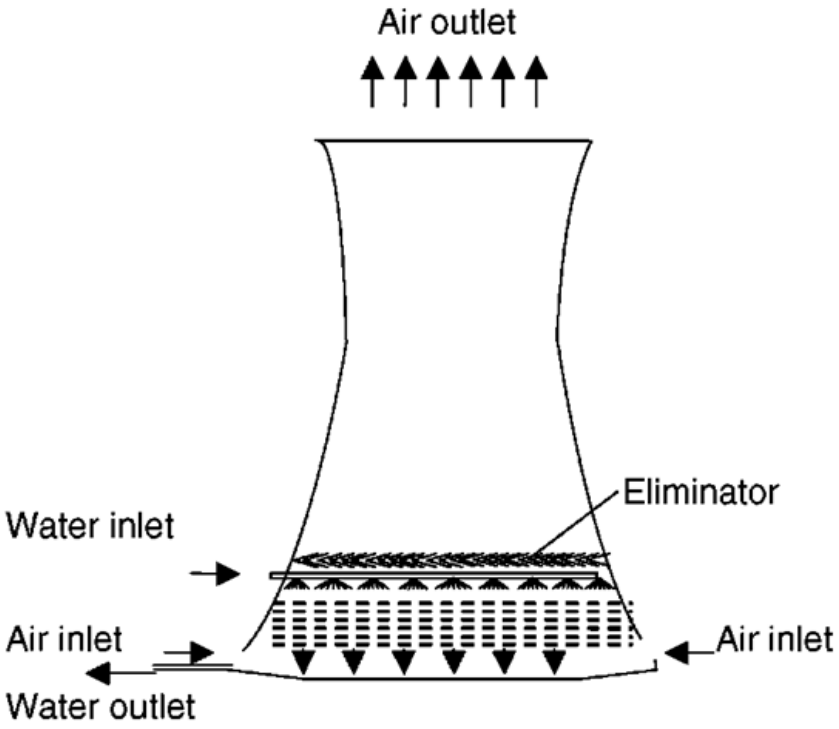

Figure 1.7 Natural draft humidifier or cooling tower [12]

In both mechanical and natural draft humidifier, the configuration of the flow of air and water (cross and counter flow) is encountered. In the counter flow arrangement, the air stream flows in the opposite direction of sprayed water as in figure 1.4, whereas in the cross flow arrangement the air and water stream flow in perpendicular direction to each other as shown in figure 1.8.

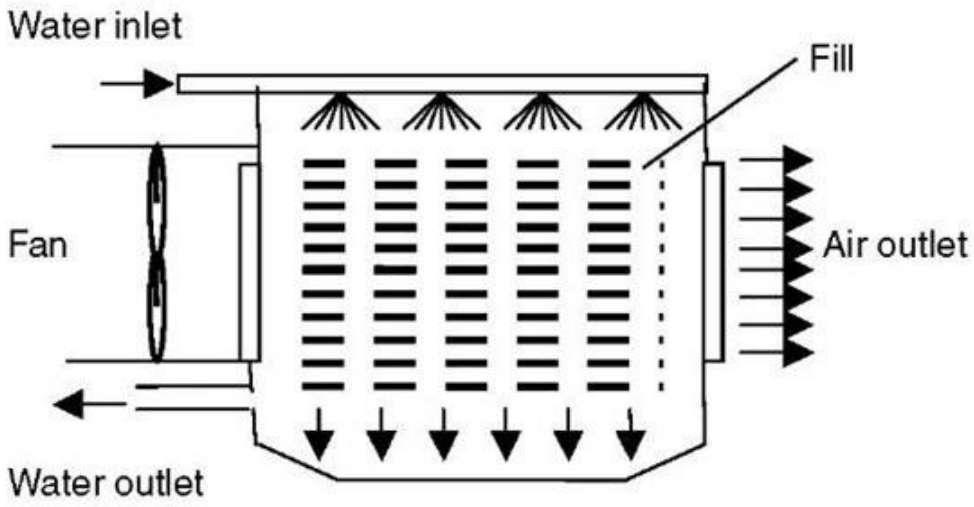

Figure 1.8 Cross flow humidifier [12]

CHAPTER 2

LITERATURE REVIEW AND OBJECTIVES

2.1 CURRENT STATUS OF HUMIDIFIER APPLICATIONS IN HDH SYSTEMS

For air humidification processes, many devices such as spray towers, packed-bed towers, bubble columns and wetted wall towers are used in HDH systems since their principles of operation are the same. In spray towers the water stream travels downward and scatters into droplets and at the same time the air stream travels upwards and mixes with water droplets. Due to existence of spray nozzles, there exists a drop on the water side whereas the pressure drop on the air side is low. Moreover, one of the disadvantages of a spray tower is its low efficiency [15, 16].

Younis [17] and Ben-Amara [18] used spray towers in HDH system as humidifiers and they concluded that there is an optimum value of the water flow rate which in turn results in highest air humidity at the outlet of humidifier.

In bubble columns the air bubbles are introduced in a vessel full of water and the water diffuses into the air inside the bubbles making the outlet air humid. El-Agouz and Abagderah [19] tested a bubble column experimentally by using seawater and they concluded that the system efficiency depends on the temperature of the seawater and velocity of air.

Muller-Holst [20] and Orfi [21] used wetted-wall towers as humidifiers in HDH systems and investigated the system efficiency; they found out that the humidification process obtained a humidity of 100%.

In packed bed towers, a fill material is used within the humidifier and there different types of fills such as film fill, see figure 2.1, trickle fill, splash fill, honeycomb…etc. These packing materials are designed in a way to force the air and water streams to take complex paths through their corrugated surfaces and therefore both streams have longer contact or higher surface area and consequently heat and mass transfer are enhanced. As indicated by Wallis and Aull [22] there have been improvements in the type of packing materials for the past years.

Film fills are the most used packing materials due to some features such as high thermal performance and low pressure drop. Many researchers used different types of packing materials in the humidifiers of HDH system and detailed review of the results can be found in [10].

Most tested HDH systems were using counter flow configuration and to the best of author's knowledge cross flow humidifier has not been incorporated in HDH system for testing before whereas there are many works on cross flow configuration in the studies of air conditioning systems and other applications. Sumathy [23] has investigated theoretically the performance of cross flow direct evaporative cooler using honeycomb paper as packing material and concluded that it can be used as humidifier in arid region.

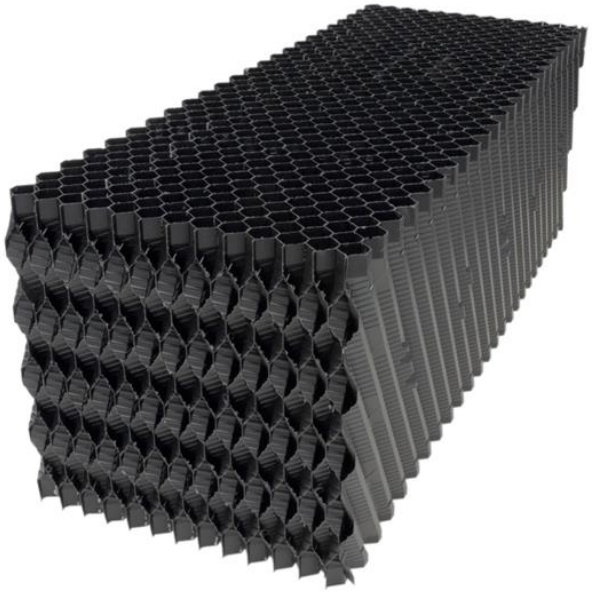

Figure 2.1Film fill [13]

2.2 CURRENT STATUS OF THE PERFORMANCE ANALYSIS OF HUMIDIFIERS AND COOLING TOWERS

Merkel, during 1920s [24] developed a method that depends on critical assumptions to make the solution of the governing equations for heat and mass transfer in the fill of a counter-flow cooling tower simple and because of his assumptions, Merkel method may not accurately represent the physics of the heat and mass transfer process in the cooling tower.

In 1970s Poppe and Rogener [25] developed a method that is not making the simplifying assumptions of Merkel method and the test results had shown a good agreement with the formulations results and values obtained for evaporated water flow rate.

Jabber and Webb [26] developed necessary equations to apply in the e-NTU method directly to counter-flow or cross-flow cooling towers. They used the same simplifying assumptions employed by Merkel to apply the e-NTU method.

Klopper and Kroger [27] represented a detailed derivation of the heat and mass transfer equations of evaporative cooling in counter flow wet-cooling towers and did a comparison study between Merkel, Poppe and e-NTU methods for counter-flow cooling towers. In [28] they studied the differences between numerical results of the three methods when applied to a cross-flow cooling tower. Detailed review of these three methods will be discussed in the next chapter.

In [29], Hajidavallo et. al. studied the effect of wet bulb temperature on the performance of a cross flow cooling tower at constant dry bulb temperature. They

used a splash fill type and employed the Merkel method to compare the numerical results of incoming air flow with the test results. They found that increasing the wet bulb temperature will increase the water outlet temperature as well as decrease the evaporation rate.

In [30] the authors studied the effect of changing the mass flow rate ratio in direct evaporative cooler by varying the air flow rate and they concluded that as the air speed is increased the system effectiveness decreases. The effectiveness defined in the study included only the temperature changes in the system. They compared the experimental results with the mathematical model of the evaporative cooler.

In the previous section, theoretical study on a cross flow direct evaporative cooler by Sumathy [23] has been reported. He showed that the system can reduce the air temperature by 9^{o}C and increase the humidity ratio by about 50%. In his work, the analysis was limited to cooling the air only without further investigation in heating and humidifying the air.

In [31] an experimental study was for different packed bed types for counter flow cooling tower. And he investigated the influence of mass flow rate ratio on the performance of the fills through its transfer characteristic, the Merkel number. He tested the system using charcoal, lauffa and bamboo fills and found out that lauffa fill performed the best among other fills and consumed less power than charcoal and bamboo fills.

Reuter [32] developed a model of heat and mass transfer in a cross-counter flow fill in a rectangular wet cooling tower for unsaturated and supersaturated air. Then, Yngvi [33] investigated Reuter model by comparing it with Merkel, e-NTU and

Poppe models numerically and presented some experimental results for cross and counter flow cooling towers using trickle fill. Numerically he showed that increasing the air mass flux from 1 to 4 kg/s.m^2 in a cross flow cooling tower increases the Merkel number per tower height from 0.5 to 0.8 m^{-1} and such results was done for fixed water mass flux of 3 kg/s.m^2 and at a water inlet temperature of 40^{o}C. The experimental results presented in the study involved only the effect of air-water mass flow rate ratio in the Merkel number.

2.3 PERFORMANCE EVALUATION OF HUMIDIFIERS AND COOLING TOWERS BY SECOND LAW OF THERMODYNAMICS

Some researchers have investigated the performance of cross and counter flow evaporative coolers by using the second law analysis. Bejan [34] has provided a general definition of the second law efficiency pertinent to humidification process which relates the total exergy leaving to the total exergy entering the humidifier.

Wepfer [35] provided a formula for total flow exergy of humid air per kilogram of dry air if the dry air and water vapor are considered ideal gases.

Prakash et. al [36] studied the entropy generation in simultaneous heat and mass transfer systems and defined a new parameter, the modified heat capacity rate ratio. Their study concluded that for a combined heat and mass exchange device, the entropy generation is minimized when the modified heat capacity rate ratio equals one irrespective of the value of other independent parameters. They showed theoretically how the entropy generation is minimized in a system of counter flow wet cooling tower.

Et. al [37] investigated the effect of entropy generation on the performance of humidification-dehumidification desalination cycles. In detailed analysis of each system component it has been shown that the entropy generation in the counter flow humidifier decreases as the mass flow rate ratio increases (up to values of heat capacity ratio greater than one), and they pointed out that the maximum gained output ratio of the HDH system does not occur at a point where all of the components have minimum entropy generation but rather where the total specific entropy generation of the whole system is minimum. The latter point is worth to be mentioned since current thesis study is concerned with the performance evaluation of a cross flow humidifier for its use in HDH desalination system.

Zubair and Qureshi [38] conducted a parametric study on a counter flow wet cooling tower using first and second laws of thermodynamics to determine the variation of second law efficiency as well as exergy destruction for various input parameters. The study shows that for different mass flow ratios, as the inlet wet bulb temperature of air increases the second law efficiency increases and such increase is associated with a decrease in the exergy destruction, at constant water inlet temperature. On the other hand, at constant inlet wet bulb temperature, the exergy destruction increases and the second law efficiency decreases as the water inlet temperature increases.

Muangnoi [39] developed a mathematical model based on heat and mass transfer principles to investigate exergy and exergy destruction of air and water through the fill material of counter flow cooling towers. It is concluded in the study that the water exergy decreases continually from the top of the fill to the bottom. For the air

side, the exergy of air by convective heat transfer initially drops at the inlet then it slightly recovers before leaving the cooling tower. Moreover, the exergy of air by evaporative heat transfer decrease from the inlet to the outlet of the cooling tower fill. In general the results show that the amount of exergy supplied by water is larger than that absorbed by air because the system produces entropy and therefore the lowest exergy destruction is located at the top of the fill.

Chengqinet. al [40] evaluated the performance of four different evaporative cooling configurations by using the principles of exergy analysis and included: direct, indirect, direct-indirect and regenerative evaporative cooling. Results showed that regenerative evaporative cooling has the best performance and the effectiveness for indirect evaporative cooling heat exchanger has great importance in performing the exergy efficiency ratio of regenerative scheme.

2.4 OBJECTIVES

In light of the previous sections, it can be concluded that there have been a lot of theoretical and experimental works in counter-flow and cross-flow cooling towers devoted to analyze the systems for evaporative cooling and other air conditioning and industrial applications. In other words, to the best of author's knowledge there has been no study dedicated to analyze cross-flow humidifiers for its application in humidification-dehumidification desalination systems as well as limited studies based on the second law analysis of cross-flow humidifier. This means a study to find the best conditions at which the humidifier will operate when it is incorporated or integrated with dehumidifier to form a complete HDH desalination system and this requires testing the cross-flow humidifier before its integration with HDH system.

Hence, an optimization study and performance evaluation is proposed to be done on a cross-flow humidifier by help of the methods of analysis stated in section 2.2 (Merkel, Poppe and e-NTU methods) and the study is performed through an experimental work in which different operating conditions or input parameters will be applied and varied, and they are going to be as follows:

1. Mass flow rate ratio m_w/m_a: the effect of varying the flow rate ratio on the air and water outlet conditions.
2. Temperature of the inlet water: how the system effectiveness is going to be when the water inlet temperature is varied at different flow rate ratios.

3. Length of the film fill: the influence of the surface are on the humidification process at different water inlet temperature and different flow rate ratios.

It is also proposed to evaluate the entropy generation or exergy destruction and second law efficiency associated with each of the above conditions in order to monitor the losses and obtain the points with least irreversibility.

Therefore, energy and exergy analysis will be discussed in the next chapter and experimental results will be later presented accordingly.

CHAPTER 3

GOVERNING EQUATIONS

As already introduced in chapter one, the process of heating or cooling and humidification in a humidifier is a combination of heat and mass transfer between air and water streams, therefore, the water stream will lose some of its mass due to evaporation and this amount will be absorbed by the air. Such process can be formulated using the first law of thermodynamics by considering the mass and energy balance over the control volume of the humidifier as shown in figure 3.1. So, the mass transfer rate is a function of the humidity ratio difference between inlet and outlet and the mass balance can be written as follows:

$$\dot{m}_{wi} = \dot{m}_a(\omega_o - \omega_i) + \dot{m}_{wo} \tag{3.1}$$

And the energy balance can be written as follows:

$$\sum E_{in} = \sum E_{out} \tag{3.2}$$

Or,

$$\dot{m}_a(h_{ao} - h_{ai}) = \dot{m}_{wi}h_{wi} - \dot{m}_{wo}h_{wo} \tag{3.3}$$

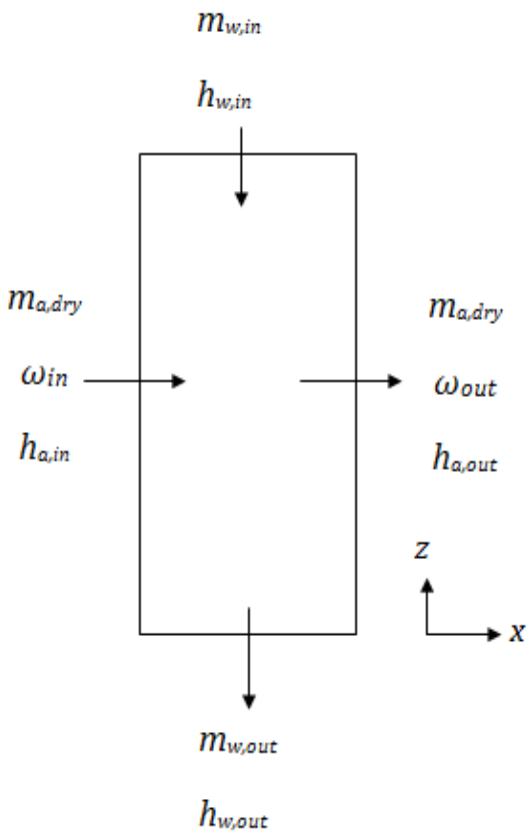

Figure 3.1 Mass and energy balance on cross-flow humidifier

From the energy balance equation, two main effectiveness definitions are introduced for the cross flow humidifier.

The first one relates the actual water change of enthalpy rate between the inlet and outlet to the maximum possible change of water enthalpy rate, and for the case of heating and humidification it can be expressed as follows:

$$\epsilon_w = \frac{\dot{m}_{wi} h_{wi} - \dot{m}_{wo} h_{wo}}{\dot{m}_{wi} h_{wi} - \dot{m}_{wo} h_{w,ideal}} \cong \frac{h_{wi} - h_{wo}}{h_{wi} - h_{ideal}} \quad (3.4)$$

Where, $h_{w,ideal}$ is the enthalpy of water at the inlet air wet bulb temperature; that is, the lowest temperature in the system.

Moreover, the second effectiveness definition that takes care of the energy transfer in the air side is relating the actual change of enthalpy rate for air-water vapor mixture between the inlet and outlet to the maximum possible change of enthalpy rate of air, and for the case of heating and humidification it can be expressed as follows:

$$\epsilon_a = \frac{\dot{m}_a (h_{ao} - h_{ai})}{\dot{m}_a (h_{a,ideal} - h_{ai})} \cong \frac{h_{ao} - h_{ai}}{h_{ideal} - h_{ai}} \quad (3.5)$$

Where, h_{ideal} is the enthalpy of air-water vapor mixture at the water inlet temperature and relative humidity equals one; that is, the highest temperature in the system.

Heat capacity rates of air and water steams in simultaneous heat and mass processes can be related through modified heat capacity ratio HCR which is introduced and defined in [36]. It relates the ratio of the maximum possible change

in total enthalpy rate of the cold stream to the maximum possible change in total enthalpy rate of the hot stream and can be expressed as follows:

$$HCR = \frac{\Delta H_{max,c}}{\Delta H_{max,h}} \tag{3.6}$$

Where,

$$\Delta H_{max,c} = \dot{m}_c\left(h_{c,ideal} - h_{ci}\right) \tag{3.7}$$

And,

$$\Delta H_{max,h} = \dot{m}_{hi}h_{hi} - \dot{m}_{ho}h_{h,ideal} \tag{3.8}$$

For heating and humidification process, the cold stream will be the air and the hot stream is the water.In such processes the water heat capacity rate is influenced significantly by the water flow rate and water temperature but the heat capacity rate of air is influenced by the air flow rate and the amount of water-vapaor absorbed into the air. Therefore, their ratio can only be recognized through the change of enthalpy rates. In general, modified heat capacity ratio is a function of mass flow rates, water temperature, and surface area for heat and mass process. Moreover, if the total losses in the humidifier are negligiable and the value of HCR equals one, it mean that the air stream is totally absorbing the energy transferred by water stream as it will be seen later in the analysis.

Heat capacity ratio is considered one of the good used tools in the current study since it provides a better insight into the system performance by pointing at the best conditions at which the humidifier processes will operate.

There are different methods for analysing the transfer characteritics in humidifiers and they are based on the analysis of the first law of thermodynamics. In the following sections three methods will be discussed in details for evaluating Merkel number.

3.1 POPPE METHOD

Since the difference between the cross-flow and counter-flow humidifiers is the direction through which the air and water flows and mixes together, Klopper and Kroger [27] procedure of deriving the governing equations for counter-flow configuration will be followed for deriving the governing equations for cross-flow humidifier. It is worth mentioning before starting the derivation that the rate at which the air enthalpy changes and water temperature changes while travelling through the fill in the cross-flow configuration is of course different than that of the counter-flow, but proceeding with deriving the final expression of Merkel number will end up with the same form for both cases. This conclusion of identical forms of Merkel number does not necessarily mean they will obtain the same values for the same water inlet temperature, but indeed the flow configuration through the fill is what governs the air capacity to absorb heat and mass from the hot water stream, and consequently the rate at which the water temperature changes in the direction of water flow for both cross-flow and counter-flow are different. Moreover, such rate of change for water temperature is one of the dependent variables by which Merkel number will change.

Klopper and Kronger [28] derived the governing equations for the cross-flow cooling tower and showed the rate of temperature change in the flow direction as well as the rate of air enthalpy change in the direction of air flow but final expression of Merkel number was not stated in the derivation. The equations will be used in the next section for Merkel method for the purpose of only making such approach clear even though they can be used in the derivation of governing equations in this section.

Consider the Control volume in figure 3.2 where the air is flowing in the x-direction and the water stream is flowing downward. As already explained; fractions of water mass will be evaporated from the water stream and absorbed into the air stream.

The mass balacnce for the control volume of the fill in figure 3.2 gives:

$$dm_w = m_a d\omega \tag{3.9}$$

The energy balance for the same control volume by using equation 3.2 is as follows:

$$(m_w + dm_w)[h_w + dh_w] + m_a h_{ma} - m_w h_w - m_a(h_{ma} + dh_{ma}) = 0 \tag{3.10}$$

Where, h_{ma} is the air-vapor mixture enthalpy.Expanding the terms in equation 3.10 yields:

$$m_w h_w + m_w dh_w + dm_w h_w + dm_w dh_w + m_a h_{ma} - m_w h_w - m_a h_{ma} - m_a dh_{ma} = 0 \tag{3.11}$$

Neglecting the second order term gives:

$$m_w dh_w + dm_w h_w - m_a dh_{ma} = 0 \tag{3.12}$$

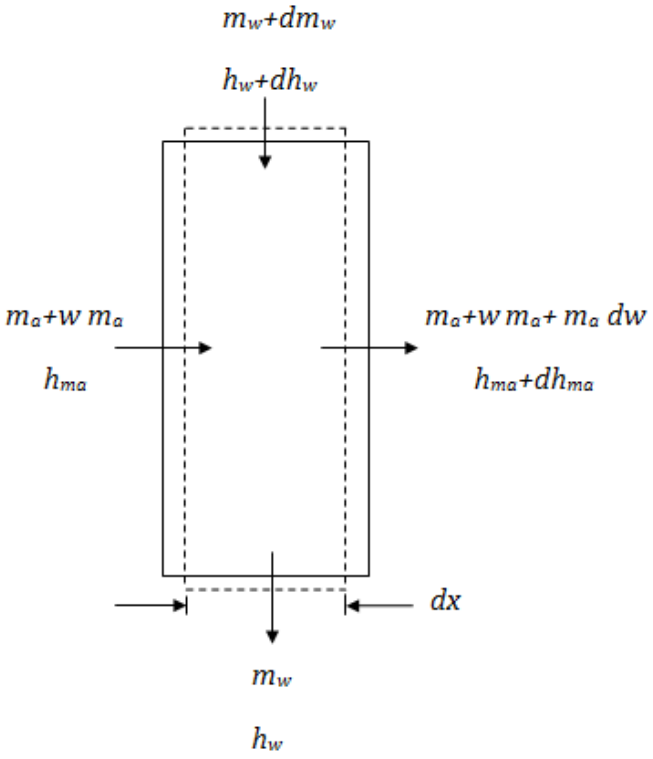

Figure 3.2 Control volume over cross-flow packed bed

Substituting equation (3.9) intoequation (3.12) gives:

$$m_w c_{pw} dT_w + m_a c_{pw} T_w d\omega - m_a dh_{ma} = 0 \tag{3.13}$$

Or,

$$dT_w = \frac{m_a}{m_w}\left[\frac{dh_{ma}}{c_{pw}} - T_w d\omega\right] \tag{3.14}$$

Further rearrangment yields:

$$\frac{d\omega}{dT_w} = \frac{1}{c_{pw} T_w}\frac{dh_{ma}}{dT_w} - \frac{1}{T_w}\frac{m_w}{m_a} \tag{3.15}$$

Or,

$$\frac{d\omega}{dT_w} = \frac{dh_{ma}}{T_w dh_w} - \frac{1}{T_w}\frac{m_w}{m_a} \tag{3.16}$$

At the interface between the water and the air, there is an enthalpy transfer associated with mass transfer due to the difference in vapor concentration between the mean stream of the air and the saturated air, as well as an enthalpy transfer associated with the heat transfer caused by the temperature difference between the air stream and water [27]. Therefore,

$$dQ = dQ_m + dQ_c \tag{3.17}$$

Where, dQ_m is the enthaply transfer assocaited mass transfer and dQ_c is the enthalpy transfer associated with heat transfer.

The amount of mass transfered at the interface between the two streams can be expressed as follows:

$$dm_w = h_d(\omega_{sw} - \omega)dA \quad (3.18)$$

Where, $\omega_{sw}$is the saturation humidity ratio of air evaluated at the local bulk water temperature, T_w , h_d is the mass transfer coefficient, kg/m^2 s and dA is the transfer area for a section dx in the fill and is expressed as follows:

$$dA = a_{fi}A_{fr}dx \quad (3.19)$$

Where,a_{fi} is the wetted area divided by the volume of the fill or area density, m^{-1} and A_{fr} is the frontal area or face area.

Therefore, the enthalpy associated with mass transfer is the product of the amount of mass transferred and the enthalpy of the water vapor h_v at the bulk water temperature T_w, and can be written as follows:

$$dQ_m = dm_w h_v = h_v h_d(\omega_{sw} - \omega)dA \quad (3.20)$$

h_v is given by:

$$h_v = h_{fgwo} + c_{pv}T_w \quad (3.21)$$

Where, h_{fgwo} is the latent heat of water at the reference temperature or at T=273.15 K. And c_{pv} is the specific heat of saturated water vapor, J/kg. K.

For the convective heat transfer dQ_c, it can be expressed as follows:

$$dQ_c = h_c(T_w - T_a)dA \quad (3.22)$$

Where h_c is the heat transfer coefficient, W/m^2 K.

The total enthalpy transfer can then be written as follows:

$$dQ = [h_c(T_w - T_a) + h_v h_d(\omega_{sw} - \omega)]dA \quad (3.23)$$

Further arrangement to equation (3.23) can be made by replacing the temperature difference with the air enthalpy differential.

The enthalpy of saturated air evaluated at the local bulk water temperature is given by:

$$h_{masw} = c_{pa}T_w + \omega_{sw}(h_{fgwo} + c_{pv}T_w) \quad (3.24)$$

And the enthalpy of the air-water vapor mixture per unit mass of dry air can be expressed as follows:

$$h_{ma} = c_{pa}T_a + \omega(h_{fgwo} + c_{pv}T_a) \quad (3.25)$$

Therfore, from equations (3.24) and (3.25):

$$h_{masw} - h_{ma} = c_{pa}T_w + \omega_{sw}(h_{fgwo} + c_{pv}T_w) - c_{pa}T_a - \omega(h_{fgwo} + c_{pv}T_a) \quad (3.26)$$

Substituting equation (3.21) into equation (3.26) gives:

$$h_{masw} - h_{ma} = (c_{pa} - \omega c_{pv})T_w - (c_{pa} - \omega c_{pv})T_a + (\omega_{sw} - \omega)h_v \quad (3.27)$$

Where,

$$(c_{pa} - \omega c_{pv}) = c_{pma} \quad (3.28)$$

Equation (3.27) can also be arranged and written as follows:

$$h_{masw} - h_{ma} = c_{pma}T_w - c_{pma}T_a + (\omega_{sw} - \omega)h_v \quad (3.29)$$

Or,

$$T_w - T_a = \frac{(h_{masw} - h_{ma}) - (\omega_{sw} - \omega)h_v}{c_{pma}} \tag{3.30}$$

Now, subtituting equation (3.30) into equation (3.23) gives:

$$dQ = \left[\left(\frac{h_c}{c_{pma}}\right)[(h_{masw} - h_{ma}) - (\omega_{sw} - \omega)h_v] + h_v h_d(\omega_{sw} - \omega)\right] dA \tag{3.31}$$

Or,

$$dQ = h_d\{(h_c/h_d\, c_{pma})(h_{masw} - h_{ma}) + (1 - (h_c/h_d\, c_{pma})h_v(\omega_{sw} - \omega)\}dA \tag{3.32}$$

The term $h_c/h_d C_{pma}$ is know as the Lewis factor Le_f and it is an indication of the relative rates of heat and mass transfer in an evaporative process. Bosnjakovic [41] developed an empirical relation for the Lewis factor for air-water vapor systems for unsaturated and saturated air. The relation developed for unsaturated air is given by:

$$Le_f = 0.865^{0.667} \frac{\left[\frac{\omega_{sw}+0.622}{\omega+0.622} - 1\right]}{\ln\left[\frac{\omega_{sw}+0.622}{\omega+0.622}\right]} \tag{3.33}$$

Equation (3.32) can be used to find the enthalpy transfer to the air stream:

$$dQ = m_a dh_{ma} \tag{3.34}$$

Or,

$$dh_{ma} = dQ/m_a$$

$$= \frac{h_d dA}{m_a}\{(h_c/h_d\, c_{pma})(h_{masw} - h_{ma}) + \big(1 - (h_c/h_d\, c_{pma}\big)h_v(\omega_{sw} - \omega)\} \quad (3.35)$$

Or,

$$dh_{ma} = \frac{h_d dA}{m_a}[Le_f(h_{masw} - h_{ma}) + (1 - Le_f)h_v(\omega_{sw} - \omega)] \quad (3.36)$$

Substituting equation (3.18) and equation (3.36) into equation (3.12) yields:

$$m_w dh_w =$$

$$h_d dA[Le_f(h_{masw} - h_{ma}) + (1 - Le_f)h_v(\omega_{sw} - \omega)] - h_d c_{pw} T_w(\omega_{sw} - \omega)dA \quad (3.37)$$

Or,

$$m_w dh_w =$$

$$h_d dA\big[h_{masw} - h_{ma} + (Le_f - 1)\{h_{masw} - h_{ma} - h_v(\omega_{sw} - \omega)\} - c_{pw} T_w(\omega_{sw} - \omega)\big] \quad (3.38)$$

Now, substiting equation (3.36) and equation (3.38) into equation (3.16) will give the ratio of the differential change of humidity ratio to the change in water temperature:

$$\frac{d\omega}{dT_w} = \frac{\frac{m_w}{m_a} c_{pw}(\omega_{sw} - \omega)}{h_{masw} - h_{ma} + (Le_f - 1)\{h_{masw} - h_{ma} - h_v(\omega_{sw} - \omega)\} - c_{pw} T_w(\omega_{sw} - \omega)} \quad (3.39)$$

The change of enthalpy for air stream to the change of water temperature can also be obtained from the same equations utilizing equation (3.16), therefore,

$$\frac{dh_{ma}}{dT_w} = \frac{m_w}{m_a} c_{pw}$$

$$\left[1 + \frac{c_{pw} T_w (\omega_{sw} - \omega)}{h_{masw} - h_{ma} + (Le_f - 1)\{h_{masw} - h_{ma} - h_v(\omega_{sw} - \omega)\} - c_{pw} T_w (\omega_{sw} - \omega)}\right] \quad (3.40)$$

From equation (3.9) and equation (3.18):

$$m_a dw = h_d (\omega_{sw} - \omega) dA \quad (3.41)$$

Rearranging the terms, gives:

$$\frac{h_d dA}{m_a} = \frac{d\omega}{(\omega_{sw} - \omega)} \quad (3.42)$$

Dividing both sides by m_w and introducing dT_w/dT_w to the right hand side and intergrate:

$$\int \frac{h_d}{m_w} dA = \int \frac{m_a}{m_w} \frac{d\omega/dT_w}{\omega_{sw} - \omega} dT_w \quad (3.43)$$

Upon integration of equation (3.43), it becomes:

$$\frac{h_d A}{m_w} = \int \frac{m_a}{m_w} \frac{d\omega/dT_w}{\omega_{sw} - \omega} dT_w \quad (3.44)$$

According to the Poppe method, equation (3.44) is defined as the Merkel number, or:

$$Me_p = \frac{h_d A}{m_w} = \int \frac{m_a}{m_w} \frac{d\omega/dT_w}{\omega_{sw} - \omega} dT_w \quad (3.45)$$

If equation (3.39) is substituted into equation (3.45), then following differential form for Merkel number with respect to water temperature is obtained:

$$\frac{Me_p}{dT_w} = \frac{c_{pw}}{h_{masw} - h_{ma} + (Le_f - 1)\{h_{masw} - h_{ma} - h_v(\omega_{sw} - \omega)\} - c_{pw}T_w(\omega_{sw} - \omega)} \quad (3.46)$$

Because the mass transfer coefficient and the specific area of the fill always contained in Merkel number, it is thereby not necessary to calculate each one of them independently. Merkel number is obtained as per equation (3.46) for Poppe method by using the integration technique of Chebychev method which is based on four points of calculation intervals then the integral in equation (3.46) can be approximated accordingly. The intervals across the temperature difference can be taken at the points 10, 40, 60 and 90% from the water outlet temperature; therefore, the integral can be approximated as follows [33]:

$$Me_P \approx \frac{c_{pw}(T_{wi} - T_{wo})}{4}\left[\frac{1}{Y_{0.1}} + \frac{1}{Y_{0.4}} + \frac{1}{Y_{0.6}} + \frac{1}{Y_{0.9}}\right] \quad (3.47)$$

Where,

$$Y_{0.1} = \Delta h_{0.1} + (Le_{f0.1} - 1)\{\Delta h_{0.1} - h_{v0.1}\Delta\omega_{0.1}\} - c_{pw}T_{w,0.1}\Delta\omega_{0.1} \quad (3.48)$$

$$\Delta h_{0.1} = \left(h_{masw,0.1} - dh_{0.1} + h_{a,i}\right) \quad (3.49)$$

$$\Delta\omega_{0.1} = \omega_{sw,0.1} - \omega_{0.1} \quad (3.50)$$

$$h_{masw,0.1} = c_{pa}T_{w,0.1} + \omega_{sw}\left(h_{fgwo} + c_{pv}T_{w,0.1}\right) \quad (3.51)$$

And,

$$T_{w,0.1} = T_{ow} + 0.1\,(T_{iw} + T_{ow}) \tag{3.52}$$

In counter-flow configuration, implementation of Chebychev method is easier than cross-flow because it is a one dimensional model, that is, the distribution of water temperature and air-water vapor mixture enthalpy across the fill length is even, therefore, it is direct substitution in the Chebychev integration equations. On the other hand, the distribution of water temperature, humidity ratio of air, and enthalpy of air-water mixture are not even in the cross-flow as presented by Kloppers in [28]. Fig. 3.3 and 3.4 show how they are distributed according to the numerical solution of governing equations of cross-flow wet cooling towers.

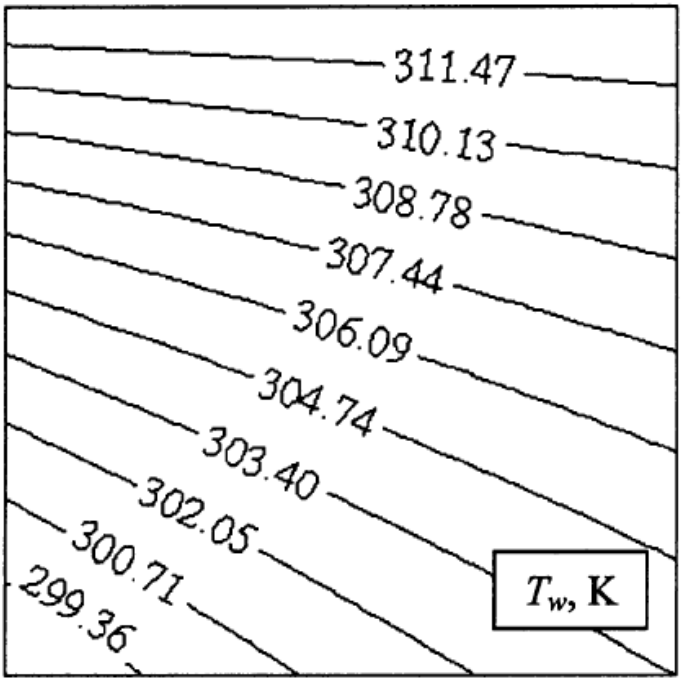

Figure 3.3 Distribution of water temperature across Film Fill height, T_{wi}=39.67°C, m_w/m_a=0.967, T_{ai}=9.7°C, T_{wb}=8.23°C [28]

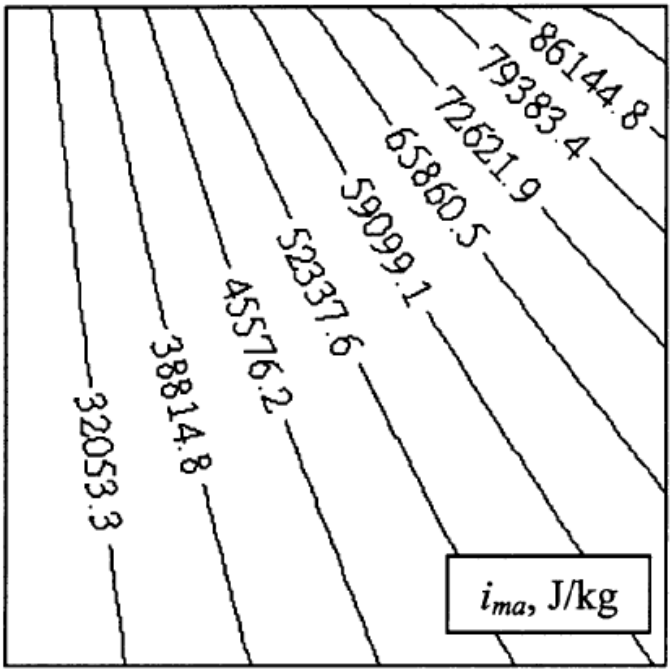

Figure 3.4 Distribution of air enthalpy across Film Fill length, , T_{wi}=39.67°C, m_w/m_a=0.967, T_{ai}=9.7°C, T_{wb}=8.23°C [28]

It can be seen that the water temperature distribution from the top to the bottom of the fill changes with fill height till it takes a positive slope. Also, the distribution of air enthalpy across the fill length from left to right takes a positive slope. The air enthalpy cannot be evaluated unless the humidity ratio at each local bulk temperature is known. In order to simplify the procedure of solving a two-dimensional problem of a cross flow configuration, two assumptions are employed to approximate the value of Merkel number by Poppe Model and these assumptions are:

1. The water temperature distribution is constant across the fill length.
2. The value of Lewis factor in the fill is the average between Lewis factors of the inlet and outlet conditions.

Figure 3.5 represents the approximated distribution of water temperature within the humidifier fill, such that each group of nodes (1, i), (2,i), (3,i) and (4,i) has the same water temperature. Since Lewis factor is assumed the same at all nodes, then values of humidity ratios at each node can be obtained and in turn the enthalpy of air-water mixture can be evaluated by equation (3.16).

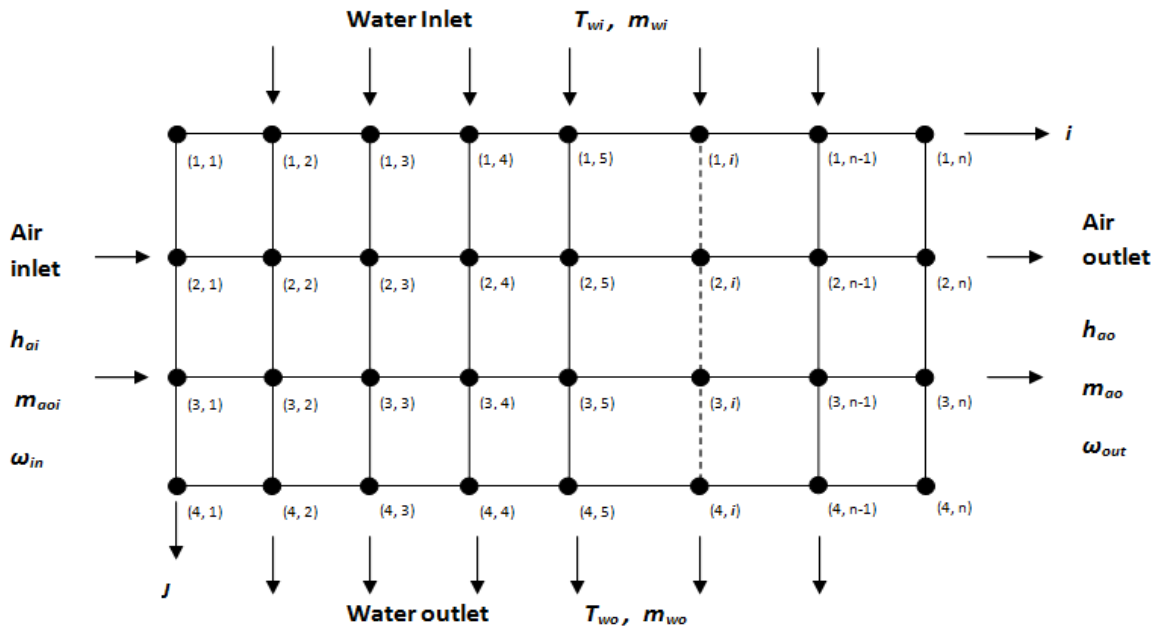

Figure 3.5 Grid for distribution of water temperature and air enthalpy across film Fill height and length

Based on these approximated distributions, Merkel number is calculated by Chebychev integration method at each divided height (i.e. first four nodes from (1, 1) up to (4, 1)), then Merkel number is calculated for the next group of nodes (i.e. from (1, 2) to (4, 2)). Eventually Merkel number can be calculated by summing all obtained values and divided by the number of intervals n, that is:

$$\mathrm{Me} = \frac{1}{n}\sum_{i=1}^{n}\sum_{j=1}^{4} \mathrm{Me}\,(j, i) \tag{3.53}$$

3.2 MERKEL METHOD

As previously stated in section 2.1, Klopper and Kroger [28] equations from first principle for cross flow cooling tower will be used and upon the derived equations in [28], expression for Merkel number will be shown.

Consider control volume in figure 3.6.

The governing equations for enthalpy change of air in the direction of air stream (x-direction in figure 3.6) and change of water temperature in the direction of water flow (z-direction in figure 3.6). The equations as per [28] are as follows:

$$\frac{dh_{ma}}{dx} = \frac{h_d a_{fi} dydz}{m_a}\{h_{masw} - h_{ma} + (Le_f - 1)\{h_{masw} - h_{ma} - h_v(\omega_{sw} - \omega)\}\} \quad (3.54)$$

And,

$$\frac{dT_w}{dz} = \frac{h_d a_{fi} dx\, dy}{c_{pw} m_w}$$

$$\{h_{masw} - h_{ma} + (Le_f - 1)\{h_{masw} - h_{ma} - h_v(\omega_{sw} - \omega)\} - c_{pw} T_w(\omega_{sw} - \omega)\} \quad (3.55)$$

Or,

$$c_{pw}\, dT_w = \frac{h_d a_{fi}\, dx\, dy\, dz}{m_w}$$

$$\{h_{masw} - h_{ma} + (Le_f - 1)\{h_{masw} - h_{ma} - h_v(\omega_{sw} - \omega)\} - c_{pw} T_w(\omega_{sw} - \omega)\} \quad (3.56)$$

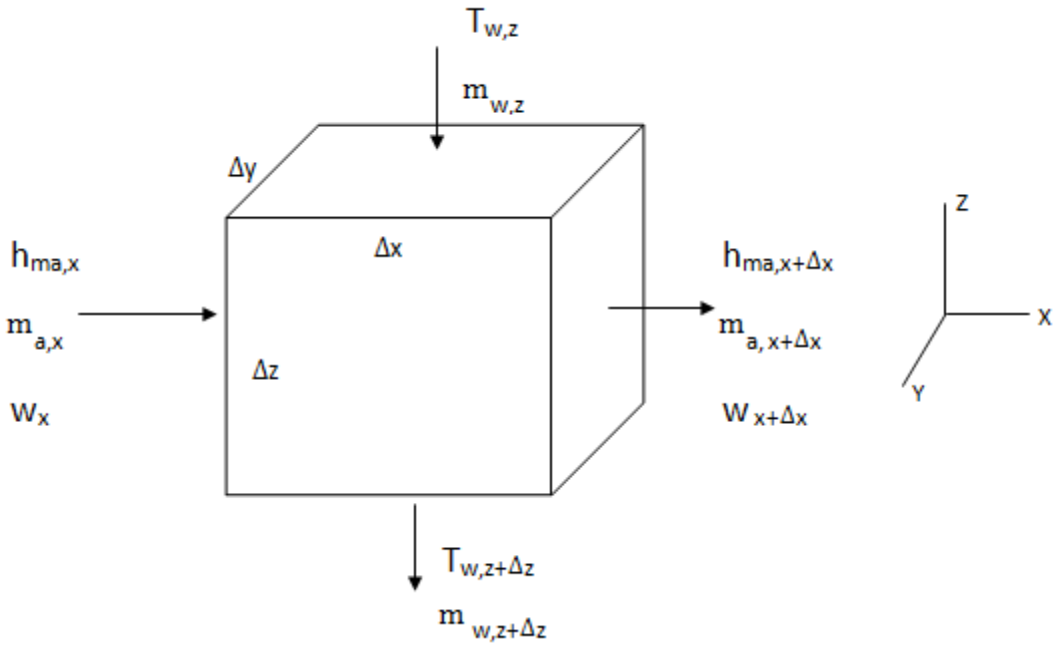

Figure 3.6 Control Volume over Cross-flow film fill

The term ($h_d\ a_{fi}\ dxdydz/m_w$) is nothing but Merkel number. If the equation is rearranged again, then it takes the form:

$$\frac{Me_p}{dT_w} = \frac{c_{pw}}{h_{masw} - h_{ma} + (Le_f - 1)\{h_{masw} - h_{ma} - h_v(\omega_{sw} - \omega)\} - c_{pw}T_w(\omega_{sw} - \omega)} \quad (3.57)$$

Which is identical to equation (3.46).

Merkel made some assumption to simplify the analysis of evaporative cooling process and these assumptions are [42]:

1. The lewis factor relating heat and mass transfer equals to 1.
2. In the energy balance the reduction of water flow rate due to evaporation is neglected.
3. The air exiting the cooling tower is saturated with water vapor and it is characterized only by its enthalpy.

When these assumptions are applied to equations (3.54) and (3.55), then they take the following forms:

$$\frac{dh_{ma}}{dx} = \frac{h_d a_{fi} dy\ dz}{m_a}\{h_{masw} - h_{ma}\} \quad (3.58)$$

And,

$$\frac{dT_w}{dz} = \frac{h_d a_{fi} dx\ dy}{c_{pw} m_w}\{h_{masw} - h_{ma}\} \quad (3.59)$$

The transfer area of the fill can easily be recognized from both equations and equation (3.59) can be put into the following form:

$$dT_w = \frac{h_d a_{fi} dz dx dy}{c_{pw} m_w} \{h_{masw} - h_{ma}\} \tag{3.60}$$

The Merkel number is therefore according to Merkel theory equals to:

$$Me_m = \frac{h_d a_{fi} V}{m_w} = \frac{h_d A}{m_w} = \int_{T_{wo}}^{T_{wi}} \frac{c_{pw} dT_w}{h_{masw} - h_{ma}} \tag{3.61}$$

The same procedure in section 3.1 is followed to evaluate Merkel number by Chebychev method of integration using equation (3.61). Since Merkel method ignores the reduction in water stream due to evaporation then there is no need to take Lewis factor into account for this method. Assuming that the water temperature values are evenly distributed across the fill lengthis enough to solve equation (3.61) because the enthalpy of air-water mixture can be evaluated directly from equation (3.16) by ignoring the change of humidity ratio. Based on Chebychev integration method, equation (3.61) becomes:

$$Me_m \approx \frac{c_{pw}(T_{iw} - T_{ow})}{4} \left[\frac{1}{\Delta h_{0.1}} + \frac{1}{\Delta h_{0.4}} + \frac{1}{\Delta h_{0.6}} + \frac{1}{\Delta h_{0.9}}\right] \tag{3.62}$$

Where,

$$\Delta h_{0.1} = \left(h_{masw,0.1} - dh_{0.1} + h_{a,i}\right) \tag{3.63}$$

The value of enthalpy change $dh_{0.1}$ can be evaluated the same way as explained in section 3.1 by knowing the sprayed water temperature and ignoring the change in humidity ratio.

3.3 EFFECTIVENESS-NTU METHOD

Jaber and Webb [26] developed the equations necessary to apply the heat exchanger Ɛ-NTU method for sensible heat transfer directly to counter-flow or cross-flow cooling towers.

The implementation of Ɛ-NTU method to evaporative air water systems is shown by Kroger [14] and the derivation for such heat and mass transfer is also explained. For evaporative air water processes, Jaber and Webb [26] showed that:

$$\frac{d(h_{masw} - h_{ma})}{(h_{masw} - h_{ma})} = h_d \left(\frac{dh_{masw}/dT_w}{m_w c_{pw}} - \frac{1}{m_a} \right) dA \tag{3.64}$$

The term dh_{masw}/dT_w is the gradient of the saturated air enthalpy-temperature curve over the control volume [14], and it can represented as follows:

$$\frac{dh_{masw}}{dT_w} = \frac{h_{maswi} - h_{maswo}}{T_{wi} - T_{wo}} \tag{3.65}$$

Where h_{maswi} and h_{maswo} are the saturated air enthalpy at the water inlet and outlet temperatures, respectively.

Equation (3.64) corresponds to the heat exchanger e-NTU method [28] where,

$$\frac{d(T_h - T_c)}{(T_h - T_c)} = -U \left(\frac{1}{m_h c_{ph}} + \frac{1}{m_c c_{pc}} \right) dA \tag{3.66}$$

It should be mentioned that the Ɛ-NTU method is derived according to the assumptions made by Merkel [24], that is the Lewis factor equals unity, then rquation (3.36) reduces to:

$$dQ = h_d(h_{masw} - h_{ma})dA \tag{3.67}$$

Where (h_{masw}-h_{ma})represents the used enthalpy driving potentail in Ɛ-NTU method in the case of evaporative cooling. Jabber and Webb [26] related the enthalpy transfer to the slope of the saturated air enthalpy and water temperature to reach finally to the final from of equation (3.64).

The correspondence of equation (3.64) to heat exchanger equation (3.66) is shown when the air capacity rate (cold fluid) is defined as m_a and the water capacity rate (hot fluid) as $m_wC_{pw}/(dh_{masw}/dT_w)$.Therefore the capacity rate ratio can be written as:

$$C_e = \frac{C_{emin}}{C_{emax}} \tag{3.68}$$

Moreover, the effectivess of the system is given by:

$$Ɛ = \frac{Q}{Q_{max}} \tag{3.69}$$

Where Q_{max} is the maximum theoritical amount of enthalpy that can be transferred and it can be given by:

$$Q_{max} = (\text{minimum capacity rate})X\ (h_{maswi} - h_{mai}) \tag{3.70}$$

Where h_{maswi} is the saturated air enthalpy at the water inlet temperature and h_{mai} is the air enthalpy at inlet condition.

Therefore,

$$\varepsilon = \frac{Q}{Q_{max}} = \frac{m_w c_{pw}(T_{wi} - T_{wo})}{C_{min}(h_{maswi} - \lambda - h_{mai})} \tag{3.71}$$

Where $\boldsymbol{\lambda}$ is a correction factor, according to Berman [43] to improve the approximation of enthalpy-temperature curve as a straight line [28] and it can be given by:

$$\lambda = \frac{h_{maswo} + h_{maswi} - 2h_{maswm}}{4} \tag{3.72}$$

For air and water streams, the number of transfer units for cross-flow arrangment for different configurations as per [26, 28] can be unmixed or mixed, or one can be mixed and the other unmixed or vice versa.

Therefore, for cross-flow with both streams mixed, NTU can be obtained according to the following equation:

$$\varepsilon = 1 - \exp\left[\frac{NTU^{0.22}[\exp(-C.NTU^{0.78}) - 1]}{C}\right] \tag{3.73}$$

And for for both streams mixed:

$$\varepsilon = \left[\frac{1}{1 - \exp(-NTU)} + \frac{C}{1 - \exp(-C.NTU)} - \frac{1}{NTU}\right]^{-1} \tag{3.74}$$

For cross flow with C_{max}mixed and C_{min} unmixed, then:

$$\varepsilon = \frac{1 - \exp\{-C[1 - \exp(-NTU)]\}}{C} \tag{3.75}$$

For cross flow with C_{max}unmixed and C_{min} mixed, then:

$$\varepsilon = 1 - \exp\left\{-\frac{[1 - \exp(-C.NTU)]}{C}\right\} \tag{3.76}$$

According to [26] there are two possible cases when the heat capaity rate of the cold fluid is less or greater than the heat capacity rate of water.

Case 1: if the heat capacity rate of cold fluid is greater than that of water,

$m_a > m_w C_{pw}/(dh_{masw}/dT_w)$

as per the definition of the heat exchanger design, the capacity rate ratio for this case can be expressed as follows:

$$C_e = \frac{C_{emin}}{C_{emax}} = \frac{m_w c_{pw}}{(dh_{masw}/dT_w)m_a} \tag{3.77}$$

And the Merkel number according to the ε-NTU method is given by:

$$Me_e = \frac{c_{pw}}{dh_{masw}/dT_w}\ NTU \tag{3.78}$$

Case 2:: if the heat capacity rate of cold fluid is less than that of water,

$m_a < m_w C_{pw}/(dh_{masw}/dT_w)$

the capacity rate ratio is then given by:

$$C_e = \frac{C_{emin}}{C_{emax}} = \frac{(dh_{masw}/dT_w)m_a}{m_w c_{pw}} \tag{3.79}$$

And Merkel number according to e-NTU method is given by:

$$Me_e = \frac{m_a}{m_w}\ \text{NTU} \tag{3.80}$$

3.4 SECOND LAW ANALYSIS

The first law of thermodynamics deals with the quantity of energy and states that energy cannot be created or destroyed. This law merely serves as a necessary tool for the quantity of energy during a process. The second law, however, deals with the quality of energy. More specifically, it is concerned with the degredation of energy during a process, the entropy generation, and the lost opportunities to do work; and it offers plenty of room for improvement [13].

Merkel, Poppe and e-NTU methods explained above were derived according to the first law of thermodynamics only. Therefore, applying the second law of thermodynamics to the air-water mixing process or in the wet cooling tower or humidifier devices is a necessary approach to examine the value of transferred energy in these processes by evaluating the irreversibilities or entropy generation and exergy destruction associated with the heat and mass transfer of mixing air and water in the cooling tower or humidifier.

From the basic definitions of second law, irreversibilities accompanying mixing of air and water streams generate entropy and any process that generates entropy always destroys exergy. In other words, the decrese of exergy principle is the counterpart of the increase of enetropy principle since both are alternative statements of the second law of thermodynamics.

Since the rate of entropy generation or the rate of exergy destruction measure the system inefficiencies, exergy analysis involves the calculation of system performance in the form of second law efficiency.

By applying the steady flow exergy balance to the crossflow humidifier as shown in figure 3.2, we simply have:

$$\sum_{\text{in}} \dot{X} - \sum_{\text{out}} \dot{X} = \dot{X}_d \tag{3.81}$$

Where X_{in} and X_{out} are the exergy transfer by mass and heat entering and leaving the system respectively. And X_d represents the exergy destruction in the process which is proportional to the entropy generation as follows:

$$X_{\text{destroyed}} = T_o S_{\text{gen}} \geq 0 \tag{3.82}$$

Where T_o is the temperature of the environment or the resteicted dead state temperature.

Equation (3.81) can be expressed in an alternative form as follows:

$$\dot{x}_d + \dot{x}_{ao} + \dot{x}_{wo} = x_{ai} + \dot{x}_{wi} + \dot{x}_{\text{makeup}} \tag{3.83}$$

Wepfer [35] provided a formula for total flow exergy of humid air per kilogram of dry air if the dry air and water vapor are considered ideal gases which can be used to expand equation (3.83), and it is given as follows:

$$X_{\text{total}} = (c_{pa} + \omega c_{pv}) T_o (T/T_o - 1 - \ln(T/T_o))$$

$$+(1 + \tilde{\omega}) R_a T_o \ln(P/P_o) + R_a T_o [(1 + \tilde{\omega}) \ln((1 + \tilde{\omega}_o)/(1 + \tilde{\omega})) + \tilde{\omega} \ln(\tilde{\omega}/\tilde{\omega}_o)] \tag{3.84}$$

Where, the humidity ratio on molal basis is given by:

$$\tilde{\omega} = 1.608\ \omega \tag{3.85}$$

Entropy generation can be found by applying the steady flow entropy balance as follows:

$$\dot{S}_{gen} = \dot{S}_{out} - \dot{S}_{in} \tag{3.86}$$

Where,

$$\dot{S}_{out} = \dot{m}_{wo} s_{wo} + \dot{m}_a s_{ao} \tag{3.87}$$

And,

$$\dot{S}_{in} = \dot{m}_{wi} s_{wi} + \dot{m}_a s_{ai} \tag{3.88}$$

Therefore, equation (3.86) can be further expanded as follows [36]:

$$\dot{S}_{gen} = \dot{m}_{wi}[s_{wo} - s_{wi}] - [\dot{m}_{wi} - \dot{m}_{wo}]s_{wo} + \dot{m}_a s_{ao} - \dot{m}_a s_{ai} \tag{3.89}$$

Entropy generation should always be greater than or equal to zero in equation (3.89).

As per Bejan [34] definition of second law efficiency which measures the irreversible losses in the humidification process, can be expressed as follows:

$$\eta_{II} = \frac{\text{total exergy leaaving}}{\text{total exergy entering}} \tag{3.90}$$

Or,

$$\eta_{II} = 1 - \frac{\dot{X}_d}{\dot{X}_{ai} + \dot{X}_{wi} + \dot{X}_{makeup}} \tag{3.91}$$

CHAPTER 4

EXPERIMENTAL WORK

An experimental work is done to evaluate the performance of a cross-flow humedifier and the points with least irreversibility by applying different operating parameters to the system which include inlet water temperature, water flow rate, and surface area of the fill or the number of fills used in the experiment.

The governing equations and methods explained in chapter three will be used to achive the objective.

4.1 EXPERIMENT SETUP

4.1.1 Overview

A cross-flow humidifier which is locally made is schematically shown in figure 4.1 and it is composed of the following components:

- The maincolumn; a transperent PVC column with dimensions: 30cm X 30 cm X 90 cm.
- Three PVC packed-beds or film fills installed inside the column with dimensions: 30 cm X 30 cm X 10 cm, and separated apart by 20 cm.

- Two fans installed at both ends of the humidifier column so that the air is blown through the fill material from left to right as shown in figure4.1.
- 150 liter water tank with 5 installed electric heaters. Three of them are 2 KW each and the other two heaters are of 1 KW power for each so that the total load these electric heaters can provide is 8 KW.
- Voltage controller or VARIAC is used and connected to one of the electric heaters (1 KW electric heater) so that it provides the required amount of power in order to achieve steady water temperature input to the humidifier and hence a steady state process.
- A pump to transfer the water from the tank to the humidifier.
- PVC pipes connecting the system components.
- One and half inch ball valve installed between the water tank and the column to regulate the flow and provide required flow rate.
- Two ball valves to control water flow over the fill materials during the tests.
- Flowmeter (Rotameter) to measure the water flow rate.
- Mist eleminator installed downstream of the third fill just before the air exiting the column to trap any moisture tending to leave the column.
- Six Omega thermocouples to measure the dry and wet bulb temperatures of air at the entry and exit of the humidifier, and inlet and outlet water temperatures.

Table 4.1 summarizes the details of the instruments used to measure the temperatures, air speed and water flow rate along with their ranges of accuracy and precision.

Table 4.1 Details of the instruments used to perform the measurements

Instrument	Model	Measured Variable	Accuracy	Precision	Calibration Method
Digital Anemometer	SMART SENSOR – AR836	Air Speed(m/s)	±3.0%	±0.1	Manufacturer data
Rotameter	OMEGA – FL-55500L	Volumetric water flow rate(LPM)	±2.0%	±0.1	Manually in Lab
Data Logger	OMEGA – HH603	Temperature(^{o}C)	±0.35	±0.1	Liquid-in-glass thermometer (including Thermocouples)

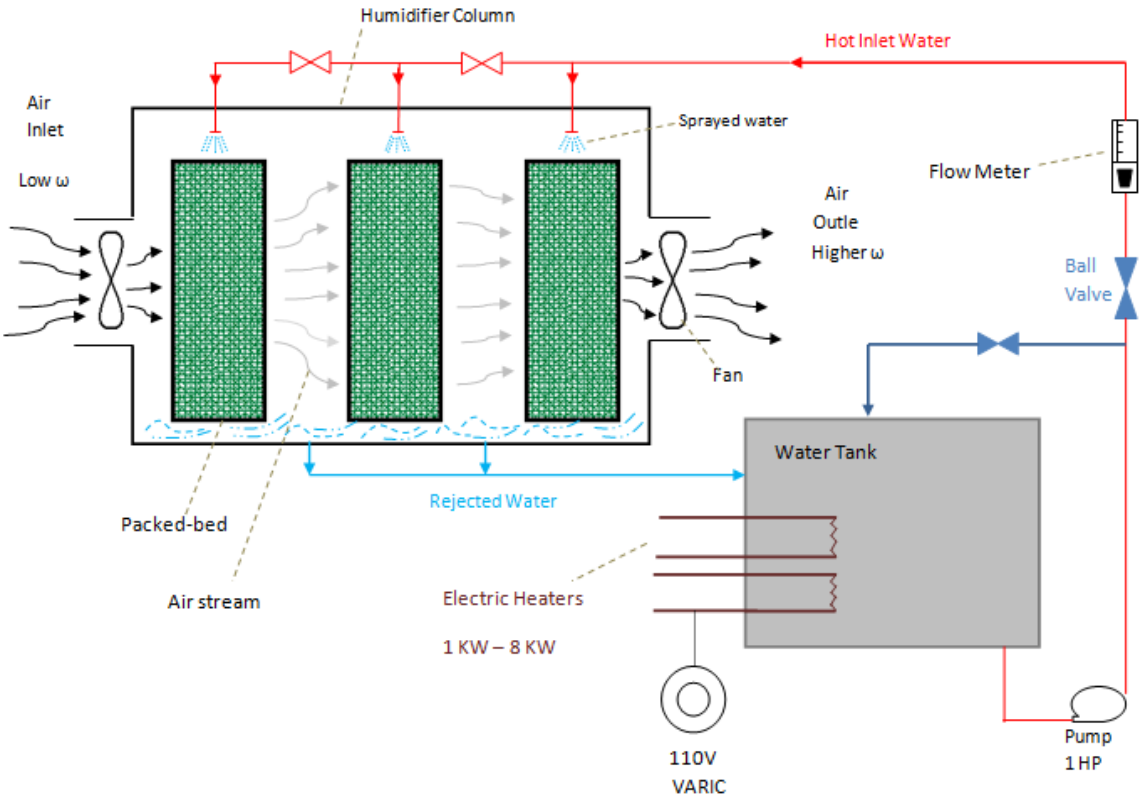

Figure 4.1Experiment setup of a cross-flow humidifier

4.1.2 System Operation

The operation of the setup shown in figure4.1 or the cross flow humidifier is simple in principle that the unsaturated air at room temperature enters the humidifier by help of the inlet and outlet fans and passes through the packed-beds as shown, Meanwhile, the humidification is accomplished by spraying hot water over the packed-bed or the fill and consequently the air is heated and humidified. Such process of heating and humidification can be represented in the psychrometric chart as alreadyshown in figure 1.5. During such process, some amounts of water from the sprayed water evaporates and is absorbed by the air.

Because the temperature of the moisture is greater than the temperature of the air, there is an overall increase in the temperture of the air.

As the process of heating and humidification takes place, the dry bulb, web bulb, and dew point temperatures of the air increases along with its relative humidity.

4.2 TEST PROCEDURE

To achieve the objective of the experiment, calculation of humidity ratio at different operating conditions, along with evaluating the system performance is what is going to be done by varying the three mentioned input parameters

Figure 4.2 shows the followed method to perform the test, that is at a given fill length the water inlet temperature is held at a specific value then the water flow rate is changed at seven different values. The same procedure is followed and repeated for three fill cases (i.e. 1, 2 and 3 fills) and four different water inlet temperatures (i.e. T_{wi}=room temperature,35, 45 and 55^{o}C), hence a total of 84 readings are obtained.

The measurements are conducted at steady state condition by help of a voltage variable device used to adjust the power input to the electric heater and therefore holding the temperature of entering water at a constant value, and it takes 30 minutes for the steady state to be reached.

The air speed is not varied so that the air-water flow rate ratio $m_r=m_w/m_a$changes as the water flow rate is changed.

The air dry bulb and web bulb temperatures of the lab ambient air is used into the test measurements as the air inlet condition (The values of these temperatures are given in section 4.4).

Table 4.2 below summarizes the parameters for the experimental measurements.

Table 4.2 Test parameters

Parameter	Symbol	Unit
Air flow rate	m_a	Kg/s
Water flow rate	m_w	Kg/s
Air inlet dry bulb Temp.	T_{ai}	^oC
Air outlet dry bulb Temp.	T_{ao}	^oC
Air inlet web bulb Temp.	$T_{i,wb}$	^oC
Aor outlet wet bulb Temp.	$T_{o,wb}$	^oC
Water inlet Temp.	T_{wi}	^oC
Water outlet Temp.	T_{wo}	^oC

All the measurements are taken at the atmospheric pressure and assumed to be P=101.325 Kpa.

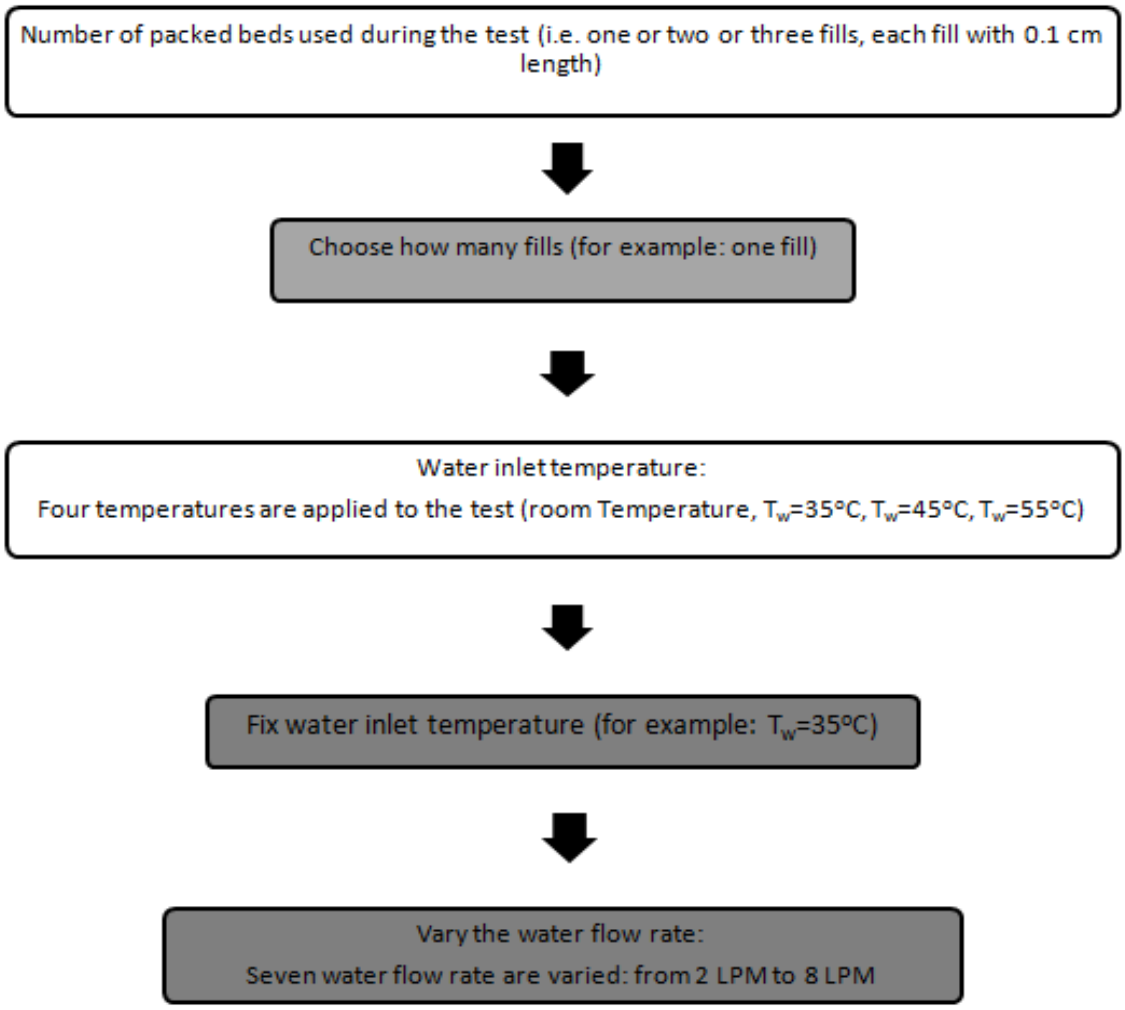

Figure 4.2 Experiment testing procedure

4.3 METHOD OF ANALYSIS

- **Air and water effectiveness (ϵ_a and ϵ_w)**

Although the main goal of the experimental work is to measure the humidity ratio of the exiting air, all other influencing aspects should be evaluated in order to examine the overall system performance. Therefore, the two main effectiveness definitions introduced in chapter 3 (equations 3.4 and 3.5) are used to analyze the performance of the cross flow humidifier. They will be calculated versus mass flow rate ratio and heat capacity ratio given by equation (3.6).

As the mass flow rate ratio is varied these two effectiveness will intersect at some point when the heat capacity rate of air and water are equal as implied before by the definition of heat capacity rate ratio HCR.

- **Merkel Number**

In regards to Merkel number calculation, the approximate method introduced in sections 3.1 and 3.2 for Poppe and Merkel models is applied on the values obtained experimentally. The method is tested and compared with the numerical results presented in [28] by using the same input data. The deviation from the exact results is about 5-10%. Table 4.3 presents the values by numerical results in [28] and by the introduced approximation method.

Table 4.3 Comparison between Merkel numbers obtained by numerical results and approximation approach by Chebychev method; T_{ai}=9.7°C, T_{wb}=8.23°C, T_{wi}=39.67°C, T_{wo}=27.7°C, m_a=4.134 kg/s, m_w=3.999 kg/s

	Merkel Model (exact)	Merkel Model (Approx.)	Diff. %	Poppe Model (exact)	Poppe Model (Approx.)	Diff. %
Me	0.7395	0.7973	8.0	0.7976	0.8495	7.0

Effectiveness-NTU method is also used to calculate Merkel number in order to compare the results with Poppe and Merkel methods.

- **Accuracy of calculated Merkel number over second and third fill**

The experiment setup includes only one flow meter which measures the total flow rate of water in case of two or three fills runs and in order to evaluate the amount of water flowing in each film fill, a manual measurement was done and the results showed the quantity of water is almost distributed evenly in each fill. Merkel number is calculated accordingly and table 4.4 represents the differences associated with the quantities of water flowing in each fill. Readings were taking at water flow rate of 4 LPM and water inlet temperature of 35°C.

Table 4.4 comparison of Merkel number for three fills with a total water flow rate of 12 LPM

Fill	T_{ai} °C	$T_{i,wb}$ °C	T_{ao} °C	$T_{o,wb}$ °C	T_{wi} °C	T_{wo} °C	Merkel Number	Difference %
1st	18.6	14.1	25.5	223.5	35	30.2	0.365	0.0
2nd	25.5	23.5	29	27.9	35	31.9	0.3586	1.78
3rd	29	27.9	32	30.5	35	32.9	0.3618	0.9

In light of the results in table 4.4, all of the readings for two and three fills cases in the experimental work are taken on the basis that the water flow rate is distributed evenly in each fill.

- **Second Law Analysis**

The entropy generation and second law efficiency of each process from the obtained experimental data will be directly calculated by equations (3.89) and (3.91).

Non-dimensional entropy generation introduced in [36] will be utilized over the experimental results for different operating conditions. The term of non-dimensional entropy generation is relating the minimum heat capacity rate to the calculated entropy generation (i.e. $S_{gen}/(m.c_p)_{min}$).

The dead state conditions required to calculate the flow exergy are taken as:

T_o=298.15 [K]

$\emptyset = 50\%$, relative humidity at dead state

P_o=101.325 [KPa]

Moreover, specific enthalpy and specific entropy at dead state are evaluated at these values of temperature and relative humidity.

4.4 RESULTS AND DISCUSSIONS

Following the procedure of section 4.2, the experimental work was conducted and completed for84 readings. The readings were taken manually by using the instruments mentioned in Table 4.1.Tables 4.5, 4.6 and 4.7 are sample readings at T_{wi}=35, 45 and 55^{o}C respectively.

Table 4.5 Experimental results at T_{wi}=35^{o}C

m_w/ m_a	T_{ai} ^{o}C	$T_{i,wb}$ ^{o}C	T_{ao} ^{o}C	$T_{o,wb}$ ^{o}C	T_{wi} ^{o}C	T_{wo} ^{o}C
0.8784	20.7	13.8	25.3	22	35	27.9
1.1458	20.8	14.1	24.6	22.1	35	29.5
1.4792	21.9	14.6	26.1	23.4	35	30.1
1.7029	21.8	11.7	26.1	22.1	35	30.3
2.0543	26	18.7	29.1	25.6	35	31.7
2.4031	26.1	18.7	29	25.8	35	32.1
3.0339	26.3	18.8	29.2	27	35	32.4

Table 4.6 Experimental results at T_{wi}=45^{o}C

m_w/ m_a	T_{ai} ^{o}C	$T_{i,wb}$ ^{o}C	T_{ao} ^{o}C	$T_{o,wb}$ ^{o}C	T_{wi} ^{o}C	T_{wo} ^{o}C
0.8784	22	14.4	28.9	26.5	45	33.3
1.1842	20.8	14.1	29.2	27.3	45	35.5
1.4792	21.9	14.6	30.1	28.4	45	36.5
1.8561	21.8	11.8	30.7	28.4	45	37
2.3695	27.2	19.5	33.5	32	45	39.2
2.7309	27.2	19.5	33.9	32.5	45	39.8
3.1727	27.2	19.5	34.1	33.3	45	40.2

Table 4.7 Experimental results at T_{wi}=55°C

m_w/ m_a	T_{ai} °C	$T_{i,wb}$ °C	T_{ao} °C	$T_{o,wb}$ °C	T_{wi} °C	T_{wo} °C
0.9028	21.5	15	33.4	31.2	55	37.9
1.3158	20.8	14.1	33.9	32.4	55	41.2
1.6667	24	14.7	34.5	33.5	55	43.7
1.9841	22.1	12	35.3	34.4	55	43.5
2.2222	22.1	12	35.7	35	55	44
2.5926	22.1	12	36.5	36.2	55	45.2
2.963	22.1	12	37.6	37.3	55	46

Calculations are performed using the Engineering Equation Solve (EES) which uses accurate equations of state for moist air and water properties; see Appendix B (1) for EES codes.

Merkel number by Poppe and Merkel models are calculated according to the approximation method introduced before. Appendix B (2) shows EES code for implementing such calculation.

The details of instruments precision and accuracy presented in table 4.1 are used to perform the uncertainty analysis by using Coleman and Steele approach [44]. The results of the uncertainty analysis can be found in Appendix A.

4.4.1 First Law Analysis

A. Effect of water flow rate

If the definitions in equations (3.4) and (3.5) for the system effectiveness of enthalpy changes of water and air sides are applied to the experimental results for different flow rate ratios, it can be conferred from figure 4.3 that the humidifier effectiveness for air side increases as the mass flow rate ratio increases, that is the water vapor content in the air exiting the humidifier increases and as a result the amount of energy content in the air or its enthalpy will be higher. This is due to the fact that the energy balance governs the outlet air humidity ratio and relative humidity in the heating and humidification process and hence they increase as the flow rate ratio increases.

If the water side in the humidifier is considered, the system effectiveness decreases as the mass flow rate increases. Such result is in a good agreement with the energy balance of the process when the decrease of enthalpy change of water is associated with an increase of enthalpy change of air. In other words, because the water flow rate is the only parameter that vary the mass flow rate ratio in the experiment, a physical meaning concerning its effect to the water outlet temperature can be elaborated through the time the water spends while travelling through the film fill of the humidifier, therefore, when the water flow rate is high or the time it spends in the fill is short, less heat transfer is resulted and hence the water inlet and outlet temperature difference will be less. The vice versa case is true when the water flow rate is large.

At a specific case of system operating conditions there is a point where the two system effectiveness for air and water sides intersects. This means that the water and air streams reached to a condition where their heat capacities are equal to each other and the amount of energies transferred by any of both streams are equal. If the same figure is plotted against heat capacity ratio, as per the definition of equation (3.6) it can be noted from figure 4.4 that this intersection takes place at HCR equals one.

At heat capacity ratios higher than one, the cold or air stream heat capacity is more than that of the hot or water stream and therefore the heat and mass transfer of the process cannot allocate the same energy differences (i.e. equal enthalpy changes for air and water).

Camargo [30] concluded from the experimental work that increasing the air speed will decrease the system effectiveness without testing the enthalpy change for water side, and this behavior is met too as in figure 4.3.

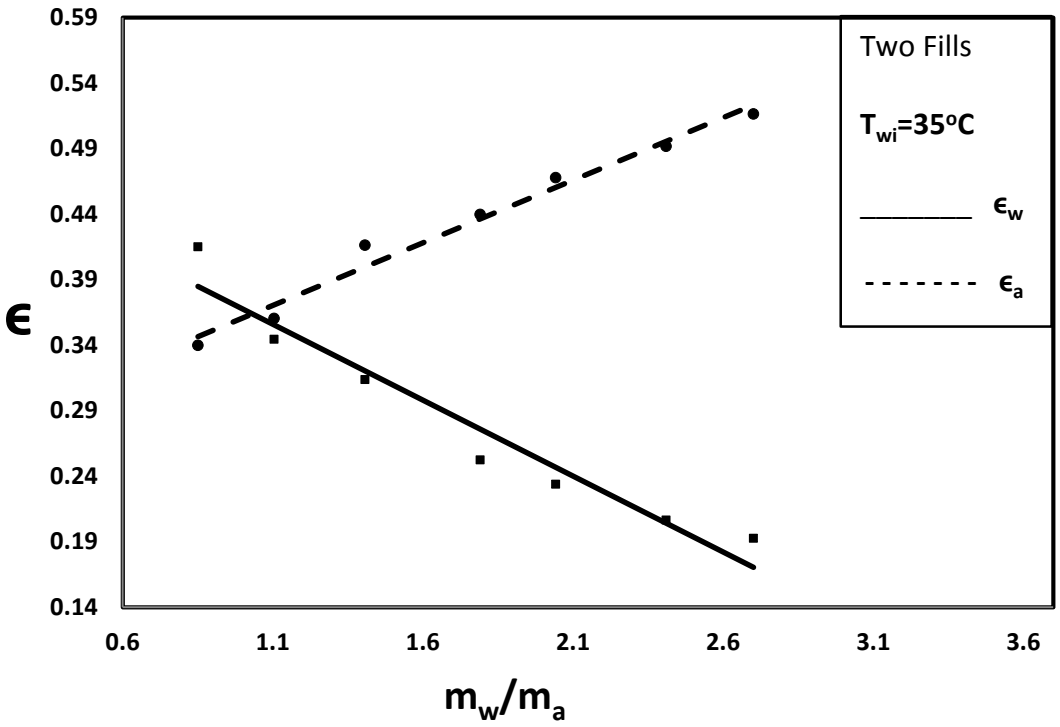

Figure 4.3 Effect of mass flow rate ratio on system effectiveness; T_{wi}=35°C, two fills

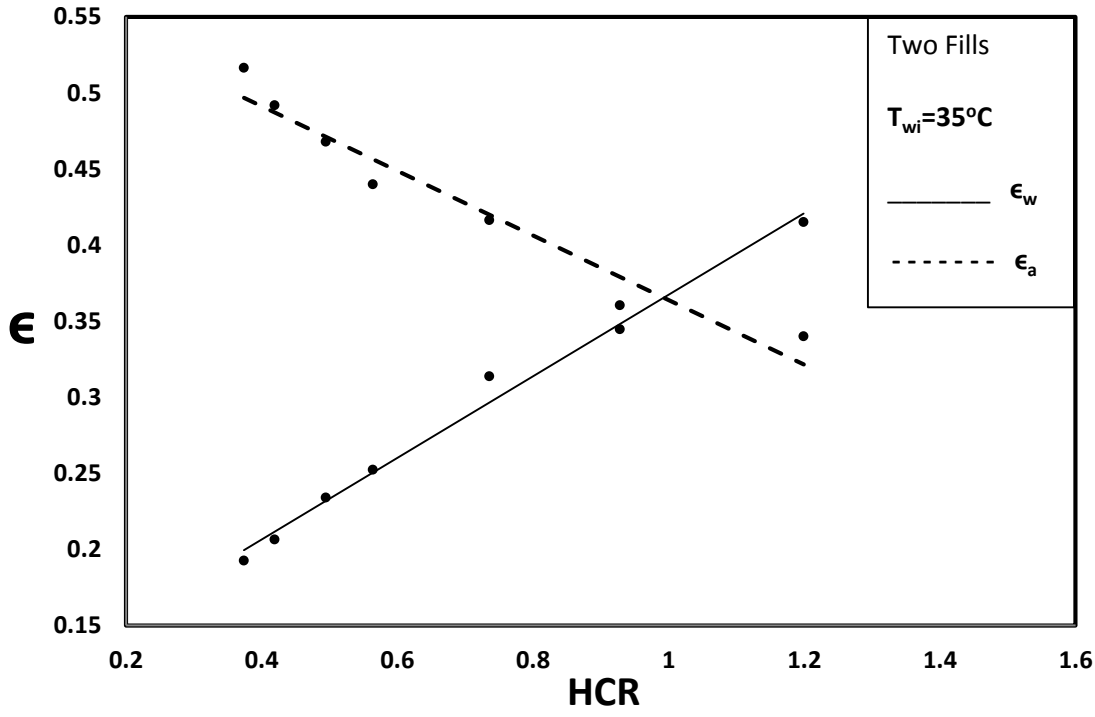

Figure 4.4 Effect of heat capacity ratio on system effectiveness; T_{wi}=35°C, two fills

B. Effect of water inlet temperature

Heating the air to higher temperatures raises its capacity to accommodate more water vapor but still the system effectiveness is what eventually can judge its overall performance. Therefore, varying the water inlet temperatures to establish heating and humidification processes for the same range of mass flow rate ratios will lead to different trends of system effectiveness as in figure 4.5. It can be seen from the figure that the two streams will behave the same way as explained earlier for each water inlet temperature, but it can be conferred from the figure that as the water inlet temperature increases the intersection points will happen at higher flow rate ratio, and these specific flow rate ratios points coincides with HCR equals one for that given water inlet temperature. Figure4.6 shows clearly these intersection points for each case at the scale of heat capacity ratio.

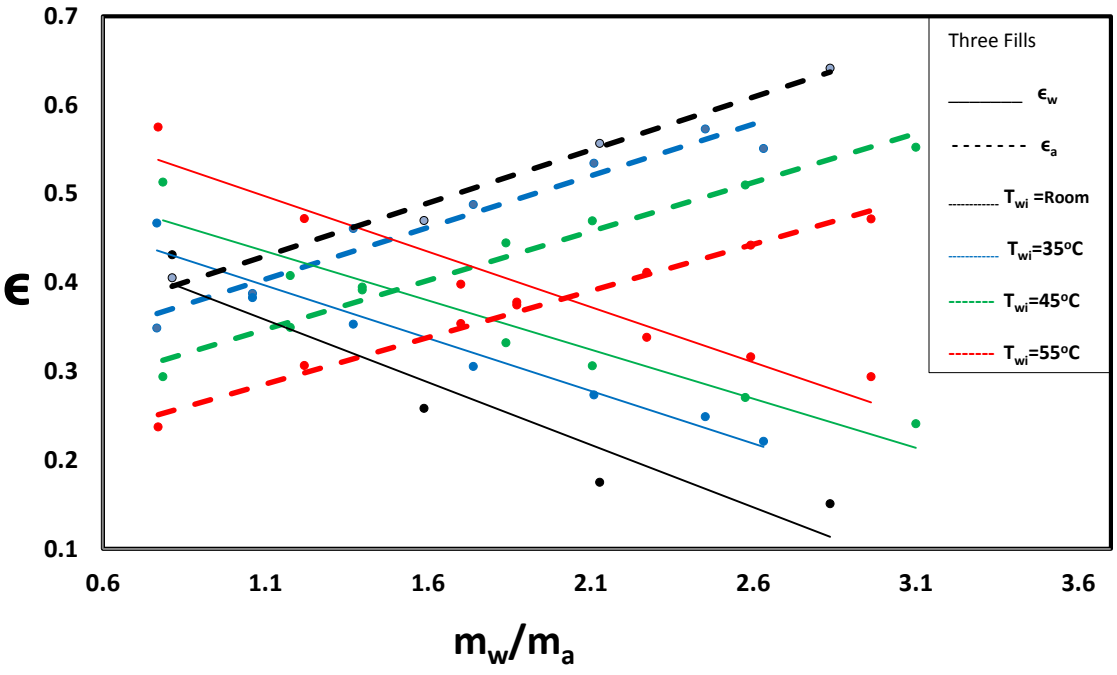

Figure 4.5 Effect of water inlet temperature on system effectiveness at different mass flow rate ratios and three fills case

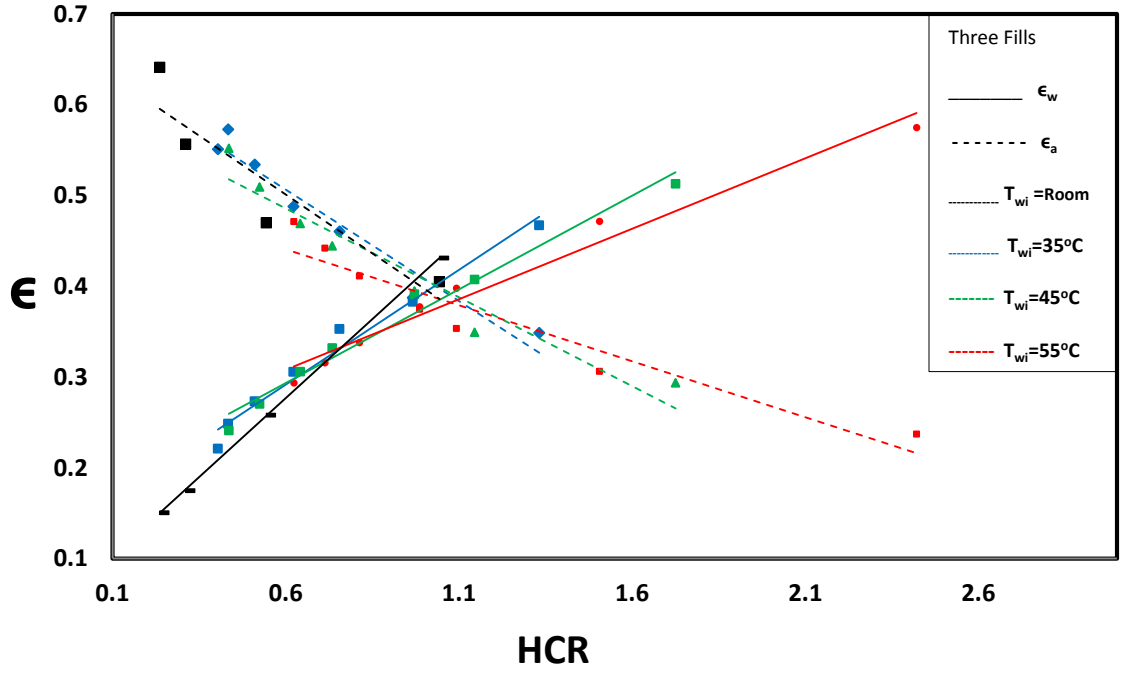

Figure 4.6 Effect of heat capacity ratio on system effectiveness at different water inlet temperatures and three fills case

If can be concluded from figure 4.5 and 4.6 that at HCR equals one the change of water inlet temperature has little effect in the value of system effectiveness or in other words for the 4 chosen temperatures the effectiveness is almost the same at these points. If these points at HCR ≈ 1 are plotted versus water inlet temperature then it can be noted from figure 4.7 the small differences in the system effectiveness which is showing that it decreases slightly as the water inlet temperature increases.

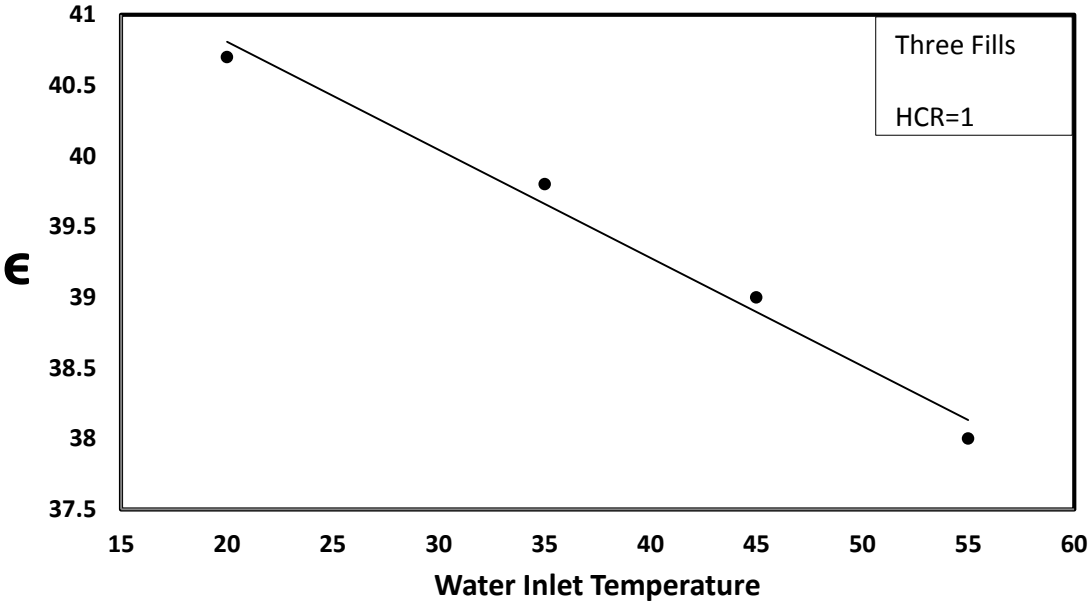

Figure 4.7 Effect of water inlet temperature on the system effectiveness at HCR=1; three fills case

C. Effect of Surface Area

Changing the number of fills used in the experiment is nothing but changing the surface area for heat and mass exchanging between the two streams of air and water. If the system effectiveness for both streams is tested for different film fills at the same water inlet temperature T_w=55^{o}C then it can be noticed from figure4.8 that the system effectiveness for both flows will be enhanced as the heat and mass surface area is increased. It should also be noted that further increase in surface area or number of fills will not necessarily contribute in increasing the system effectiveness at the same percentages presented in the figure. The reason behind that is as the surface area is increased the two streams will have more chance to exchange heat and mass and hence the air would have no more capacity to absorb energy from the hot water streams and any further increase in the moisture content in the air will be given out and condensed. For these specific results in figure4.8 most of mass and heat transfer takes place in the first fill and if a profile of the amount of water-vapor absorbed by the air is established for these three cases, then 70-75% of mass exchange will take place in the first fill, 15-20% in the second fill and 5-10% in the third film fill.

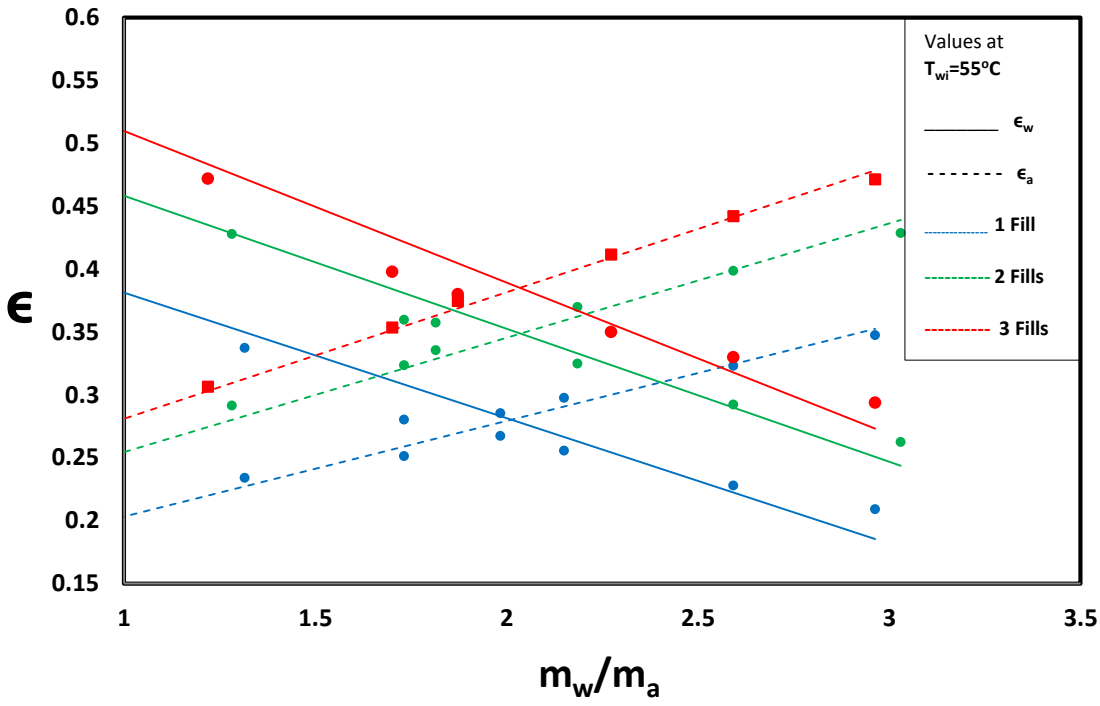

Figure 4.8 Effect of surface area on system effectiveness for different mass flow rate ratios and water inlet temperature equals 55°C

The effect of water inlet temperature to the intersection point's location at the flow rate ratio scale has been presented earlier. Unlike the water inlet temperature effect, changing the surface area has no effect on the locations of these points at the same scale of flow rate ratios and it can be seen from figure4.8 that these points take place at the same mass flow rate ratio. This is simply explained from the energy balance of the process which is a function only of the heat capacities of the two streams as well as the water inlet temperatures.

As a consequence of figure4.8 if the system effectiveness for both streams is plotted against heat capacity ratio then figure4.9 shows where they are equal at HCR ≈ 1.

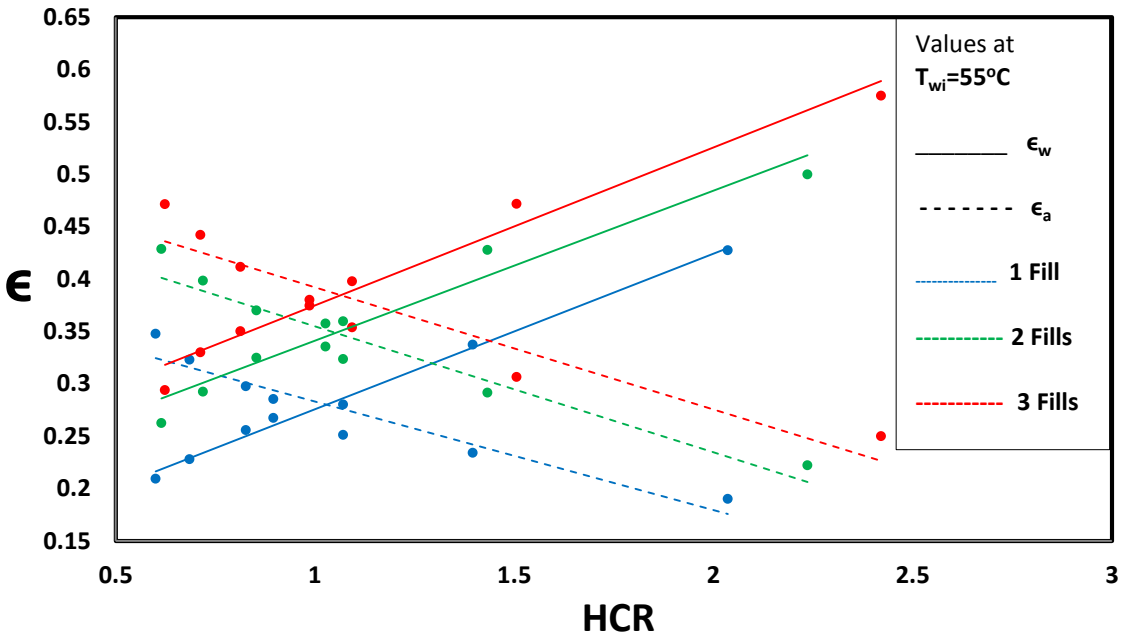

Figure 4.9 Effect of surface are on system effectiveness for different heat capacity ratios and water inlet temperature equals 55°C

4.4.2 Second Law Analysis

A. Effect of mass flow rate ratio

From the basic definitions of the second law of thermodynamics, evaluation of the entropy generation of the process of heat and mass transfer would tests the losses or irreversibility associated with such process. And due to the fact that energies are transferred to or from the cold and hot streams according to their amount of heat capacities, there must be a specific operating condition when the losses are minimal along the different heat capacity ratios of both streams.

Since variation of mass flow rate ratios changes the values of HCR then non-dimensional entropy generation defined in section 4.3 can be directly plotted against HCR as shown in figure4.10 with emphasis that the relative humidity of inlet air for these particular values are almost the same . So, the figure shows how the non-dimensional entropy generation varies when changing the flow rate ratios or the heat capacity ratio at fixed surface area and water inlet temperature. It can be noticed that the lowest values of entropy generation are around HCR ≈ 1.

And by Bejan [34] definition for the second law efficiency, equation (3.91), the results showed that when the entropy generation is minimum, the second law efficiency is maximum as can be conferred from figure 4.11. So there is an optimum point from the perspective of the second law analysis which in turn points at the best operating condition at which the cross-flow humidifier will perform.

When Wepfer [35] definition for total flow exergy of humid air is used, then the obtained 2nd law efficiency will be almost the same as the value obtained by EES built-in equations.

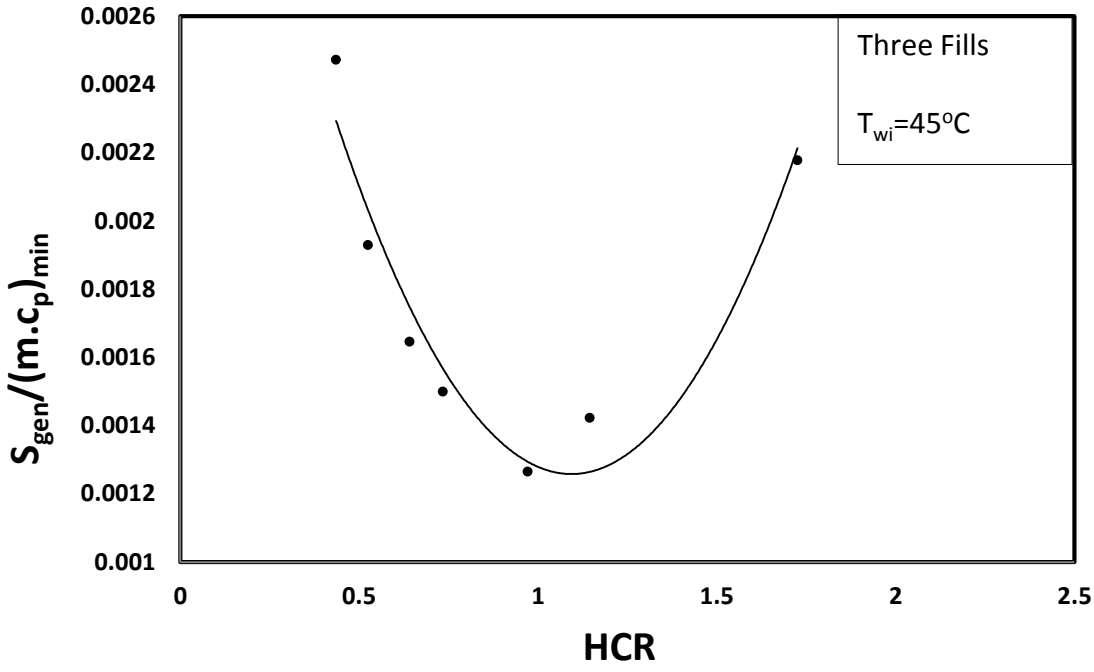

Figure 4.10 Effect of heat capacity ratio on the non-dimensional entropy generation; three fills, T_{wi}=45°C

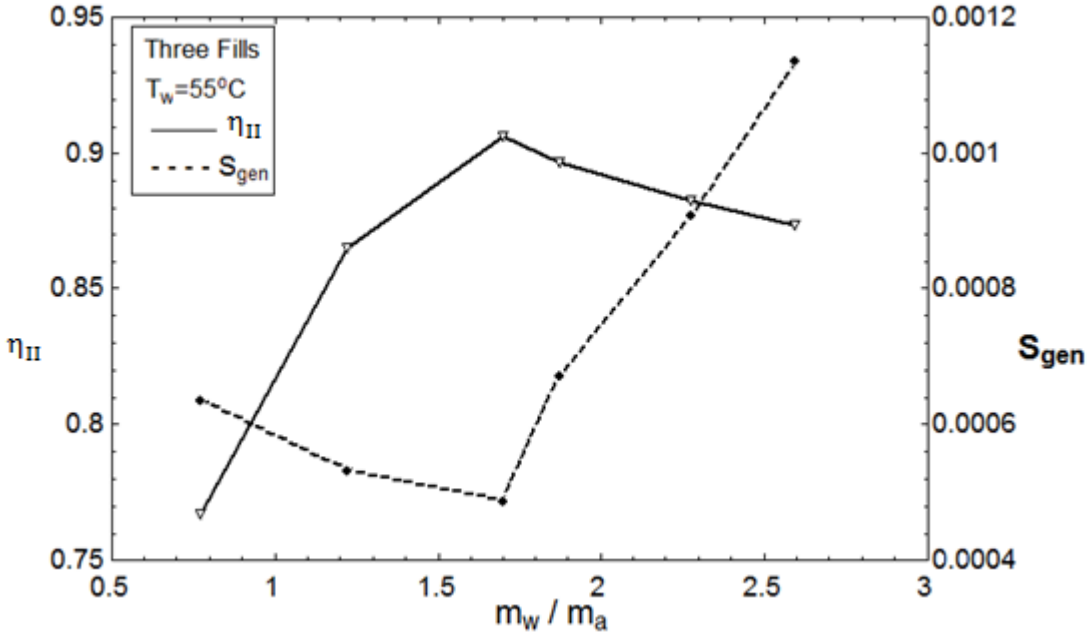

Figure 4.11 Mass flow rate ratio versus rate of entropy generation and 2nd law efficiency; three fills, T_w=55°C

It is worth mentioning that the effect of the inlet air relative humidity to the second law efficiency is not significant at the same mass flow rate ratio as presented in [38] for counter-flow cooling towers. It has been shown that for a relative humidity range from 0.35 to 0.85 for mass flow rate ratio of 0.5 the second law efficiency changes in a range of 0.0 to 2.5% and for a mass ratio of 1.0 the second law efficiency changes from 0.0 to 1.6%. For the presented study of cross-flow humidifier these conclusions are almost the same as presented in [38]. Table 4.8 shows three different conditions of inlet air along with their second law efficiencies values. The change of relative humidity from 0.35 to 0.72 for cross-flow humidifier for a fixed mass ratio of 1.7 has an effect to increase the second law efficiency up to almost 0.8%. Therefore, the optimum point in figure4.11 is still valid to be the maximum because it was evaluated at low value of relative humidity and if its relative humidity is changed to be the same as other points in the same figure then the second law efficiency at that particular point will be higher.

Table 4.8 effect of relative humidity of inlet air on the 2nd law efficiency at fixed mass flow rate ratio; three fills, T_{wi}=55°C.

M_r	Ø	T_{wi}, °C	No. of Fills	η_{II}
1.7	0.35	55	3	0.9062
1.7	0.5	55	3	0.901
1.7	0.72	55	3	0.9134

If the results of figure 4.11 are plotted versus HCR then figure 4.12 is a normal conclusion that the optimum point takes place HCR ≈ 1.

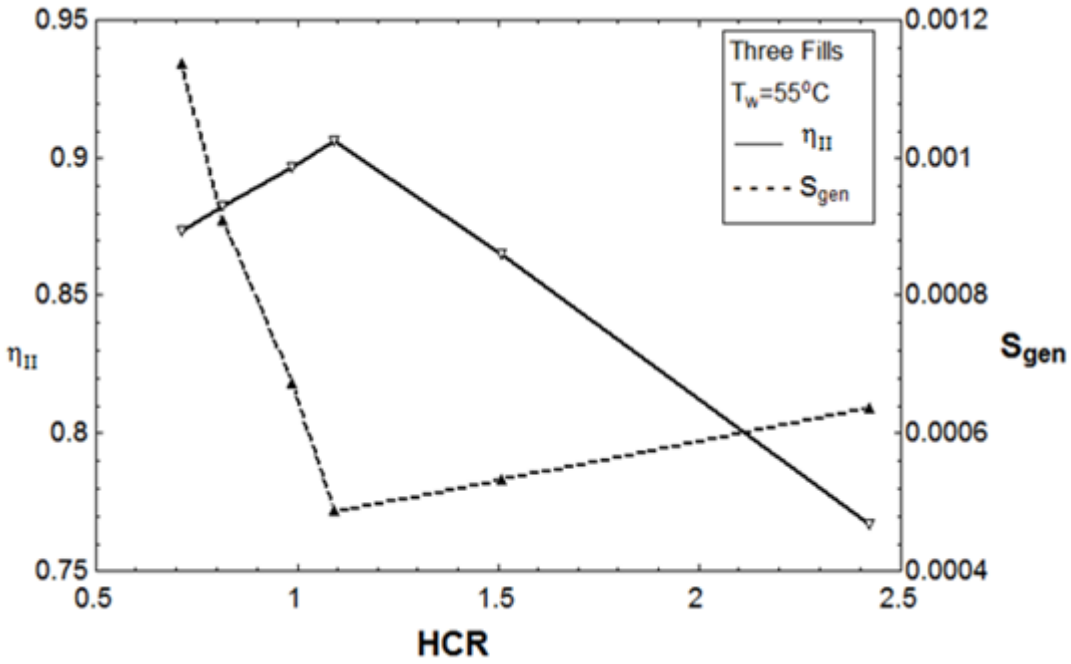

Figure 4.12 Heat capacity ratio versus rate of entropy generation and 2nd law efficiency; three fills, T_w=55°C

B. Effect of water inlet temperature

By the analysis of the first law of thermodynamics it has been shown in figure4.6 that for a fixed surface area the system effectiveness has nearly the same value at HCR ≈ 1 for different water inlet temperatures. If the second law analysis is used to evaluate these results and non-dimensional entropy generation is plotted versus HCR then it can be clearly noticed from figure4.13 that as the water inlet temperature increases the non-dimensional entropy generation increases. Therefore, at the points of intersection in figure4.5 the losses or irreversibility is the minimum in the processes of heat and mass exchanging.

It has been shown in figures 4.11 and 4.12 that the second law efficiency is maximum when the entropy generation is the least. Therefore, for the results presented in figure 4.13, the operating conditions with minimal losses will be examined from the perspective of the 2^{nd} law efficiency for different water inlet temperatures. Figure 4.14 shows how the 2^{nd} law efficiency of the points with minimal losses in figure 4.13 changes for fixed surface area and HCR equals one. As the water inlet temperature increases the second law efficiency decreases and this due to the irreversibility associated with such heat and mass exchanging processes.

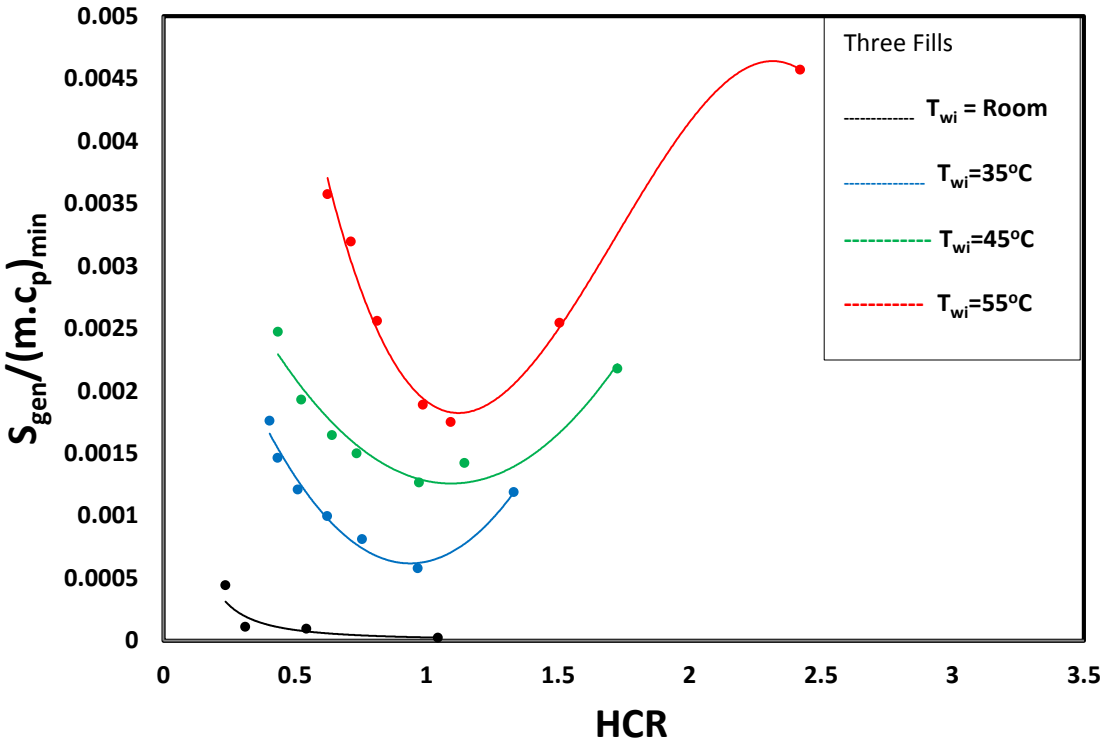

Figure 4.13 Non-dimensional entropy generation versus heat capacity ratio for different water inlet temperatures and fixed surface area (three fills)

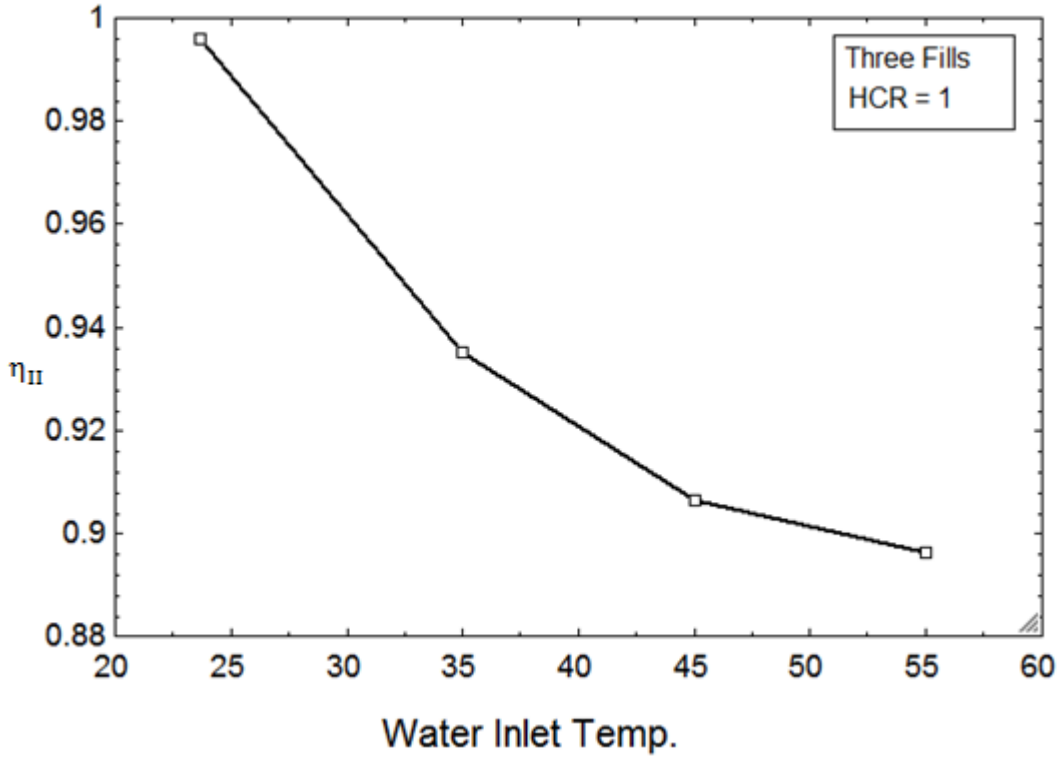

Figure 4.14 Effect of water inlet temperature on the 2nd law efficiency at HCR=1 and fixed surface area

C. Effect of Surface Area

The first law analysis showed that the system effectiveness is enhanced when the surface area or the number of film fill is increased, see figure4.9. If the exergy destruction or the entropy generation principles are used to test the quality of the transferred energies as the surface area of the cross-flow humidifier is changed then it can be conferred from figures 4.15 and4.16 that increasing the surface area will result in an increase of entropy generation rate with minimal losses at heat capacity ratios equal one.

And at a specific water inlet temperature the second law efficiency increases as the number of film fills used is reduced, see figure 4.17.

Increasing the surface area gives the hot and cold streams more chances to exchange heat with surrounding, moreover, for the mass transfer side some of the water vapor in the air will tend to condense and this can be thought of as the energy that has been spent and consumed to evaporate and absorb the water-vapor from the water stream to the air stream is dissipated through the condensation process which happens before the air leaves the humidifier, therefore, that amount of energy is considered lost and such loss is reflected in increasing the entropy generation and in turn decreasing the second law efficiency.

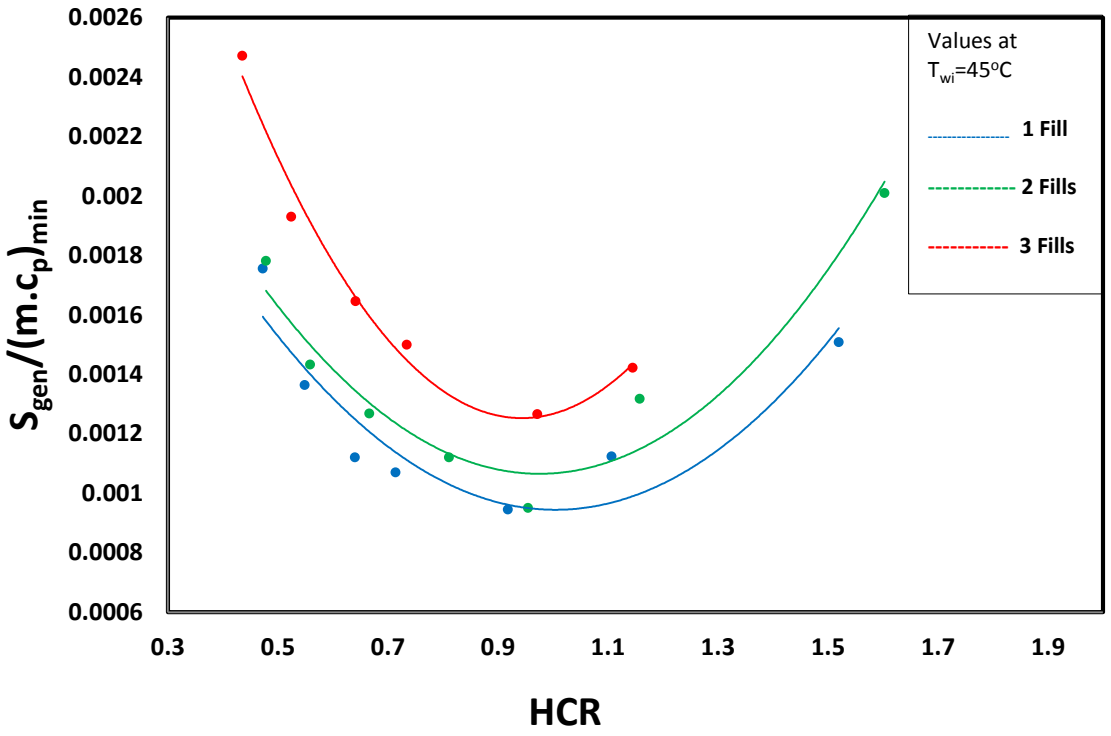

Figure 4.15 Effect of surface area on the non-dimensional entropy generation at fixed water inlet temperature of 45°C

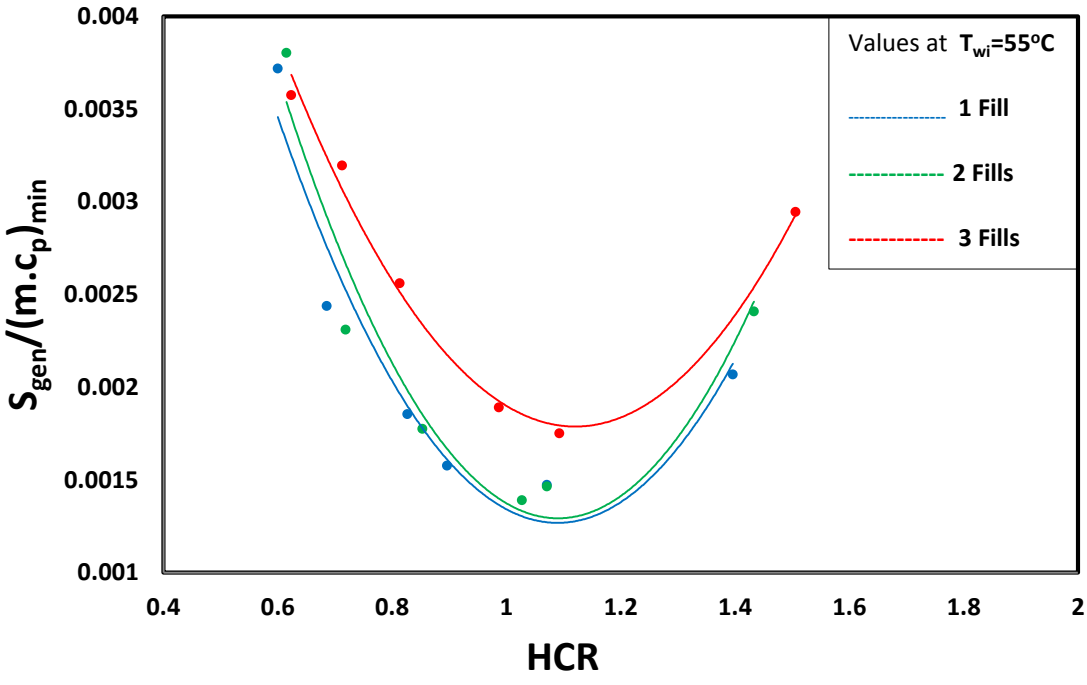

Figure 4.16 Effect of surface area on the non-dimensional entropy generation at fixed water inlet temperature of 55°C

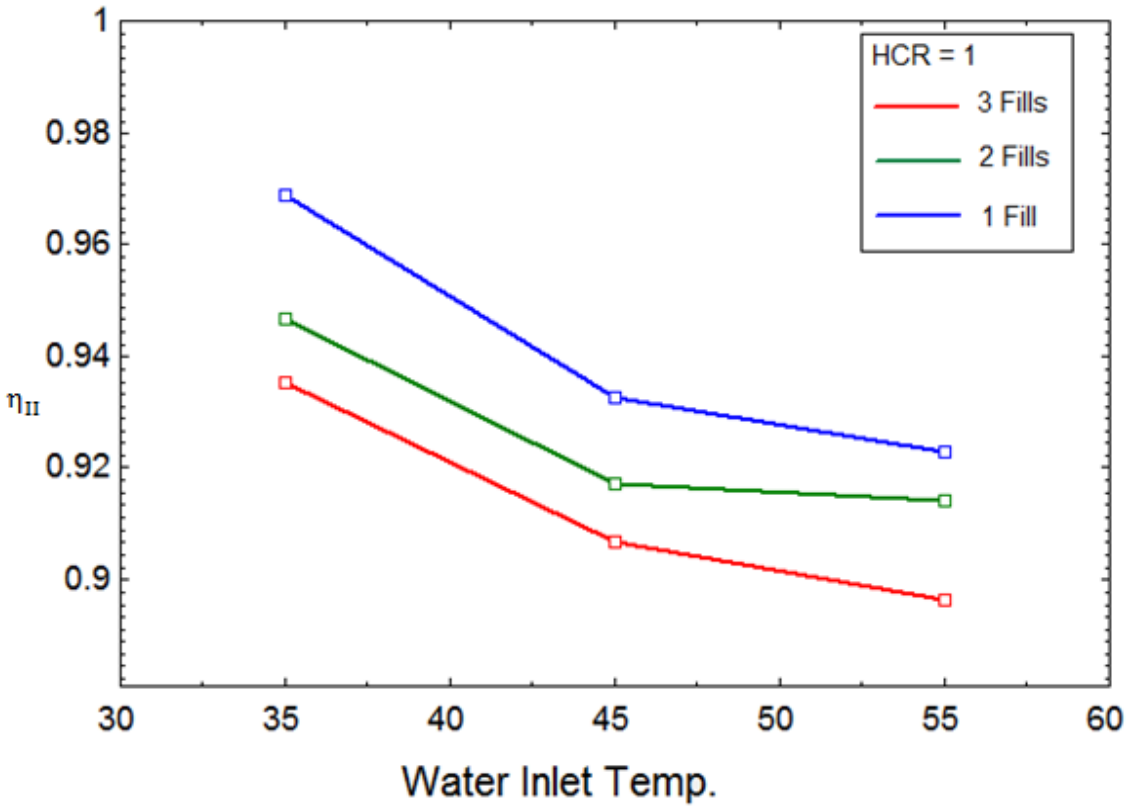

Figure 4.17 Effect of surface area and water inlet temperature on 2nd law efficiency at HCR=1

4.4.3 Merkel Number

Effectiveness-NTU method is used in the following three sections to study the effect of mass flow rate ratio, water inlet temperature and the fill length because using any method will lead to same behavior or trends but of course the values of Merkel number will be different if other methods are considered. The comparison between the three introduced methods in chapter 3 is done in the last section.

A. Effect of mass flow rate ratio

The transfer characteristic or the Merkel number is a strong function of the water flow rate as it is shown in figure4.18. From the definition of Merkel number, in addition to the product of mass transfer coefficient and surface area per unit volume inside the Merkel number, water flow rate is also included. And unlike these two characteristics of the fill which are practically difficult to be determined, water flow rate can easily be varied to change the final value of Merkel number. Therefore, as the flow rate increases the Merkel number decreases as it can be noticed in the figure.

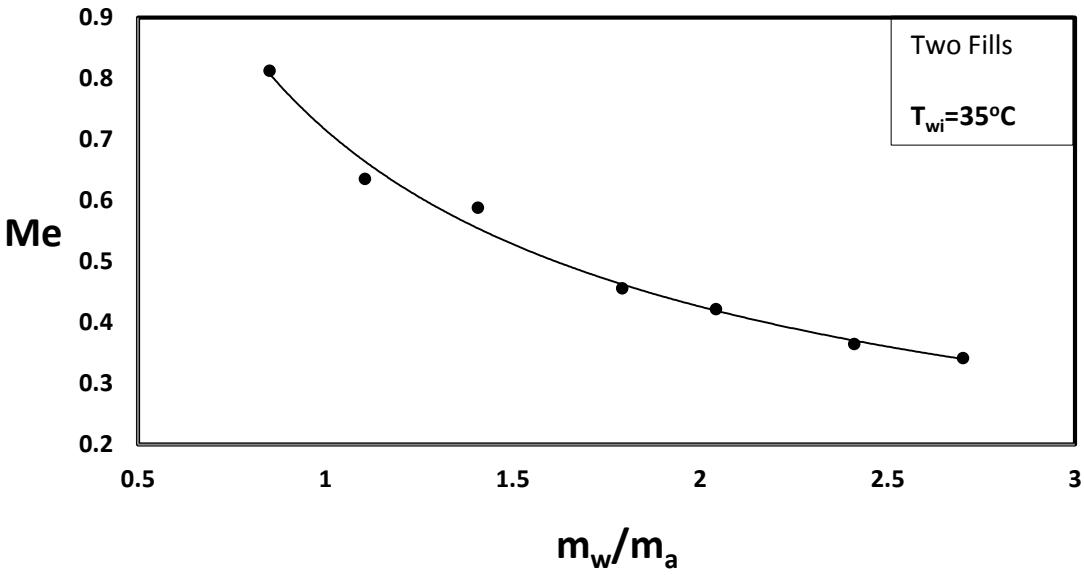

Figure 4.18 Effect of mass flow rate ratio on Merkel number; T_{wi}=35°C, two fills case, relative humidity=50%

B. Effect of Water inlet Temperature

It has been shown experimentally [45] that increasing the water inlet temperature decrease the Merkel number for counter-flow cooling tower. For the present study of a cross-flow configuration the same result is achieved as shown in figure4.19. These trends in figure 4.19 can be obtained by using any methods mentioned earlier for analyzing the performance of cross-flow humidifier and in this figure e-NTU method is used.

As already explained, the driving potential in the evaporative process inside cross-flow humidifier is the difference between the enthalpy of the air at the interface with water and the air at the free stream, and such difference is included in the integral form of Merkel number. Moreover, as the water inlet temperature increases, the difference between the inlet and outlet temperatures for water becomes larger. Even though such difference is large, the Merkel number is smaller when it is compared with less water inlet temperature. The reason behind that is the air enthalpy difference which dominates at higher temperatures, and therefore reduces the value of Merkel number.

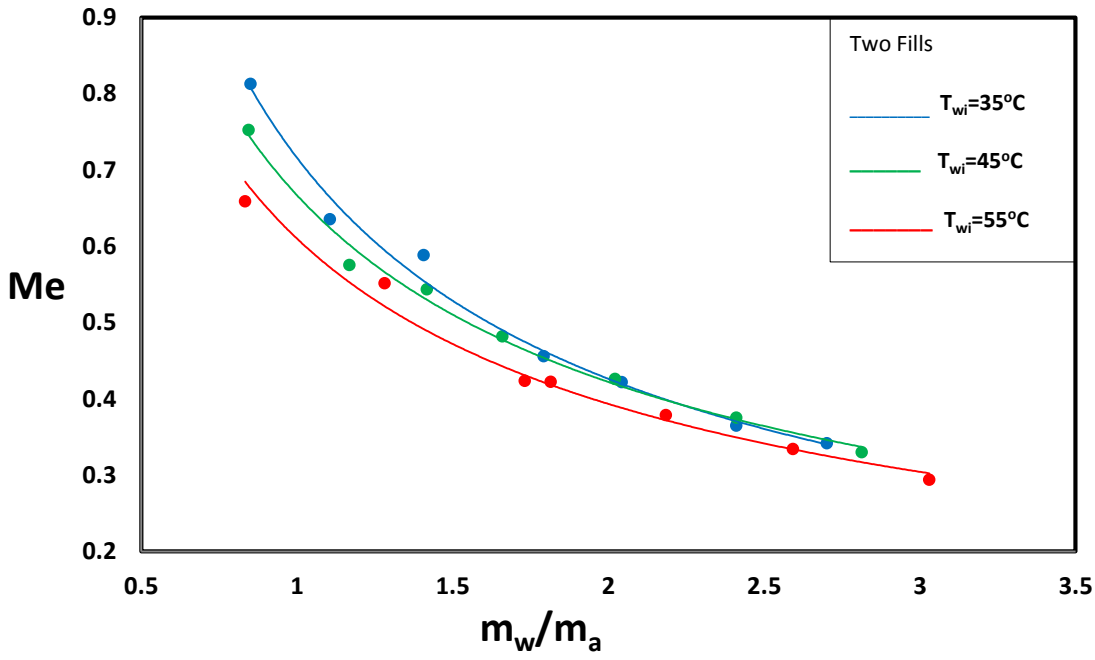

Figure 4.19 Effect of water inlet temperature on Merkel number for different mass flow rate ratios and fixed surface area

C. Effect of fill length or surface area

The transfer surface area of the fill is a product of the volume of the fill and the surface area per unit volume which is a characteristic of the fill itself. Therefore, changing the fill length will result in changing its volume and in turn the surface area for heat and mass transfer.

The potential difference in temperature and water concentration between the air and water streams are higher at the inlet sides of the fill, then such potential decreases as the air becomes more saturated, until it cannot sustain to absorb more water vapor which may allow the process of condensation to happen. Therefore, increasing the surface area for heat and mass transfer is limited to the air capacity to absorb water-vapor, for example, doubling the surface area for the same inlet conditions does not mean that the amount of water vapor absorbed by the air will be doubled too. This fact can be observed simply in the variation of Merkel number for different surface areas as shown in figure4.20. The value of the transfer characteristic or Merkel number for two fills increased by 45% (from the value of Merkel number for one fill case) and for three fill case it increased by 20% (from the value of Merkel number for two fill case). Such reduction in the percentage of Merkel number increase draws a limit in designing a humidifier that adding more fills or increasing the surface area is not necessarily mandatory if the objective is to make the air humid.

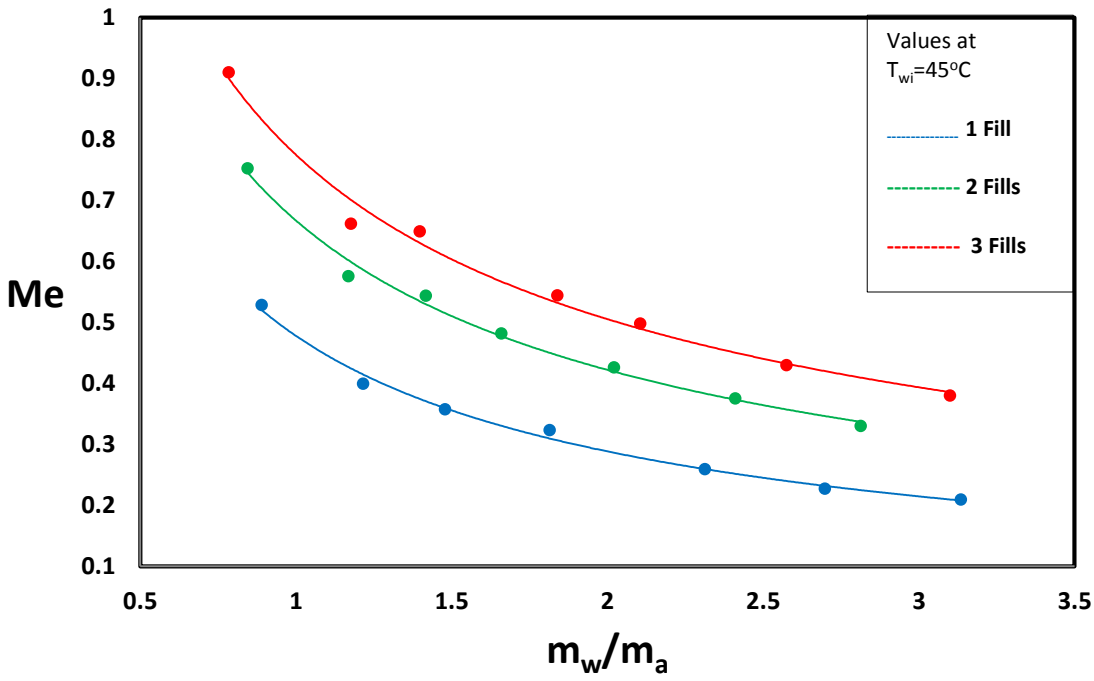

Figure 4.20 Effect of surface area on Merkel number at T_{wi}=45°C

D. Merkel number by Merkel, Poppe and e-NTU methods

As mentioned earlier, unlike counter-flow arrangement, the calculation of Merkel number in cross-flow configuration should be conducted in two dimensional schemes. And evaluation of integrals for Merkel number in equations (3.46) and (3.61) can be done by Chebychev integration method and for cross-flow it is more complicated than the case of counter-flow.

As already explained, the introduced approximation method for such evaluation showed that the obtained Merkel number by both Merkel and Poppe methods gave values higher by 5-10% than the exact solution. Table 4.3 shows a comparison between Merkel number obtained by numerical calculation and by the proposed approximation method by using available data in [28] for 1.5 X 1.878 m film fill. The used approximation method has also been tested for counter-flow arrangements and produced exactly the same results with zero deviations.

Taking such differences into consideration, the obtained values of Merkel number by all methods are compared to each other. Figure4.21 shows that Merkel number by Poppe method gives higher values than Merkel and e-NTU methods because it is supposed to be more rigorous and accurate. On the other hand, Merkel and e-NTU which are using the same simplifying assumptions produced almost the same values even though Merkel numbers by Merkel method are calculated by the approximation method. Therefore, the deviation might not be as large as stated in table 4.3 because the fill size for the values in figure4.21 (0.1 X 0.3 m) is much

smaller than the fill size of the values obtained numerically [28] in tables 4.3 (1.5 X 1.878 m).

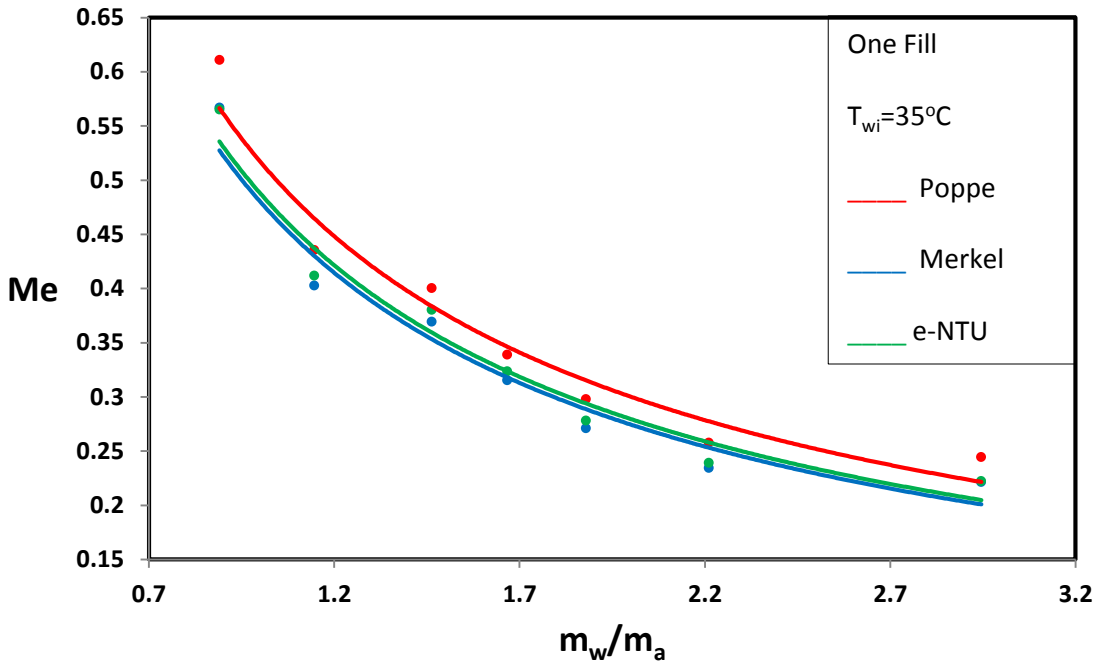

Figure 4.21 Comparison between Merkel numbers by Poppe, Merkel and e-NTU models, at water inlet temperature equals 35°C and one fill case

4.4.4 Best operating conditions and performance comparison with counter flow humidifiers

In light of previous analysis of first and second law of thermodynamics, the best operating conditions of the cross flow humidifier are the ones with least losses or irreversibility; that is at HCR equals 1.0. Since the humidifier is tested for the aim of using it in HDH system then the exit air is preferred to contain more water vapor. And hence, higher qualities of humid air can be achieved at higher mass flow rate ratios but as it has been noticed such higher qualities of air are on the expense of higher energy input to the system or in other words higher losses.

From the collected experimental results, the best operating condition for the tested cross flow humidifier took place when the water is provided into the humidifier at room temperature and at a fill length of 0.3 meter or the highest length available. The system effectiveness at this point is calculated to be 46%.

If a cross flow configuration is compared with a counter flow configuration, the results available in literature showed that more water vapor evaporates from water stream in the counter flow humidifiers, and such results can be noticed through Merkel number. For example, in [32] the results for both configurations are evaluated and the comparison is made. Table 4.9 shows that Merkel number for counter flow arrangement is higher by 14% than the cross flow humidifier.

Table 4.9 Merkel number comparison between counter and cross-flow humidifier [32]

	T_{wi}	m_w/m_a	Me_p/Le_{fi}
Counter-Flow Humidifier	38.13	1.87	0.65
Cross-Flow Humidifier	38.27	1.88	0.57

If the system performance of cross and counter flow humidifiers is compared to each other, then the air and water effectiveness (ϵ_w and ϵ_a) of the counter flow humidifier showed higher values by nearly 19-25% than the cross flow humidifier. Results of experimental data for counter flow cooling tower in [46] are used for comparison with the results of current study. Table 4.10 shows Merkel number and air and water effectiveness for counter and cross flow humidifiers.

Table 4.10 System effectiveness comparison between counter and cross flow humidifiers

	m_w/m_a	T_{wi} (^oC)	Me_p	ϵ_a	ϵ_w
Counter-Flow Humidifier	1.5	31.5	0.54	0.43	0.29
Cross-Flow Humidifier	1.5	31	0.46	0.37	0.23

CHAPTER 5

CONCLUSION AND RECOMMENDATIONS

Experimental work for cross flow humidifier has been done for one, two and three film fills set up and readings were taken for different mass flow rate ratios and water inlet temperatures. First and second law of thermodynamics were used to analyze the results by evaluating the variation of effectiveness or enthalpy changes for air and water streams as a function of input parameters as well as the associated entropy generation rate for each process.

The results showed that as mass flow rate ratio is varied, the heat capacity ratio of the hot and cold streams of air and water changes and when they are equal to each other the system effectiveness for both definitions of equations (3.4) and (3.5) becomes equal. The water inlet temperature influences the enthalpy change of humid air so that as it decreases the change in the humid air enthalpy is enhanced. Moreover, it has an effect to the heat capacity ratio at which the system effectiveness for both cases becomes equal.

It has also been shown that increasing the surface area or increasing the number of film fills enhances the heat and mass transfer and therefore the system effectiveness increases accordingly.

Second law analysis has been conducted for measured values and it showed the entropy generation rate is the least at HCR ≈ 1 in all cases. And as the water inlet

temperature increases the irreversibility in the system increases and the associated second law efficiency decreases.

Moreover, the effect of increasing the surface area has strong influence in increasing the losses in the system and hence the 2nd law efficiency decreases as the number of fills used increases.

At HCR equals one, second law efficiency was also tested and figure 4.17 showed that decreasing the number of fills contribute in increasing the 2nd law efficiency.

On the other hand, Merkel number was calculated by three different methods, Merkel, Poppe and e-NTU models. And all these models the mass flow rate ratio showed an influence to the value of Merkel number, that is, Merkel number decreases as the mass flow rate ratio increases. And it increases as the surface area is increased.

The effect of water inlet temperature is not as significant as the other parameters (i.e. mass flow rate ratio and surface area).

An approximation method was introduced and implemented to calculate Merkel number by Merkel and Poppe models with help of Chebychev integration method and it deviates from exact solutions by almost 8.0%.

Comparison between the three methods was made and since e-NTU and Merkel models are employing the same simplifying assumptions, they showed similar results. And because Poppe model is more accurate, the Merkel number obtained is greater than the ones evaluated by other two methods.

Since the flow rate of water during the test of three film fills case is the total flow rate on these fills, the partial flow rate over each fill is the same for all but the

associated heat capacity ratio is different for each one due to the fact that the incoming air temperature to the second and third fill is higher. Therefore, it is recommended to regulate the flow rate of water over each fill in order to achieve HCR equals one which is according to the results will maintain the minimum losses in the system.

Although the results of cross flow humidifier showed less performance than the counter flow humidifier, it is recommended to continue investigating how a cross flow humidifier will perform when it is incorporated with dehumidifier to form an HDH unit and in turn how much of GOR it will obtain.

APPENDIX A

UNCERTAINTY ANALYSIS

Coleman and Steele [44] approach for uncertainty analysis is used to examine the results of the experimental measurements. The proposed propagation equation estimates a 95% confidence interval. The proposed equation is:

$$U_r^2 = B_r^2 + P_r^2 \tag{A. 1}$$

Where U_r is the total uncertainty error, B_r is the Bias error, and P_r is the precision error.

Bias and precision errors can be evaluated as follows:

$$P_r^2 = \sum_{j=1}^{n} \left(\frac{\partial V}{\partial X_j} \right)^2 P_{Xj}^2 \tag{A. 2}$$

And,

$$B_r^2 = \sum_{j=1}^{n} \left(\frac{\partial V}{\partial X_j} \right)^2 B_{Xj}^2 \tag{A. 3}$$

Where X is the increment for the measured value and V is the measured variable.

The sensitivity of ϵ_w , ϵ_a , HCR , Me and μ_{II} to the changes of air and water flow rates, dry and wet bulb temperatures of air and water inlet and outlet temperatures, are evaluated by considering different values that ranges from low to high flow rates and from low to high temperatures.

Tables A.1, A.2 and A.3 below represent the calculation of the total uncertainty errors for ϵ_w , ϵ_a , HCR , Me and $\boldsymbol{\eta}_{II}$.

Table A.1 Uncertainty analysis for 3 fills readings at T_{wi}=55°C and $\dot{m}_w$=2 LPM.

	parameter	unit	Δx_j	$\epsilon_{a,x}$	$\epsilon_{a,x+\Delta x}$	$\frac{\partial \epsilon_a}{\partial X_j}$	P_{xj}	$\left(\frac{\partial \epsilon_a}{\partial X_j}\right)^2 P_{Xj}^2$	B_{xj}	$\left(\frac{\partial \epsilon_a}{\partial X_j}\right)^2 B_{Xj}^2$
ϵ_a	V_a	m/s	0.1	23.72	23.72	0	0.1	0	0.1	0
	$\dot{\forall}_{inlet,w}$	LPM	0.1	23.72	23.72	0	0.1	0	0.15	0
	$T_{dry,\ in}$	°C	0.15	23.72	23.72	0	0.1	0	0.35	0
	$T_{wet,\ in}$	°C	0.15	23.72	23.62	-0.667	0.1	0.0044	0.35	0.054
	$T_{dry,\ out}$	°C	0.15	23.72	23.72	0	0.1	0	0.35	0
	$T_{wet,\ out}$	°C	0.15	23.72	24.01	1.933	0.1	0.03737	0.35	0.457878
	$T_{water,\ in}$	°C	0.15	23.72	23.52	-1.333	0.1	0.0178	0.35	0.21778
	$T_{water,\ out}$	°C	0.15	23.72	23.72	0	0.1	0	0.35	0
								0.0596		0.7301
							P_r	0.24413	B_r	0.8544
							U_r	0.8886		

	parameter	unit	Δx_j	$\epsilon_{w,x}$	$\epsilon_{w,x+\Delta x}$	$\frac{\partial \epsilon_w}{\partial X_j}$	P_{xj}	$\left(\frac{\partial \epsilon_w}{\partial X_j}\right)^2 P_{Xj}^2$	B_{xj}	$\left(\frac{\partial \epsilon_w}{\partial X_j}\right)^2 B_{Xj}^2$
ϵ_w	V_a	m/s	0.1	57.49	57.49	0	0.1	0	0.1	0
	$\dot{\forall}_{inlet,w}$	LPM	0.1	57.49	57.49	0	0.1	0	0.15	0
	$T_{dry,\ in}$	°C	0.15	57.49	57.49	0	0.1	0	0.35	0
	$T_{wet,\ in}$	°C	0.15	57.49	57.71	1.467	0.1	0.021511	0.35	0.26351
	$T_{dry,\ out}$	°C	0.15	57.49	57.49	0	0.1	0	0.35	0
	$T_{wet,\ out}$	°C	0.15	57.49	57.49	0	0.1	0	0.35	0
	$T_{water,\ in}$	°C	0.15	57.49	57.65	1.067	0.1	0.011378	0.35	0.139378
	$T_{water,\ out}$	°C	0.15	57.49	57.12	-2.467	0.1	0.06084	0.35	0.74534
								0.093733		1.14823
							P_r	0.306159	B_r	1.0715
							U_r	1.114435		

	parameter	unit	Δx_j	$Me_{,x}$	$Me_{,x+\Delta x}$	$\frac{\partial Me}{\partial X_j}$	P_{xj}	$\left(\frac{\partial Me}{\partial X_j}\right)^2 P_{Xj}^2$	B_{xj}	$\left(\frac{\partial Me}{\partial X_j}\right)^2 B_{Xj}^2$
Me	V_a	m/s	0.1	0.9088	0.9041	-0.047	0.1	2.209E-05	0.1	2.209E-05
	$\dot{\forall}_{inlet,w}$	LPM	0.1	0.9088	0.9242	0.154	0.1	0.00023716	0.15	0.00053361
	$T_{dry,\ in}$	°C	0.15	0.9088	0.9088	0	0.1	0	0.35	0
	$T_{wet,\ in}$	°C	0.15	0.9088	0.9133	0.03	0.1	9E-06	0.35	0.00011025
	$T_{dry,\ out}$	°C	0.15	0.9088	0.9088	0	0.1	0	0.35	0
	$T_{wet,\ out}$	°C	0.15	0.9088	0.9088	0	0.1	0	0.35	0
	$T_{water,\ in}$	°C	0.15	0.9088	0.9125	0.024667	0.1	6.08444E-06	0.35	7.45344E-05
	$T_{water,\ out}$	°C	0.15	0.9088	0.8929	-0.106	0.1	0.00011236	0.35	0.00137641
								0.000386694		0.002116894
							P_r	0.019664548	B_r	0.046009721
							U_r	0.050035876		

	parameter	unit	Δx_j	$HCR_{,x}$	$HCR_{,x+\Delta x}$	$\frac{\partial HCR}{\partial X_j}$	P_{xj}	$\left(\frac{\partial HCR}{\partial X_j}\right)^2 P_{Xj}^2$	B_{xj}	$\left(\frac{\partial HCR}{\partial X_j}\right)^2 B_{Xj}^2$
HCR	V_a	m/s	0.1	2.421	2.46	0.39	0.1	0.001521	0.1	0.001521
	$\dot{\forall}_{inlet,w}$	LPM	0.1	2.421	2.355	-0.66	0.1	0.004356	0.15	0.009801
	$T_{dry,\ in}$	°C	0.15	2.421	2.421	0	0.1	0	0.35	0
	$T_{wet,\ in}$	°C	0.15	2.421	2.427	0.04	0.1	1.6E-05	0.35	0.000196
	$T_{dry,\ out}$	°C	0.15	2.421	2.421	0	0.1	0	0.35	0
	$T_{wet,\ out}$	°C	0.15	2.421	2.421	0	0.1	0	0.35	0
	$T_{water,\ in}$	°C	0.15	2.421	2.433	0.08	0.1	6.4E-05	0.35	0.000784
	$T_{water,\ out}$	°C	0.15	2.421	2.421	0	0.1	0	0.35	0
								0.005957		0.012302
							P_r	0.077181604	B_r	0.110914381
							U_r	0.135125867		

	parameter	unit	Δx_j	$\mu_{II,x}$	$\mu_{II,x+\Delta x}$	$\frac{\partial \mu_{II}}{\partial X_j}$	P_{xj}	$\left(\frac{\partial \mu_{II}}{\partial X_j}\right)^2 P_{Xj}^2$	B_{xj}	$\left(\frac{\partial \mu_{II}}{\partial X_j}\right)^2 B_{Xj}^2$
η_{II}	V_a	m/s	0.1	0.7602	0.72	-0.402	0.1	0.00161604	0.1	0.00161604
	$\forall_{inlet,w}$	LPM	0.1	0.7602	0.88	1.198	0.1	0.01435204	0.15	0.03229209
	$T_{dry,\ in}$	°C	0.15	0.7602	0.7597	-0.00333	0.1	1.11111E-07	0.35	1.36111E-06
	$T_{wet,\ in}$	°C	0.15	0.7602	0.7846	0.162667	0.1	0.000264604	0.35	0.003241404
	$T_{dry,\ out}$	°C	0.15	0.7602	0.7608	0.004	0.1	1.6E-07	0.35	1.96E-06
	$T_{wet,\ out}$	°C	0.15	0.7602	0.7118	-0.32267	0.1	0.001041138	0.35	0.012753938
	$T_{water,\ in}$	°C	0.15	0.7602	0.7852	0.166667	0.1	0.000277778	0.35	0.003402778
	$T_{water,\ out}$	°C	0.15	0.7602	0.7344	-0.172	0.1	0.00029584	0.35	0.00362404
								0.017847711		0.056933611
							P_r	0.133595326	B_r	0.238607651
							U_r	0.273461738		

Table A.2 Uncertainty analysis for 3 fills readings at T_{wi}=45°C and m_w=8 LPM.

	parameter	unit	Δx_j	$\epsilon_{a,x}$	$\epsilon_{a,x+\Delta x}$	$\frac{\partial \epsilon_a}{\partial X_j}$	P_{xj}	$\left(\frac{\partial \epsilon_a}{\partial X_j}\right)^2 P_{Xj}^2$	B_{xj}	$\left(\frac{\partial \epsilon_a}{\partial X_j}\right)^2 B_{Xj}^2$
ϵ_a	V_a	m/s	0.1	55.22	55.22	0	0.1	0	0.1	0
	$\dot{\forall}_{inlet,w}$	LPM	0.1	55.22	55.22	0	0.1	0	0.2	0
	$T_{dry,\,in}$	°C	0.15	55.22	55.22	0	0.1	0	0.4	0
	$T_{wet,\,in}$	°C	0.15	55.22	55.11	-0.733	0.1	0.005378	0.4	0.065878
	$T_{dry,\,out}$	°C	0.15	55.22	55.21	-0.0667	0.1	4.44E-05	0.4	0.000544
	$T_{wet,\,out}$	°C	0.15	55.22	55.82	4	0.1	0.16	0.4	1.96
	$T_{water,\,in}$	°C	0.15	55.22	54.73	-3.2667	0.1	0.106711	0.4	1.307211
	$T_{water,\,out}$	°C	0.15	55.22	55.22	0	0.1	0	0.4	0
								0.272133		3.33363
							P_r	0.521664004	B_r	1.825824015
							U_r	1.898885638		

	parameter	unit	Δx_j	$\epsilon_{w,x}$	$\epsilon_{w,x+\Delta x}$	$\frac{\partial \epsilon_w}{\partial X_j}$	P_{xj}	$\left(\frac{\partial \epsilon_w}{\partial X_j}\right)^2 P_{Xj}^2$	B_{xj}	$\left(\frac{\partial \epsilon_w}{\partial X_j}\right)^2 B_{Xj}^2$
ϵ_w	V_a	m/s	0.1	24.1	24.1	0	0.1	0	0.1	0
	$\dot{\forall}_{inlet,w}$	LPM	0.1	24.1	24.1	0	0.1	0	0.2	0
	$T_{dry,\,in}$	°C	0.15	24.1	24.1	0	0.1	0	0.4	0
	$T_{wet,\,in}$	°C	0.15	24.1	24.22	0.8	0.1	0.0064	0.4	0.0784
	$T_{dry,\,out}$	°C	0.15	24.1	24.1	0	0.1	0	0.4	0
	$T_{wet,\,out}$	°C	0.15	24.1	24.1	0	0.1	0	0.4	0
	$T_{water,\,in}$	°C	0.15	24.1	24.47	2.4667	0.1	0.060844	0.4	0.745344
	$T_{water,\,out}$	°C	0.15	24.1	23.61	-3.2667	0.1	0.10671	0.4	1.30721
								0.173956		2.130956
							P_r	0.417079795	B_r	1.459779283
							U_r	1.518193371		

	parameter	unit	Δx_j	$Me_{,x}$	$Me_{,x+\Delta x}$	$\frac{\partial Me}{\partial X_j}$	P_{xj}	$\left(\frac{\partial Me}{\partial X_j}\right)^2 P_{Xj}^2$	B_{xj}	$\left(\frac{\partial Me}{\partial X_j}\right)^2 B_{Xj}^2$
Me	V_a	m/s	0.1	0.4056	0.3979	-0.077	0.1	5.929E-05	0.1	5.929E-05
	$\forall_{inlet,w}$	LPM	0.1	0.4056	0.4102	0.046	0.1	2.116E-05	0.2	4.761E-05
	$T_{dry,\ in}$	°C	0.15	0.4056	0.4056	0	0.1	0	0.4	0
	$T_{wet,\ in}$	°C	0.15	0.4056	0.4077	0.014	0.1	1.96E-06	0.4	2.401E-05
	$T_{dry,\ out}$	°C	0.15	0.4056	0.4056	0	0.1	0	0.4	0
	$T_{wet,\ out}$	°C	0.15	0.4056	0.4056	0	0.1	0	0.4	0
	$T_{water,\ in}$	°C	0.15	0.4056	0.416	0.069333333	0.1	4.80711E-05	0.4	0.000588871
	$T_{water,\ out}$	°C	0.15	0.4056	0.39	-0.104	0.1	0.00010816	0.4	0.00132496
								0.000238641		0.002044741
							P_r	0.015448013	B_r	0.045218814
							U_r	0.047784749		

	parameter	unit	Δx_j	$HCR_{,x}$	$HCR_{,x+\Delta x}$	$\frac{\partial HCR}{\partial X_j}$	P_{xj}	$\left(\frac{\partial HCR}{\partial X_j}\right)^2 P_{Xj}^2$	B_{xj}	$\left(\frac{\partial HCR}{\partial X_j}\right)^2 B_{Xj}^2$
HCR	V_a	m/s	0.1	0.4357	0.4458	0.101	0.1	0.00010201	0.1	0.00010201
	$\forall_{inlet,w}$	LPM	0.1	0.4357	0.4305	-0.052	0.1	2.704E-05	0.2	6.084E-05
	$T_{dry,\ in}$	°C	0.15	0.4357	0.4357	0	0.1	0	0.4	0
	$T_{wet,\ in}$	°C	0.15	0.4357	0.4368	0.0073	0.1	5.378E-07	0.4	6.58778E-06
	$T_{dry,\ out}$	°C	0.15	0.4357	0.4357	0	0.1	0	0.4	0
	$T_{wet,\ out}$	°C	0.15	0.4357	0.4357	0	0.1	0	0.4	0
	$T_{water,\ in}$	°C	0.15	0.4357	0.4376	0.01267	0.1	1.60444E-06	0.4	1.96544E-05
	$T_{water,\ out}$	°C	0.15	0.4357	0.4357	0	0.1	0	0.4	0
								0.000131192		0.000189092
							P_r	0.011453917	B_r	0.013751081
							U_r	0.017896493		

	parameter	unit	Δx_j	$\mu_{II,x}$	$\mu_{II,x+\Delta x}$	$\frac{\partial \mu_{II}}{\partial X_j}$	P_{xj}	$\left(\frac{\partial \mu_{II}}{\partial X_j}\right)^2 P_{Xj}^2$	B_{xj}	$\left(\frac{\partial \mu_{II}}{\partial X_j}\right)^2 B_{Xj}^2$
η_{II}	V_a	m/s	0.1	0.9078	0.871	-0.368	0.1	0.00135424	0.1	0.00135424
	$\dot{\forall}_{inlet,w}$	LPM	0.1	0.9078	0.921	0.132	0.1	0.00017424	0.2	0.00039204
	$T_{dry,\ in}$	°C	0.15	0.9078	0.9076	-0.00133	0.1	1.778E-08	0.4	2.17778E-07
	$T_{wet,\ in}$	°C	0.15	0.9078	0.9131	0.0353	0.1	1.2484E-05	0.4	0.000152934
	$T_{dry,\ out}$	°C	0.15	0.9078	0.908	0.0013	0.1	1.778E-08	0.4	2.17778E-07
	$T_{wet,\ out}$	°C	0.15	0.9078	0.89	-0.11867	0.1	0.00014081	0.4	0.001725018
	$T_{water,\ in}$	°C	0.15	0.9078	0.9322	0.16267	0.1	0.000264604	0.4	0.003241404
	$T_{water,\ out}$	°C	0.15	0.9078	0.8784	-0.196	0.1	0.00038416	0.4	0.00470596
								0.002330582		0.011572032
							P_r	0.048276104	B_r	0.107573381
							U_r	0.117909348		

Table A.3 Uncertainty analysis for 1 fill readings at T_{wi}=35°C and m_w=5 LPM.

	parameter	unit	Δx_j	$\epsilon_{a,x}$	$\epsilon_{a,x+\Delta x}$	$\frac{\partial \epsilon_a}{\partial X_j}$	P_{xj}	$\left(\frac{\partial \epsilon_a}{\partial X_j}\right)^2 P_{Xj}^2$	B_{xj}	$\left(\frac{\partial \epsilon_a}{\partial X_j}\right)^2 B_{Xj}^2$
ϵ_a	V_a	m/s	0.1	32.91	32.91	0	0.1	0	0.1	0
	$\dot{\forall}_{inlet,w}$	LPM	0.1	32.91	32.91	0	0.1	0	0.15	0
	$T_{dry,\ in}$	°C	0.15	32.91	32.91	0	0.1	0	0.35	0
	$T_{wet,\ in}$	°C	0.15	32.91	32.66	-1.66667	0.1	0.027778	0.35	0.340278
	$T_{dry,\ out}$	°C	0.15	32.91	32.9	-0.06667	0.1	4.44E-05	0.35	0.000544
	$T_{wet,\ out}$	°C	0.15	32.91	33.2	1.933333	0.1	0.037378	0.35	0.457878
	$T_{water,\ in}$	°C	0.15	32.91	32.57	-2.26667	0.1	0.051378	0.35	0.629378
	$T_{water,\ out}$	°C	0.15	32.91	32.91	0	0.1	0	0.35	0
								0.116578		1.428078
							P_r	0.341435	B_r	1.195022
							U_r	1.242842		

	parameter	unit	Δx_j	$\epsilon_{w,x}$	$\epsilon_{w,x+\Delta x}$	$\frac{\partial \epsilon_w}{\partial X_j}$	P_{xj}	$\left(\frac{\partial \epsilon_w}{\partial X_j}\right)^2 P_{Xj}^2$	B_{xj}	$\left(\frac{\partial \epsilon_w}{\partial X_j}\right)^2 B_{Xj}^2$
ϵ_w	V_a	m/s	0.1	20.17	20.17	0	0.1	0	0.1	0
	$\dot{\forall}_{inlet,w}$	LPM	0.1	20.17	20.17	0	0.1	0	0.15	0
	$T_{dry,\ in}$	°C	0.15	20.17	20.17	0	0.1	0	0.35	0
	$T_{wet,\ in}$	°C	0.15	20.17	20.3	0.866667	0.1	0.007511	0.35	0.092011
	$T_{dry,\ out}$	°C	0.15	20.17	20.17	0	0.1	0	0.35	0
	$T_{wet,\ out}$	°C	0.15	20.17	20.17	0	0.1	0	0.35	0
	$T_{water,\ in}$	°C	0.15	20.17	20.68	3.4	0.1	0.1156	0.35	1.4161
	$T_{water,\ out}$	°C	0.15	20.17	19.53	-4.26667	0.1	0.182044	0.35	2.230044
								0.305156		3.738156
							P_r	0.552409	B_r	1.933431
							U_r	2.010799		

	parameter	unit	Δx_j	$Me_{,x}$	$Me_{,x+\Delta x}$	$\frac{\partial Me}{\partial X_j}$	P_{xj}	$\left(\frac{\partial Me}{\partial X_j}\right)^2 P_{Xj}^2$	B_{xj}	$\left(\frac{\partial Me}{\partial X_j}\right)^2 B_{Xj}^2$
Me	V_a	m/s	0.1	0.3236	0.3193	-0.043	0.1	1.85E-05	0.1	1.85E-05
	$\dot{\forall}_{inlet,w}$	LPM	0.1	0.3236	0.3252	0.016	0.1	2.56E-06	0.15	5.76E-06
	$T_{dry,\ in}$	°C	0.15	0.3236	0.3236	0	0.1	0	0.35	0
	$T_{wet,\ in}$	°C	0.15	0.3236	0.3255	0.012667	0.1	1.6E-06	0.35	1.97E-05
	$T_{dry,\ out}$	°C	0.15	0.3236	0.3236	0	0.1	0	0.35	0
	$T_{wet,\ out}$	°C	0.15	0.3236	0.3236	0	0.1	0	0.35	0
	$T_{water,\ in}$	°C	0.15	0.3236	0.3348	0.074667	0.1	5.58E-05	0.35	0.000683
	$T_{water,\ out}$	°C	0.15	0.3236	0.3096	-0.09333	0.1	8.71E-05	0.35	0.001067
								0.000166		0.001794
							P_r	0.012865	B_r	0.042355
							U_r	0.044266		

	parameter	unit	Δx_j	$HCR_{,x}$	$HCR_{,x+\Delta x}$	$\frac{\partial HCR}{\partial X_j}$	P_{xj}	$\left(\frac{\partial HCR}{\partial X_j}\right)^2 P_{Xj}^2$	B_{xj}	$\left(\frac{\partial HCR}{\partial X_j}\right)^2 B_{Xj}^2$
HCR	V_a	m/s	0.1	0.5905	0.608	0.175	0.1	0.000306	0.1	0.000306
	$\dot{\forall}_{inlet,w}$	LPM	0.1	0.5905	0.582	-0.085	0.1	7.23E-05	0.15	0.000163
	$T_{dry,\ in}$	°C	0.15	0.5905	0.5905	0	0.1	0	0.35	0
	$T_{wet,\ in}$	°C	0.15	0.5905	0.5921	0.010667	0.1	1.14E-06	0.35	1.39E-05
	$T_{dry,\ out}$	°C	0.15	0.5905	0.5905	0	0.1	0	0.35	0
	$T_{wet,\ out}$	°C	0.15	0.5905	0.5905	0	0.1	0	0.35	0
	$T_{water,\ in}$	°C	0.15	0.5905	0.5928	0.015333	0.1	2.35E-06	0.35	2.88E-05
	$T_{water,\ out}$	°C	0.15	0.5905	0.5905	0	0.1	0	0.35	0
								0.000382		0.000512
							P_r	0.019545	B_r	0.022618
							U_r	0.029892		

	parameter	unit	Δx_j	$\mu_{II,x}$	$\mu_{II,x+\Delta x}$	$\frac{\partial \mu_{II}}{\partial X_j}$	P_{xj}	$\left(\frac{\partial \mu_{II}}{\partial X_j}\right)^2 P_{Xj}^2$	B_{xj}	$\left(\frac{\partial \mu_{II}}{\partial X_j}\right)^2 B_{Xj}^2$
η_{II}	V_a	m/s	0.1	0.9528	0.902	-0.508	0.1	0.002581	0.1	0.002581
	$\dot{\forall}_{inlet,w}$	LPM	0.1	0.9528	0.972	0.192	0.1	0.000369	0.15	0.000829
	$T_{dry,\ in}$	°C	0.15	0.9528	0.952	-0.00533	0.1	2.84E-07	0.35	3.48E-06
	$T_{wet,\ in}$	°C	0.15	0.9528	0.965	0.081333	0.1	6.62E-05	0.35	0.00081
	$T_{dry,\ out}$	°C	0.15	0.9528	0.9534	0.004	0.1	1.6E-07	0.35	1.96E-06
	$T_{wet,\ out}$	°C	0.15	0.9528	0.934	-0.12533	0.1	0.000157	0.35	0.001924
	$T_{water,\ in}$	°C	0.15	0.9528	0.931	-0.14533	0.1	0.000211	0.35	0.002587
	$T_{water,\ out}$	°C	0.15	0.9528	0.934	-0.12533	0.1	0.000157	0.35	0.001924
								0.003541		0.010662
							P_r	0.059509	B_r	0.103256
							U_r	0.119177		

APPENDIX B

EES CODES

1. Engineering Equation Solver (EES) Code for calculating system effectiveness, rate of entropy generation, second law efficiency, Merkel number by effectiveness-NTU method.

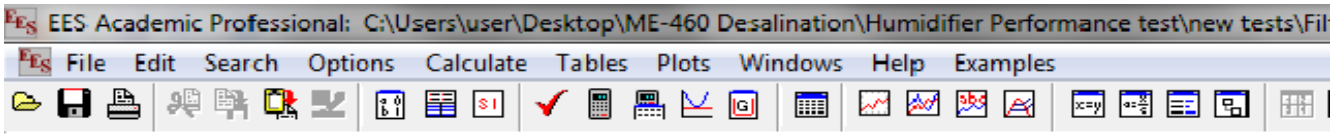


```
"m_a=0.037"          "air flow rate, kg/s"
"flowrate=1.95"
m_w=flowrate/60      "water flow rate, kg/s"
Mr=m_w/m_a
"db1=20.7"          "inlet air dry bulb Temp., C"
"wb1=13.8"          "inlet air wet bulb Temp., C"
rh1=RelHum(AirH2O,T=db1,B=wb1,P=P1)
rho=Density(AirH2O,T=db1,B=wb1,P=P1)
"db2=25.3"          "outlet air dry bulb Temp., C"
"wb2=22"            "outlet air wet bulb Temp., C"
rh2=RelHum(AirH2O,T=db2,B=wb2,P=P1)
"T_in=35"            "water inlet Temp., C"
"T_out=27.9"         "water outlet Temp., C"
T_in1=T_in+273.15
T_out1=T_out+273.15
T_w=(T_in+T_out)/2
P1=101.325
h1=Enthalpy(AirH2O,T=db1,B=wb1,P=P1)      "enthalpy of inlet air, kJ/kg"
cp1=Cp(AirH2O,T=db1,B=wb1,P=P1)
h2=Enthalpy(AirH2O,T=db2,B=wb2,P=P1)      "enthalpy of outlet air, kJ/kg"
cp2=Cp(AirH2O,T=db2,B=wb2,P=P1)
Cpma=(cp1+cp2)/2
omega1=HumRat(AirH2O,T=db1,B=wb1,P=P1)  "humidity ratio of inlet air, kg of water vapor/ kg dry air"
omega2=HumRat(AirH2O,T=db2,B=wb2,P=P1)  "humidity ratio of outlet air,  kg of water vapor/ kg dry air"
h_in=Enthalpy(Water,T=T_in,P=P1)          "enthalpy of inlet water, kJ/kg"
h_out=Enthalpy(Water,T=T_out,P=P1)        "enthalpy of outlet water, kJ/kg"
h_mean=Enthalpy(AirH2O,T=T_w,r=1,P=P1)
DELTA_h_w=h_in-h_out
DELTA_h_a=h2-h1
```

```
"heat loss"
Q_loss=(m_w*(h_in-h_out))-(m_a*(h2-h1))
q=(Q_loss/(m_w*(h_in-h_out)))*100

"water heat transfer effectiveness"
h_coldest=Enthalpy(Water,T=wb1,P=P1)
eff_water=(h_in-h_out)/(h_in-h_coldest)      "system effectiveness for enthalpy change of water side"
DELTA_H_w_max=(h_in-h_coldest)

"air heat transfer effectiveness"
h_max=Enthalpy(AirH2O,T=T_in,r=1,P=P1)
eff_air=(h2-h1)/(h_max-h1)                    "system effectiveness for enthalpy change of air side"
DELTA_H_a_max=(h_max-h1)

"system effectiveness"
omega_max=HumRat(AirH2O,T=T_in,r=1,P=P1)

eff_sys=(omega2-omega1)/(omega_max-omega1)


"Modified Heat Capacity Ratio"
HCR=(m_a*DELTA_H_a_max)/(m_w*DELTA_H_w_max)

"Lewis Factor for unsaturated air case"
omega_s=HumRat(AirH2O,T=T_w,r=1,P=P1)      "Hum. Ratio of sat. air at local bulk Temp."
Le_f=(0.865^0.667)*(((omega_s+0.622)/(omega1+0.622))-1)/(ln((omega_s+0.622)/(omega1+0.622)))


" entropy production"

s_in=Entropy(Water,T=T_in,P=P1)
s_out=Entropy(Water,T=T_out,P=P1)
s_1=Entropy(AirH2O,T=db1,B=wb1,P=P1)
s_2=Entropy(AirH2O,T=db2,B=wb2,P=P1)
S_gen_h=m_w*(s_out-s_in)+m_a*(s_2-s_1)   "entropy generation rate, W/K"

"e_NTU method"

h_maswi=h_max
h_maswo=Enthalpy(AirH2O,T=T_out,r=1,P=P1)
di_T_gradiant=(h_maswi-h_maswo)/(T_in-T_out)
C1=(m_w*cp_w)/di_T_gradiant
C2=m_a
C=C2/C1                                          "heat capacity ratio"
lamda=(h_maswo+h_maswi-(2*h_mean))/4
Q_max=C2*(h_maswi-lamda-h1)
Q1=(m_w*cp_w)*(T_in-T_out)
e=Q1/Q_max                                        "effectiveness"
e1=e
e1=1-exp(((NTU1^0.22)/C)*(exp(-C*(NTU1^0.78))-1))   "for both streams unmixed"
Me_e1=NTU1*(cp_w/di_T_gradiant)
Me_e11=(1/Mr)*NTU1                               "Merkel number by e-NTU method"
```

"Exergy and Second law eff."

```
t=0
T_o=t+273.15
T_a=db1+273.15
R_a=0.287
P_o=101.325
c_pa=Cp(AirH2O,T=db1,w=0,P=P1)
c_pv=Cp(Water,T=db1,x=1)
w=1.608*omega1
rh=0.5
omega_o=HumRat(AirH2O,T=t,r=rh,P=P_o)
w_o=1.608*omega_o
x_1=((c_pa+(omega1*c_pv))*T_o*((T_a/T_o)-1-(ln(T_a/T_o))))
x_2=((1+w)*R_a*T_o*(ln(P1/P_o)))+R_a
x_3=T_o*(((1+w)*(ln((1+w_o)/(1+w))))+(w*(ln(w/w_o))))
x_in=m_a*(x_1+x_2*x_3)                "total exergy flow for humid air by Wepfer, KJ"

h_oa=Enthalpy(AirH2O,T=t,r=rh,P=P_o)
s_oa=Entropy(AirH2O,T=t,r=rh,P=P_o)
h_o=Enthalpy(Water,T=t,P=P_o)
s_o=Entropy(Water,T=t,P=P_o)
x_w_in=m_w*((h_in-h_o)-(T_o*(s_in-s_o)))
x_a_in=m_a*((h1-h_oa)-(T_o*(s_1-s_oa)))
X_D=T_o*S_gen_h

eff_secondlaw=1-(X_D/(x_in+x_w_in))        "second law efficiency by using Wepfer definition"
eff_2law=1-(X_D/(x_a_in+x_w_in))
```

2. EES code for calculating Merkel number by Poppe and Merkel methods using the approximation approach and Checychev method of integration.

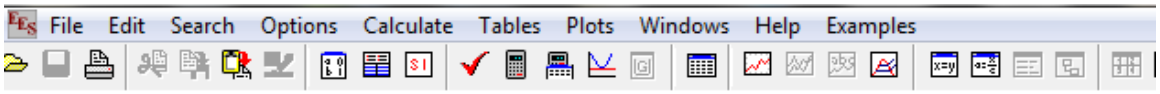


```
flowrate=4.7
m_w=flowrate/60
m_a=0.047
mr=m_w/m_a
T_in=35
T_out=30.3
db1=21.8
wb1=11.7
db2=26.1
wb2=22.1
P1=101.325
h_air_in=Enthalpy(AirH2O,T=db1,B=wb1,P=P1)
h_air_out=Enthalpy(AirH2O,T=db2,B=wb2,P=P1)
cp1=Cp(Water,T=T_in,P=P1)
cp2=Cp(Water,T=T_out,P=P1)
c_pwm=(cp1+cp2)/2
omega1=HumRat(AirH2O,T=db1,B=wb1,P=P1)
omega2=HumRat(AirH2O,T=db2,B=wb2,P=P1)
T1=T_out+(0.1*(T_in-T_out))          "water bulk temperature at 0.1"
T2=T_out+(0.4*(T_in-T_out))
T3=T_out+(0.6*(T_in-T_out))
T4=T_out+(0.9*(T_in-T_out))
h1sat=Enthalpy(AirH2O,T=T1,r=1,P=P1)      "enthalpy of air-water vapor at water bulk temperature (0.1)"
h2sat=Enthalpy(AirH2O,T=T2,r=1,P=P1)
h3sat=Enthalpy(AirH2O,T=T3,r=1,P=P1)
h4sat=Enthalpy(AirH2O,T=T4,r=1,P=P1)

T=(T_in+T_out)/2
omega_s=HumRat(AirH2O,T=T,r=1,P=P1)
Le_f_in=(0.865^0.667)*(((omega_s+0.622)/(omega1+0.622))-1)/(ln((omega_s+0.622)/(omega1+0.622)))
Le_f_out=(0.865^0.667)*(((omega_s+0.622)/(omega2+0.622))-1)/(ln((omega_s+0.622)/(omega2+0.622)))
Le_f_avg=(Le_f_in+Le_f_out)/2

z=0.3                    "Height of the Fill"
z1=0.1*z
z2=0.4*z
z3=0.6*z
z4=0.9*z
"delta_x=0"          "Length"
```

```
"delta_x=0"              "Length"

massflux_ratio=mr*3
b=massflux_ratio

"values of air-water vapor enthalpy by Merkel method"
dh1=((T1-T_out)*b*c_pwm*delta_x)/z1
dh2=((T2-T_out)*b*c_pwm*delta_x)/z2
dh3=((T3-T_out)*b*c_pwm*delta_x)/z3
dh4=((T4-T_out)*b*c_pwm*delta_x)/z4

"Difference between saturated and unsaturated enthalpies of air"
DELTA_h_1=h1sat-(dh1+h_air_in)
DELTA_h_2=h2sat-(dh2+h_air_in)
DELTA_h_3=h3sat-(dh3+h_air_in)
DELTA_h_4=h4sat-(dh4+h_air_in)

X=(1/DELTA_h_1)+(1/DELTA_h_2)+(1/DELTA_h_3)+(1/DELTA_h_4)
Me=((T_in-T_out)/4)*X*c_pwm          "Merkel number by Chebychev method and Merkel Model"

"distribution of humidity ratio across the film fill"
Le_f1=Le_f_avg
Le_f2=Le_f_avg
Le_f3=Le_f_avg
Le_f4=Le_f_avg

"values of air enthalpy distribution at water bulk temperature by Poppe Model"
dh1p=c_pwm*((((T1-T_out)*b*delta_x)/z1)+T1*w1)
dh2p=c_pwm*((((T2-T_out)*b*delta_x)/z2)+T2*w2)
dh3p=c_pwm*((((T3-T_out)*b*delta_x)/z3)+T3*w3)
dh4p=c_pwm*((((T4-T_out)*b*delta_x)/z4)+T4*w4)
```

```
"values of humidity ratios of saturated air at water local bulk temperature"
omega_s1=HumRat(AirH2O,T=T1,r=1,P=P1)
omega_s2=HumRat(AirH2O,T=T2,r=1,P=P1)
omega_s3=HumRat(AirH2O,T=T3,r=1,P=P1)
omega_s4=HumRat(AirH2O,T=T4,r=1,P=P1)
"Lewis factor at local bulk temperature of water"
Le_f1=(0.865^0.667)*(((omega_s1+0.622)/(w1+0.622))-1)/(ln((omega_s1+0.622)/(w1+0.622)))
Le_f2=(0.865^0.667)*(((omega_s2+0.622)/(w2+0.622))-1)/(ln((omega_s2+0.622)/(w2+0.622)))
Le_f3=(0.865^0.667)*(((omega_s3+0.622)/(w3+0.622))-1)/(ln((omega_s3+0.622)/(w3+0.622)))
Le_f4=(0.865^0.667)*(((omega_s4+0.622)/(w4+0.622))-1)/(ln((omega_s4+0.622)/(w4+0.622)))

w_1=omega_s1-w1
w_2=omega_s2-w2
w_3=omega_s3-w3
w_4=omega_s4-w4

h_v1=Enthalpy(Water,T=T1,x=1)
h_v2=Enthalpy(Water,T=T2,x=1)
h_v3=Enthalpy(Water,T=T3,x=1)
h_v4=Enthalpy(Water,T=T4,x=1)
"difference between sat. and unsat. air enthalpies per Popper model"
DELTA_h_1p=h1sat-(dh1p+h_air_in)
DELTA_h_2p=h2sat-(dh2p+h_air_in)
DELTA_h_3p=h3sat-(dh3p+h_air_in)
DELTA_h_4p=h4sat-(dh4p+h_air_in)

denom1=DELTA_h_1p+((Le_f1-1)*(DELTA_h_1p-(h_v1*w_1)))-(c_pwm*w_1*T1)
denom2=DELTA_h_2p+((Le_f2-1)*(DELTA_h_2p-(h_v2*w_2)))-(c_pwm*w_2*T2)
denom3=DELTA_h_3p+((Le_f3-1)*(DELTA_h_3p-(h_v3*w_3)))-(c_pwm*w_3*T3)
denom4=DELTA_h_4p+((Le_f4-1)*(DELTA_h_4p-(h_v4*w_4)))-(c_pwm*w_4*T4)
Y=(1/denom1)+(1/denom2)+(1/denom3)+(1/denom4)
Me_P=((T_in-T_out)/4)*Y*c_pwm        "Merkel number by Checychev Method and Poppe Model"
```

NOMENCLATURE

A	area, m^2
a_{fi}	surface area per unit volume of the fill, m^{-1}
C	heat capacity rate, W/K
c_{pw}	specific heat of water at constant pressure, J/kg K
c_{pv}	specific heat of water-vapor at constant pressure, J/kg K
c_{pa}	specific heat of air at constant pressure, J/kg K
E	total energy transfer, KJ
e	effectiveness
h_c	heat transfer coefficient, W/m^2 s
h_d	mass transfer coefficient, Kg/m^2 s
h	enthalpy, J/kg
h_v	enthalpy of water vapor, J/kg
h_{ma}	enthalpy of moist air, J/kg
h_{fgwo}	latent heat of water at T=273.15 K, J/kg
h_{masw}	enthalpy of sat. air evaluated at local bulk temperature of water, J/kg

h_{maswm}	enthalpy of sat. air evaluated at mean temperature of water, J/kg
h_w	enthalpy of water, J,kg
HCR	heat capacity ratio
Le_f	lewis factor
m_v	mass of water vapor, Kg
m_g	mass of water vapor at saturated vapor condition, Kg
$\dot{m}_a$	mass flow rate of air, Kg/s
$\dot{m}_{wi}$	mass flow rate of inlet water, Kg/s
$\dot{m}_{wo}$	mass flow rate of outlet water, Kg/s
Me_p	merkel number by Poppe method
Me_m	merkel number by Merkel method
Me_e	merkel number by effectiveness-NTU method
NTU	number of transferred units
P	pressure, KPa
P_a	pressure of dry air, KPa
P_v	pressure of water vapor, KPa

P_o	pressure at dead state, KPa
$\dot{Q}$	heat transfer rate, KW
Q_m	energy transfer due to mass transfer, KJ
Q_c	energy transfer due to heat transfer, KJ
R_a	specific gas constant for dry air, KJ/Kg K
s_{ai}	specific entropy of inlet air, KJ/Kg K
s_{ao}	specific entropy of outlet air, KJ/Kg K
s_{wi}	specific entropy of inlet water, KJ/Kg K
s_{wo}	specific entropy of outlet air, KJ/Kg K
$\dot{S}_{gen}$	entropy generation rate, W/K
T_{wi}	water inlet temperature, K
T_{wo}	water outlet temperature, K
T_{ai}	dry bulb temperature of inlet air, K
T_{ao}	dry bulb temperature of outlet air, K
$T_{i,wb}$	wet bulb temperature of inlet air, K
$T_{o,wb}$	wet bulb temperature of outlet air, K

T_c temperature of cold stream, K

T_h temperature of hot stream, K

T_o temperature at dead state, K

U overall heat transfer coefficient, $W/m^2 K$

$\dot{X}$ flow exergy, KW

$\dot{X}_d$ exergy destruction, KW

$\dot{x}_{ai}$ specific exergy of inlet air, KJ/Kg

$\dot{x}_{ao}$ specific exergy of outlet air, KJ/Kg

$\dot{x}_{wi}$ specific exergy of inlet water, KJ/Kg

$\dot{x}_{wo}$ specific exergy of outlet water, KJ/Kg

Greek Symbols

Ω humidity ratio, $Kg_{water\text{-}vapor}/Kg_{dry\text{-}air}$

ω_{sw} humidity ratio of saturated air at water local bulk temperature, $Kg_{water\text{-}vapor}/Kg_{dry\text{-}air}$

$\widetilde{\omega}$ mole fraction ratio, $Kmol_{water\text{-}vapor}/Kmol_{dry\text{-}air}$

$\widetilde{\omega}_o$ mole fraction ratio at dead state, $Kmol_{water\text{-}vapor}/Kmol_{dry\text{-}air}$

$\emptyset$	relative humidity
η_{II}	second law efficiency
ϵ	system effectiveness
$\boldsymbol{\lambda}$	correction factor

Subscripts

A	Air
A_i	inlet air
A_o	outlet air
Fi	Fill
Fr	frontal
max	Maximum
min	Minimum
I	Inlet
O	Outlet
V	Vapor

W	Water
w_i	inlet water
w_o	outlet air
wb	wet bulb

REFERENCES

[1] J. Bendfeld, Ch. Broker, K. Menne, E. Ortjohann, L. Temme, J. Vob and P.C. M. Carvallo, "Design of a PV-Powered Reverse Osmosis Plant for Desalination of Brackish Water," Proceedings of 2nd World Conference and Exhibition on Photovoltaic Solar Energy Conversion, Vienna, 6-10 July 1998, 3075-3077.

[2] United Nations Inter-Agency Water, www.unwater.org

[3] S. Kalogirou, "Economic Analysis of a Solar Assisted Desalination System," Renewable Energy, Vol. 12, No. 4, 1997, 351-367.

[4] A. E. Kabeel, Mofreh H. Hamed, Z. M. Omara, S. W. Sharshir, "Water Desalination Using a Humidification-Dehumidification Technique-A Detailed Review," Natural Resources, 2013, 4, 286-305.

[5] A. Cipollina, C. Micale, L. Rizzuti, Seawater Desalination-Conventional and Renewable Energy Processes. Springer, Italy, 2009.

[6] H.T. El-Dessouky and H.M. Ettouney, Fundamentals of Salt Water Desalination. Elsevier Science B.V., University of Kuwait, 2002.

[7] G. Thiel, "Entropy Generation Minimization of a Heat and Mass Exchanger for Use in a Humidification-Dehumidification Desalination System," Master's Thesis, Massachusetts Institute of Technology, 2012.

[8] G. Parakash Narayan, Mostafa H. Sharwawy, John H. Lienhard, Syed M. Zubair, "Thermodynamic analysis of humidification dehumidification desalination cycles," Desalination and Water Treatment, April 2010, 16, 339-353.

[9] G. Parakash Narayan, Mostafa H. Sharwawy, Edward K. Summers , John H. Lienhard, Syed M. Zubair, M. A. Antar, "The potential of solar-driven humidification-dehumidification desalination for small-scale decentralized

water production," Renewable and Sustainable Energy Reviews, 14.4 (2010): 1187-1201.

[10] G. Parakash Narayan, Ronan K. McGovern, Gregory P. Thiel, Jacob A. Miller, Mostafa H. Sharqawy ,John H. Lienhard, Syed M. Zubair, M. A. Antar, "Status of humidification dehumidification desalination technology," World Congress-Perth Convention and Exhibition Centre (PCEC), Perth, Western Australia, Sep. 2011.

[11] M. A. Antar, "Introduction to Humidification-Dehumidification Desalination System," Lectures at KFUPM, Fall term, 2013.

[12] http://what-when-how.com/energy-engineering/cooling-towers-energy-engineering

[13] Yunus A. Cengel and Michael A. Boles, Thermodynamics an Engineering Approach, 5th Ed., McGraw-Hill College, Boston, MA, 2006.

[14] Detlev G. Kroger, Air-Cooled Heat Exchangers and Cooling Towers. PennWell Corp., Tulsa, OK, 2004.

[15] Treybal R. E., 1980. Mass Transfer Operations.3rd edition, McGraw-Hill, NY.

[16] Kreith F. and Bohem R. R., 1988. Direct-Contact heat transfer, Hemisphere Pub. Corp., Washington.

[17] Yousin, M.A., Darwish, M.A., Juwayhel, F., 1993. Experimental and theoretical study of a humidification dehumidification desalting system. Desalination 94, 11-24.

[18] Ben-Amara, M., Houcine, I., Guizani, A., Maalej, M., 2004. Experimental study of a multiple-effect humidification solar desalination technique. Desalination 170, 209-221.

[19] El-Agouz, S.A. and Abagderah M., 2008. Experimental analysis of humidification process by air passing through seawater, Energy Conversion and Management, Vol. 49 (12), 3698-3703.

[20] United Muller-Holst, H., Engelhardt, M., Herve, M., Scholkopf, W., 1998. Solar thermal seawater desalination systems for decentralized use. Renewable Energy 14(1-4), 311-318.

[21] Orfi, J., Laplante, M., Marmouch, H., Galanis, N., Benhamou B., Nasallah S. B., Nguyen C.T., 2004. Experimental and theoretical study of a humidification dehumidification water desalination system using solar energy. Desalination 168, 151.

[22] Wallis J.S. and Aull R.J., 1999. Improving Cooling Tower Performance, Hydrocarbon Engineering, pp. 92-95, May.

[23] Y.J. Dai and K. Sumathy, " Theoretical study on a cross-flow direct evaporative cooler using honeycomb paper as packing material," Applied Thermal Engineering, 22 (2002) 1417-1430.

[24] United F. Merkel, VerdunstungsKuhlung, VDI-Zeitchrift 70 (1925) 123-128.

[25] United M. Poppe, H. Rogener, Berechnung von Ruckkuhlwerken, VDI-Warmeatlas (1991) Mi 1-Mi 15.

[26] H. Jaber, R.L. Weeb, Design of cooling towers by the effectiveness-NTU method, J. Heat Transfer 111 (1989) 837-843.

[27] J.C. Kloppers and D.G. Kroger, "A critical investigation into the heat and mass transfer analysis of counter-flow wet-cooling towers," International Journal of heat and mass transfer, 48 (2005) 765-777.

[28] J.C. Kloppers and D.G. Kroger, "A critical investigation into the heat and mass transfer analysis of cross-flow wet-cooling towers," Numerical Heat Transfer, Part A, 46: 785-806, 2004. [28]

[29] Ebrahim Hajid avalloo, Reza Shakeri, Mozaffar A. Mehrabian, "Thermal performance of cross flow cooling towers in variable web bulb temperature," Energy Conversion and Management, 51 (2010) 1298-1303.

[30] J.R. Camargi, C.D. Ebinuma, S. Cardoso, "A mathematical Model for direct evaporative cooling air conditioning system," EngenhariaTermica, No. 4, 2003 P. 30-34.

[31] L.O. Liburd, "Solar-driven humidification dehumidification desalination for potable use in Haiti," Master's Thesis, Massachusetts Institute of Technology, 2010.

[32] Reuter, H C R, 2010, Performance evaluation of natural draught cooling towers with anisotropic fills, PhD Thesis, Stellenbosch University, South Africa.

[33] Yugvi G., "Performance evaluation of wet-cooling tower fills with computational fluid dynamics," Master Thesis, Stellenbosch University, March 2012.

[34] A. Bejan, Advanced Engineering Thermodynamics, Second ed., John Willey & Sons, New York, 1997.

[35] W.J. Wepfer, R.A. Gaggioli, E.F. Obert, Proper evaluation of available energy for HVAC, ASHRAE Transactions, Part I 85 (1979) 214-230.

[36] G. Prakash Narayan, John H. Lienhard, Syed M. Zubair, Entropy generation minimization of combined heat and mass transfer devices. International Journal of thermal Sciences, 49 (2010) 2057-2066.

[37] Karan H. Mistry, John H. Lienhard, Syed M. Zubair, "Effect of entropy generation on the performance of humidification dehumidification desalination cycles," International Journal of Thermal Sciences, 49 (2010) 1837-1847.

[38] B.A. Qureshi and S.M. Zubair, “Second-Law based performance evaluation of cooling towers and evaporative heat exchangers,” International Journal of Thermal Sciences, 46 (2007) 188-198.

[39] T. Muangnoi, W. Asvapoositkul, S. Wongwises, “ An exergy analysis on the performance of a counter-flow wet cooling tower,” Applied Thermal Engineering, 27 (2007) 910-917.

[40] R. Chenngqin, Li Nianping, Tang Guangfa, “Principles of exergy analysis in HVAC and evaluation of evaporative cooling schemes,” Building and Environment, 37 (2002) 1045-1055.

[41] F. Bosnjakovic, Technische Thermodinamik, Theodor Steinkopf, Dresden, 1965.

[42] J.C. Kloppers and D.G. Kroger, “Cooling Tower Performance: A critical Evaluation of the Merkel Assumption,” R&D Journal, 2004, 20 (1).

[43] L.D. Berman, Evaporative cooling of Circulating Water, 2nd ed., pp. 94-99, H. Sawistowski, ed., translated from Russian by R. Hardbottle, Pergamon Press, New York, 1961.

[44] H. W. Coleman and W. G. Glenn Steele, Experimentation, Validation, and Uncertainty Analysis for Engineers, 3rd Ed., A John Willy & Sons, INC. USA, 2009.

[45] J. C. KloppersandD. G. Kroger, “Refinement of the transfer characteristic correlation of wet-cooling Tower fills”, Heat Transfer Engineering. 26 (4): 35-41, 2005.

[46] Iqbal Husain, “Performance evaluation of seawater counter flow cooling towers,” Master Thesis, King Fahd University of Petroleum and Minerals, May 2011.

Vitae

Name	Ibrahim Saad Al-Shalawi
Nationality	Saudi
Date of Birth	28/8/1980
Email	Ibrhaim.shalawi@hotmail.com
Adress	Saudi Arabia Khobar Azeziyah – Noras District Phone: +966505552997
Academic Background	M.S (Mechanical Engineering) - May 2014 King Fahd University of Petroleum & Minerals Dhahran, Saudi Arabia B.S (Mechanical Engineering) - January 2005 King Fahd University of Petroleum & Minerals Dhahran, Saudi Arabia
Career	SAUDI ARAMCO COMPANY January 2005 – August 2013